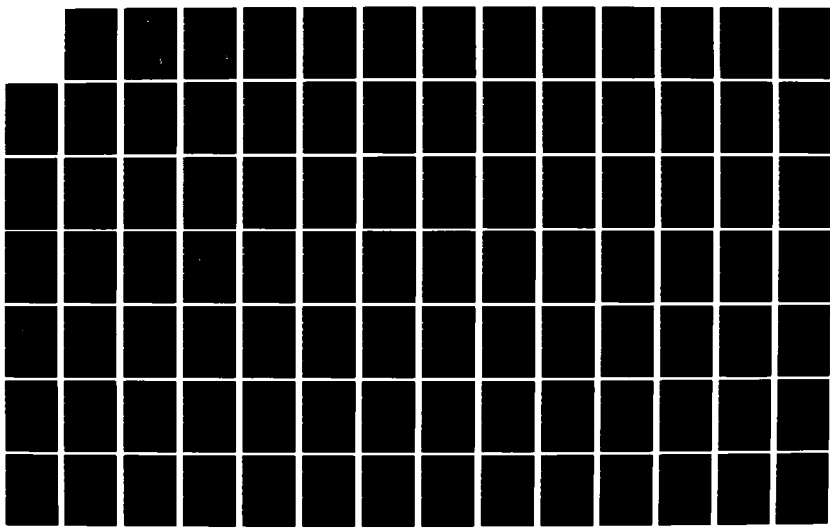
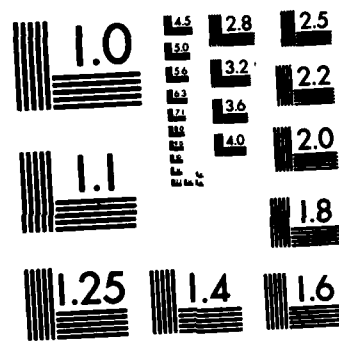


AD-A124 774 COMPARISON OF ALUMINUM AND COPPER FUSE OPENING SWITCHES 1/2
UNDER ROOM AND CR. (U) AIR FORCE INST OF TECH
WRIGHT-PATTERSON AFB OH SCHOOL OF ENGI. J C BUECK
UNCLASSIFIED DEC 82 AFIT/GE/EE/82D-22 F/G 9/1 NL



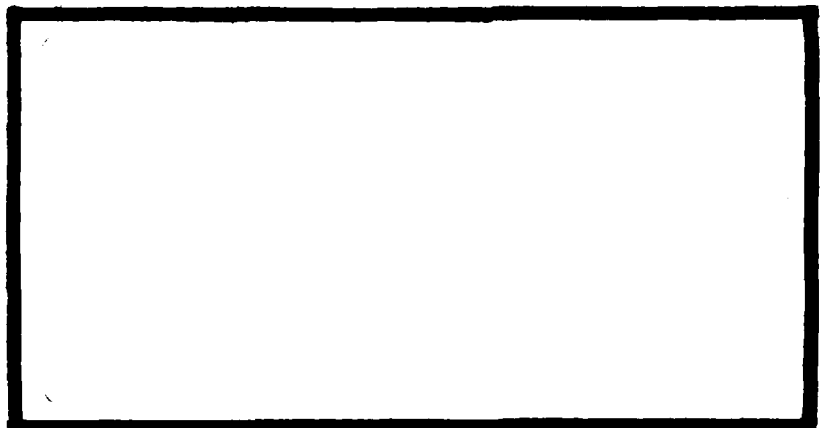


MICROCOPY RESOLUTION TEST CHART
NATIONAL BUREAU OF STANDARDS-1963-A

AD A112474



1



This document has been approved
for public release and sale; its
distribution is unlimited.

DTIC
SELECTED
S FEB 22 1983

A

DEPARTMENT OF THE AIR FORCE
AIR UNIVERSITY (ATC)

AIR FORCE INSTITUTE OF TECHNOLOGY

DTIC FILE COPY

Wright-Patterson Air Force Base, Ohio

2

COMPARISON OF ALUMINUM
AND COPPER FUSE OPENING SWITCHES
UNDER ROOM AND CRYOGENIC
TEMPERATURE CONDITIONS

THESIS

AFIT/GE/EE/82D-22

Jerry C. Bueck
Capt USAF

DTIC
SELECTED
S A
FEB 22 1983

Approved for Public Release; Distribution Unlimited

COMPARISON OF
ALUMINUM AND COPPER FUSE OPENING SWITCHES
UNDER ROOM AND CRYOGENIC TEMPERATURE CONDITIONS

THESIS

Presented to the Faculty of the School of Engineering
of the Air Force Institute of Technology
Air University
in Partial Fulfillment of the
Requirements for the Degree of
Master of Science

by
Jerry C. Bueck, B. S.
Capt USAF

December 1982

Classification For	
MAY 19 1981	
1981 E&B	
Advanced	
Classification	
Distribution/	
Availability Codes	
1st	2nd
Special	
A	



Approved for Public Release; Distribution Unlimited

Acknowledgements

This project would not have been possible without the efforts of Dr. Robert E. Reinovsky. Dr. Reinovsky not only sponsored the topic but provided me with continuous guidance and support throughout this summer. His insights and encouragement made many a difficult time bearable. Funding was provided by the Air Force Weapons Laboratory and the Defense Nuclear Agency.

The many helpful and knowledgeable people assigned to the Advanced Concepts Branch, Applied Physics Division, at the Air Force Weapons Laboratory deserve my gratitude. Without exception help of all sorts was readily available to me on many topics about which I knew little. I would like to single out several individuals for special mention. First, Capt R. E. "Crunch" Henderson helped me keep the transient digitizers in operation. Without his help I would have had almost invincible difficulties. My data was processed under the watchful eye and computer routines of 2Lt Steve Payne. Steve put in as much time as I did in working with the results of my experiments. Finally, Maj Bill McCullough gave me many insights into the fuse operation on the SHIVA-STAR.

Dan Porter is an outstanding engineering student from the University of New Mexico. He worked hand and glove with

me and kept the experiment going on an even keel. I owe much to this dedicated and hard working young man. This experiment was as much his as it was mine.

The Maxwell contractor personnel gave me invaluable technical and logistic support. Their professional and prompt assistance allowed me to progress through the early learning experience in a most painless way. My thanks to all of them.

Finally, I must mention the people who suffered most while I spent the summer in sunny New Mexico, my wife and children. They gave up an entire summer to allow me to complete this work, a sacrifice not many have been asked to make. To them I owe more than just gratitude.

Jerry C. Bueck

Contents

	<u>Page</u>
Acknowledgements	ii
List of Figures	vi
List of Tables	x
Abstract	xi
I. Introduction	1-1
Problem and Scope	1-3
Assumptions	1-5
General Approach	1-5
Sequence of Presentation	1-6
II. Theory	2-1
Basic Fuse Theory	2-1
Early Fuse Concepts	2-2
Voltage Multiplication and Pulse Compression	2-8
Extension of Fuses to Higher Energies ..	2-10
Thermal Considerations	2-13
III. Equipment	3-1
Capacitor Storage Bank	3-1
Inductive Store	3-3
Closing Switches	3-3
Triggering	3-4
Transmission Line	3-4
Fuse Fixture, Fuse Mounting	3-4
Current and Voltage Sensors	3-10
Signal Recorders	3-12
Calibration	3-13
Final Calibration	3-18
Time Correlation	3-20
IV. Results	4-1
Data Processing	4-1
Fuses in Sand at Room Temperature	4-6
Fuses in Cold Sand	4-17
Fuses in Liquid Nitrogen	4-22
Fuses in Deionized Water	4-29
Other Copper Fuse Configurations	4-29

Contents

	<u>Page</u>
V. Summary, Conclusions, and Recommendations ..	5-1
Summary	5-1
Conclusions	5-1
Recommendations	5-2
Bibliography	Bi-1
Appendix A	A-1
Appendix B	B-1
Appendix C	C-1
Vita	V-1

List of Figures

<u>Figure</u>		<u>Page</u>
1	Basic Circuit Model With a Load	2-3
2	Maisonnier's Circuit Model	2-3
3	DiMarco's Circuit Model	2-7
4	Bedford's Circuit Model	2-7
5	Experimental Device	3-2
6	Instrumentation Arrangement	3-5
7	General Fuse Geometry	3-6
8	Fuse Mounting, Sand Quench	3-8
9	Cold Soaking Device	3-9
10	Sensor Mounting and Locations	3-11
11	Short Circuit I-Dot Coil Signal	3-15
12	Calculated Signal Overlay of Measured Signal	3-16
13	Typical Calibration Output	3-15
14	Typical Raw Voltage and Current Data	3-21
15	Characteristic Voltage Step On Fuse Signal	3-22
16	Experimental and Computed Voltage and Current	4-5
17	Processed Voltage and Current	4-7
18	Preprocessed Voltage and Current	4-8
19	Processed Resistivity Vs. Specific Energy	4-9
20	Processed and Preprocessed Resistivity Vs. Specific Energy	4-10

List of Figures

<u>Figure</u>		<u>Page</u>
21	Processed and Preprocessed Resistivity Vs. Specific Energy	4-11
22	Processed Resistivity	4-12
23	Preprocessed Resistivity	4-13
24	Processed Resistance	4-14
25	Processed Power	4-15
26	Processed Energy	4-16
27	Preprocessed Voltage and Current	4-18
28	Preprocessed Resistivity Vs. Specific Energy	4-19
29	Preprocessed Resistivity	4-20
30	Baseline Preprocessed Resistivity Vs. Specific Energy	4-21
31	Preprocessed Voltage and Current	4-23
32	Preprocessed Resistivity Vs. Specific Energy	4-24
33	Preprocessed Resistivity	4-25
34	Preprocessed Voltage and Current	4-26
35	Preprocessed Resistivity Vs. Specific Energy	4-27
36	Preprocessed Resistivity	4-28
37	Preprocessed Voltage and Current	4-30
38	Preprocessed Resistivity Vs. Specific Energy	4-31
39	Preprocessed Resistivity	4-32
40	Preprocessed Resistivity Vs. Specific Energy	4-34

List of Figures

<u>Figure</u>		<u>Page</u>
41	Flow Chart, Initial Signal Processing	A-2
42	Flow Chart, Full Data Processing	A-3
43	Bank Current	B-2
44	Fuse dI/dt , Restrike	B-3
45	Fuse Voltage, Restrike	B-4
46	Fuse Voltage, Air Quench	B-5
47	Bank dI/dt , Air Quench	B-6
48	Fuse Voltage	B-7
49	Bank dI/dt	B-8
50	Bank Current	B-9
51	Fuse Voltage	B-10
52	Bank dI/dt	B-11
53	Bank Current	B-12
54	Fuse Voltage	B-13
55	Bank dI/dt	B-14
56	Bank Current	B-15
57	Preprocessed Resistivity Vs. Specific Energy	C-2
58	Original and Processed Fuse Voltage	C-3
59	Original and Processed Fuse Current	C-4
60	Original Fuse Currents	C-5
61	Original Fuse Voltages	C-6
62	Processed and Calculated Fuse Voltage and Current	C-7
63	Resistivity, Copper Fuse in Air	C-8

List of Figures

<u>Figure</u>		<u>Page</u>
64	Voltage and Current, Copper Fuse in Air	C-9
65	Relative Timing, Voltage, Current, and Resistance	C-10
66	Fuse Energy	C-11
67	Relative Timing, Voltage, Current, and Resistance	C-12

List of Tables

<u>Table</u>		<u>Page</u>
I	Aluminum Fuse Shots	4-2
II	Copper Fuse Shots	4-3

Abstract

The characteristics of electrically exploded aluminum and copper foil fuses are investigated and compared under varying temperature conditions. A 34 to 39 KJ system is used to explode the fuses in room temperature glass beads (sand), sand cooled to approximately -77 C, liquid nitrogen, and deionized water. The temperature of the quench medium is seen to have an effect on fuse behavior with aluminum fuses being more affected.

Two data processing methods are used and are found to produce quite different results. Because of this difference only a qualitative comparison of the behavior of the fuses is given. The first method involved using voltage and current data scalefactored and integrator droop corrected to compute resistivity. The second method used a self consistent solution to the circuit model to recalibrate the voltage and current signals and then compute resistivity.

COMPARISON OF
ALUMINUM AND COPPER FUSE OPENING SWITCHES
UNDER ROOM AND CRYOGENIC TEMPERATURE CONDITIONS

I. INTRODUCTION

The effective use of magnetic energy storage devices requires that the current flowing through the device be interrupted. Exploding foil fuses have proven to be effective opening switches at energies approaching two megajoules. Plasma physics experiments conducted at the Air Force Weapons Laboratory (AFWL) routinely use fuses as opening switches (Ref 1) to transfer energy from inductive stores to inductive loads.

There are several significant advantages in using magnetic storage for high energy plasma physics experiments. The energy density in magnetic storage is 100 to 1000 times greater than that of electrostatic energy storage. This allows a lot of energy to be stored close to the experimental load. Energy transfer to the load can then be expedited due to the reduction of inductance between energy source and load. Figure 1 shows a circuit model of a magnetic energy system. Two switches are used, one for connecting to the load (a closing switch), and one for

interrupting the current through the inductor (an opening switch).

The requirements for a good opening switch include low resistance as the current reaches its maximum level for maximum magnetic energy storage, rapid opening (rapid increase in resistance in the case of fuses) at the desired time, and good hold off of voltages several times the voltage applied to the original system. The exploding foil fuse has been found to possess these attributes and routinely interrupts megamps and holds off several hundred kilovolts (Ref 2). Resistivities of several hundred micro-ohms centimeter are common in the open state. The fuse is also convenient in that a slow energy storage system, such as a capacitor bank, can be used as a prime energy source, the energy transferred to the storage inductor and switched into a load with a voltage multiplication of several times and time compression of the pulse (see the Theory section for details of these phenomena).

The voltage standoff of foil fuses has been significantly improved by the use of quenching materials and mediums surrounding the fuse. Many different kinds of quench materials have been tested and used (Ref 3,4,18,19). To date the use of glass beads (usually referred to as sand in this report) has proven most effective (Ref 4).

It was realized that foil or wire fuses might prove to be an effective switch for inductive energy storage in 1975 and recommendations to begin studies were made at that time (Ref 5). Investigations into the behavior of electrically exploded foil fuses have been going on at the Air Force Weapons Laboratory for some time and this report constitutes a continuation of that study.

Problem and Scope

There are two basic but interrelated problems investigated in this report. One is the investigation of fuse properties and characteristics in varied environments. The second is the investigation of the potential of using fuses as opening switches at energy levels exceeding two megajoules.

The properties and characteristics of fuses were investigated by using an ongoing fuse physics experiment. A 36.25 microfarad capacitive storage system operated at 42-47 kilovolts is the prime energy storage system. Using this system, the effects of different quench mediums and temperatures are tested. Voltage and current data were obtained and the resistive nature of the fuse analyzed. Of special interest was the effect of initial temperature on the early resistivity of the fuse. Experiments to investigate this effect were conducted.

The second problem was a first order investigation into the feasibility of using fuses in energy applications exceeding the presently known two Megajoule level. At the AFWL, a pulse power system used in plasma physics experiments called the SHIVA-STAR has been built. It is capable of storing energies approaching 10 megajoules in a large capacitor bank and uses inductive power conditioning to increase the power delivered to the load. Provisions for fuse opening switches are included in this system. Plans for even higher energy systems exist and the simplicity of fuse opening switches make them an attractive candidate for the opening switch.

The scope of this experiment was limited to the investigation of aluminum and copper fuses in the environments of sand, cryogenically cooled sand, liquid nitrogen, and deionized water. Some variation in fuse geometry was also investigated. The second part of the problem was limited to a first order examination of the effects of increasing the energy of the system driving the fuse. The whole of this report is directed to the equipment and procedures in use at this writing at the Advanced Concepts Branch, Applied Physics Division, Air Force Weapons Laboratory, Kirtland Air Force Base, New Mexico, where the experimentation took place.

Assumptions

The basic assumption made and supported by some theoretical study and past experience (Ref 1) is that the experimental results using a relatively low energy source may be applied directly to the high energy SHIVA-STAR system. The experimental apparatus was specifically designed to have the same order time constant as the larger SHIVA-STAR. The High Energy Applications section of the Theory Chapter provides further information.

General Approach

The experimental approach used was to adopt an aluminum fuse design that was currently undergoing test. This fuse shape was used throughout a series of tests designed to investigate the environmental effects on the fuse. Initially the fuse was tested in a room temperature environment and several experiments were done to obtain a baseline for the fuse. Next, attempts to cool the sand to near liquid nitrogen temperature without introducing the liquid nitrogen into the sand were made and tests were conducted. To further isolate the effects of very cold temperatures, fuses were exploded in liquid nitrogen and in room temperature deionized water, two incompressible liquids differing primarily in temperature. This same series of experiments was then performed with copper fuses. An attempt was made

using the Masionnier cross sectional area (Ref 6) to make the two fuses similar in performance; explosion time and total energy required to vaporize the fuse.

Some additional experiments were performed with copper fuses including multisectional fuses, thicker fuses, and a relatively solid quench. One air environment shot was performed to baseline the air quench. The basic approach was to structure the experiments so as to gain some understanding of the effect of thermal transfer on the fuse performance.

Sequence of Presentation

This report begins with a theory chapter which details several of the more important aspects of foil fuses and their association with the load under consideration. Included in this chapter is a basic analysis of the fuse in higher energy systems than those currently in use. This is one of the problems that was to be addressed in this study. The equipment chapter then describes the experimental apparatus, the instrumentation and the calibration procedures. Included in this chapter is a novel approach to the calibration of data using known circuit parameters. This procedure was developed by the computational physics section at the AFWL and implemented in the analysis of the data. Next comes the results chapter followed by the conclusions

and recommendations chapter. Several recommendations are given for further fuse studies. The Appendices contain flow charts, and much of the data from the many experiments that were performed during the course of this study.

II. THEORY

The theory of fuse operation is very much in a state of development. There is much about the physics of fuse operation that is not understood. Most of the work done in the area of exploding opening foil fuses is predicated on the works of Maisonnier, et al. and DiMarco, et al. (Ref 6,7). This section introduces the basic works of Maisonnier and DiMarco. Next those aspects that are closely related to the work being performed at the Air Force Weapons Laboratory are discussed. Following that is a brief investigation into the effects of the electric field along the length of the fuse as higher energy systems are considered for future plasma physics investigations. Finally a few related works are mentioned to give the reader a feel for the breadth of works in the area of fuse physics and applications.

Basic Fuse Theory

The concept behind electrically exploded foil fuse is very simple. The foil is heated by the current passing through it. Initially this joule heating is small since the foil is in its solid, and most conductive state. As the heating increases over a time frame too short to allow much heat transport to the surrounding medium, enough energy is

delivered to the metal to cause a state change. When the state changes from solid to liquid the resistivity increases; this increases the joule heating hastening the next phase change. As temperature increases, the vapor state is reached explosively and a high resistivity medium results, hence the fuse interrupts the current. The advantages of the fuse are obvious. The early low resistivity allows a capacitive or slow energy source to transfer energy to a magnetic storage device close to the load. When the fuse interrupts the flowing current, energy is transferred to the load with little inductance between the storage device and the load, allowing rapid energy transfer.

Early Fuse Concepts

Maisonnier (Ref 6) proposed the use of foil fuses as a promising candidate for extracting energy from inductive stores. Exploding wires had been used to switch magnetic energy at low levels (Ref 8) so a precedent was in existence. Using the circuit seen in Figure 2 as the basis of the analysis, Maisonnier proposed two conditions for an effective energy transfer using a fuse:

(1) Condition one: The explosion occurs when the stored magnetic energy is at a maximum. This condition exists at time t_0 :

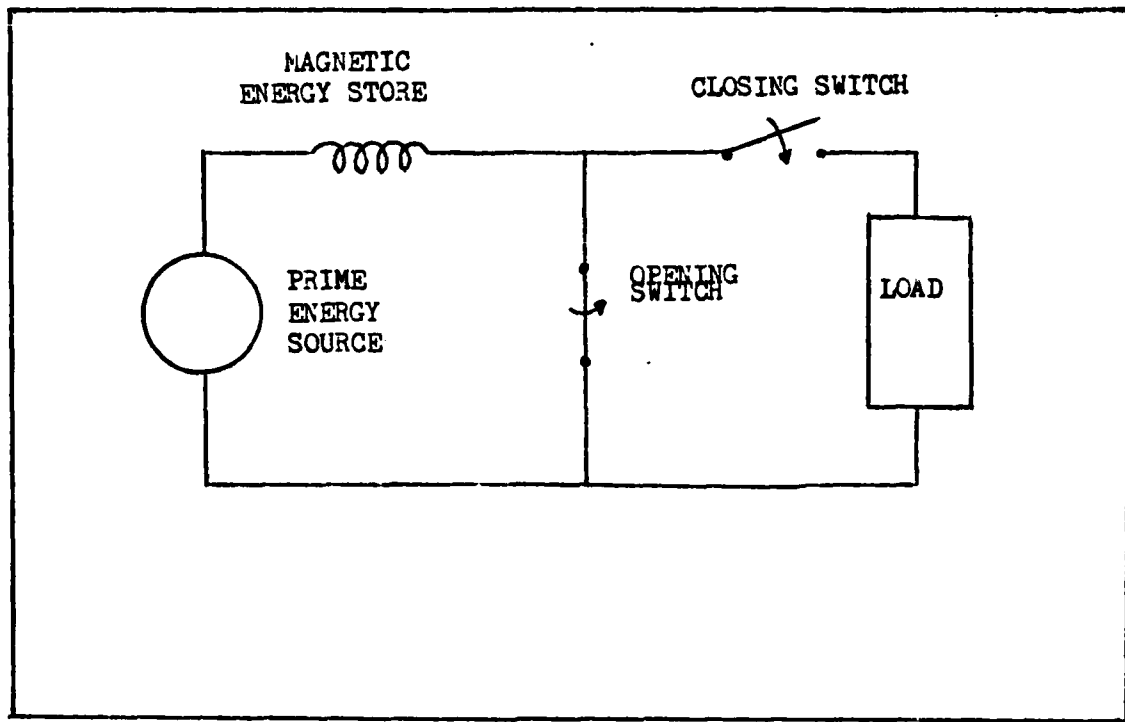


Fig 1. Basic Circuit Model With a Load

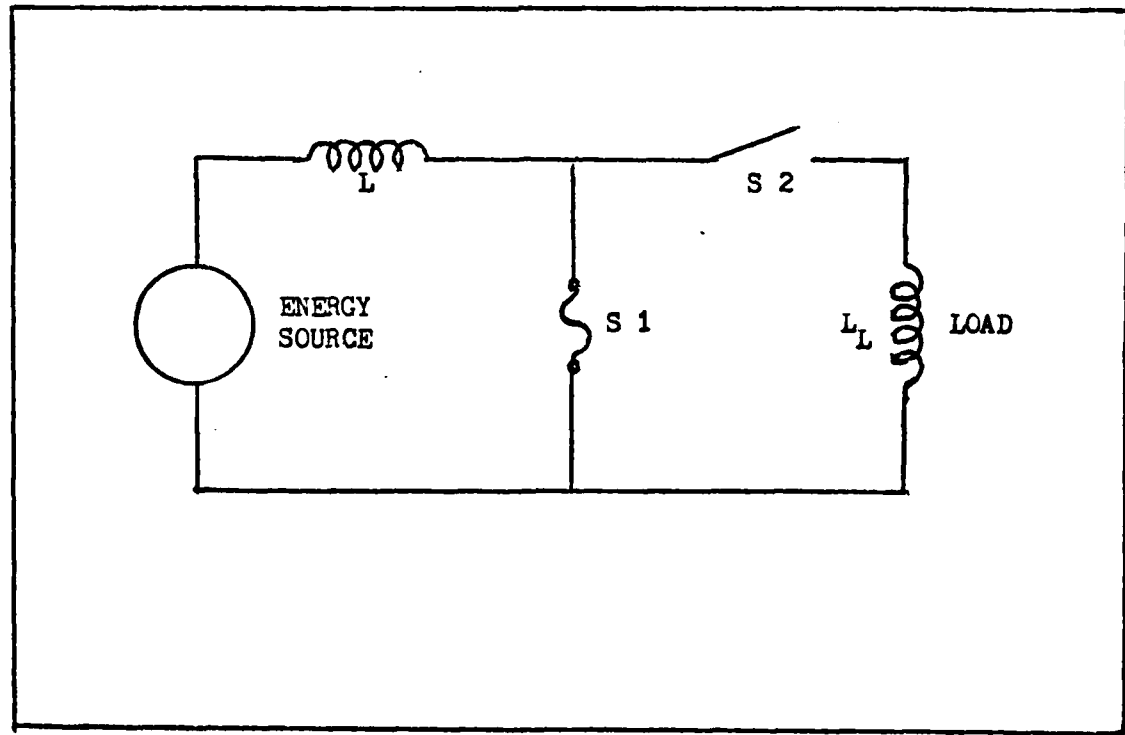


Fig 2. Maisonnier's Circuit Model

$$t_o = \frac{1}{2} \cdot \pi^{1/2} (L/C)^{1/2} \quad (1)$$

(2) Condition two: The energy required to be dissipated in the switch as a result of flux conservation in the circuit is just equal to the energy necessary to vaporize the foil.

Condition one may be met if the joule heating during the first quarter cycle is equal to the energy necessary to bring the fuse to the vaporization point. This implies the following:

$$\rho \cdot \frac{h}{s} I^2 = m \frac{de}{dt} \quad (2)$$

where

ρ is the resistivity of the foil (variable with time)

h is foil height or length

s is foil cross sectional area

I is current in the foil

m is mass of the foil

e is internal energy per unit mass of the foil

The current may be assumed to be a sinusoid
 $I = I(t_o) \sin \omega t$ with $\omega = 1/LC)^{1/2}$ since the fuse resistance has negligible effect on the frequency prior to the explosion. Also the resistivity is a function of

temperature and energy. In principle then resistivity is a function of energy since temperature is a function of energy. Eq(2) is then rewritten

$$\frac{m}{\rho(e)} de = \frac{h}{s} I^2 \sin 2\omega t dt \quad (3)$$

Integrating this equation between time 0 and t_0 and substituting circuit values one arrives at the equation for the cross sectional area of the fuse:

$$s^2 = \frac{W(0)^{3/2}}{V(0) L^{1/2} k a} \quad (4)$$

where

$W(0)$ is initial energy in the system

$V(0)$ is initial charge voltage

L is systems inductance

k is a constant between 1 and 3 that accounts for the adiabatic heating data used to compute a .

a is a nondimensional term defined as:

$$a = \frac{2^{1/2}}{\pi} \gamma \int_{T_1}^{T_2} \frac{1}{\rho} de \quad (5)$$

where γ is the density of the foil and the limits of integration go from the initial temperature, T_1 , to the

vaporization temperature, T_2 (heat of vaporization excluded).

Now that the cross sectional area of the foil has been determined the length of the fuse is determined by the energy that the fuse must absorb. This energy is dependent on the circuit parameters. The reader is referred to the original paper for further information on this topic. Experience has shown that good results are attained with fuses whose cross sectional area is about 70 percent of the Maisonnier criteria with $k = 2$ (Ref 9).

DiMarco and Burkhardt (Ref 7) in a 1970 paper titled "Characteristics of a Magnetic Energy Storage System Using Exploding Foils" expanded on the use of foil fuses. Using the results of Maisonnier, (Ref 6), and the switching techniques employed by Early and Martin (Ref 10), experiments were performed using exploding foils. Operating at 15 kilovolts and 34 kilojoules the characteristics of the fuse with and without a load were examined. Some of the more important aspects of DiMarco's work are presented in the following paragraphs.

In analyzing the basic circuit of Figure 3 we may find an expression for I_2 -dot (the time derivative of I_2):

$$I_2\text{-dot} = \frac{V}{L_2} e^{-\frac{R(t - t_0)}{L_3}} \quad (6)$$

where L_3 is the parallel combination of L_1 and L_2 .

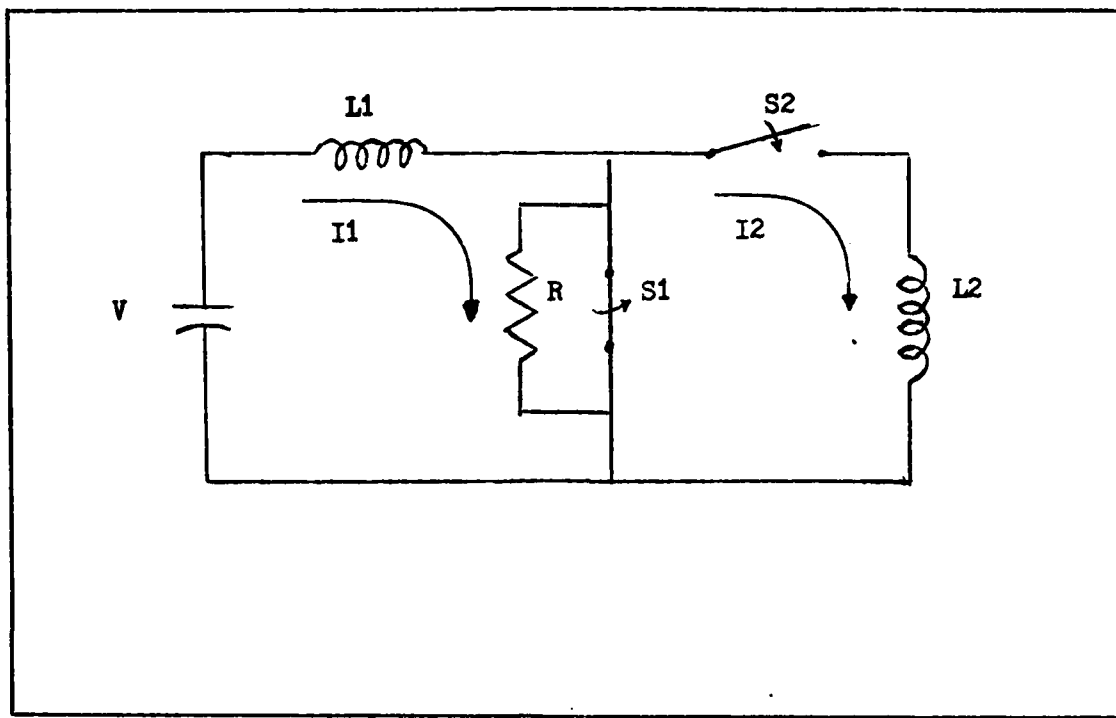


Fig 3. DiMarco's Circuit Model

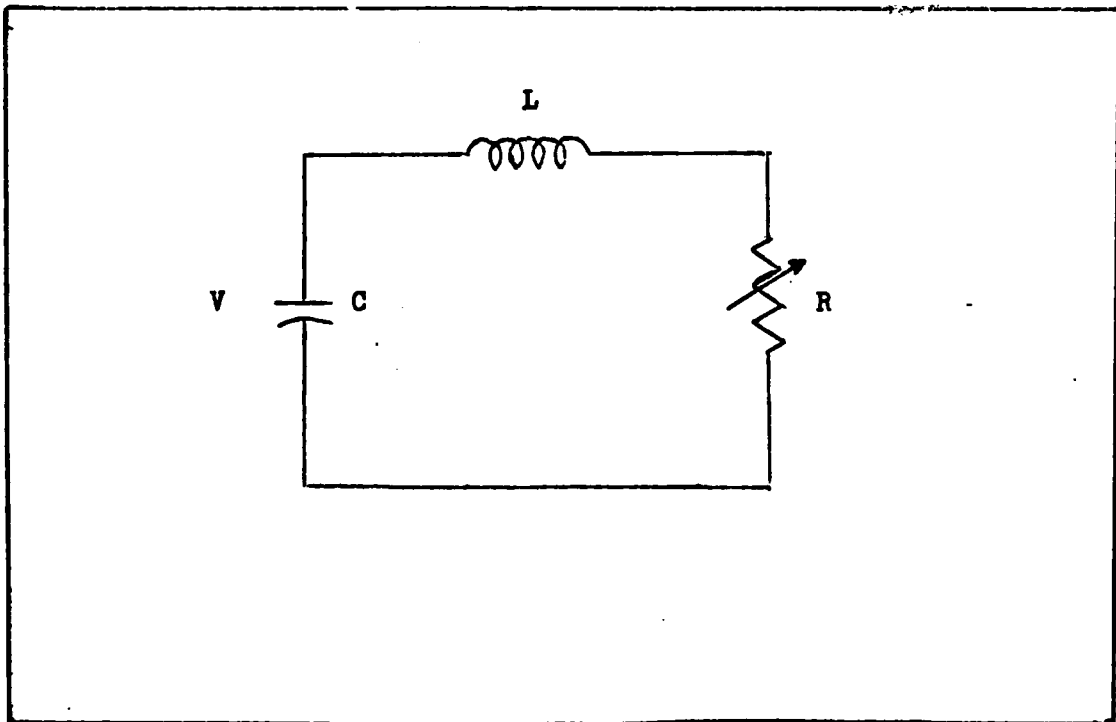


Fig 4. Benford's Circuit Model

From examining Eq(6) one can conclude that, for rapid current transfer into the load, large fuse voltage and small load inductance are desired. It is interesting to note that for maximum energy transfer $L_1 = L_2$ (Ref 6). Additionally the e-folding time for the fuse resistance must be on the same order as the experiment.

DiMarco also examined a range of copper fuses without a load. These fuses varied in cross sectional area, thickness, and assembled geometries. A good fit with the data obtained and Maisonnier's criteria was found using a value of $k=2$. A wide variation of cross section and length was found to give satisfactory performance. In one set of experiments the length was varied between two limits. The first limit was fuse too short, producing restrike with electric fields breaking down along the fuse at about 6 kilovolts per centimeter. The second limit in performance was fuse too long where the energy needed to vaporize the mass of the foil was greater than the energy available.

Voltage Multiplication and Pulse Compression

Two advantages of opening switches and inductive energy storage are the phenomena of voltage multiplication and pulse compression. J. Benford et al. built upon DiMarco's works mentioned above and investigated these concepts (Ref 11).

They also developed some scaling laws for application to different fuse circuits.

Using the circuit model of Figure 4 and characterizing the fuse resistance as a step, the voltage multiplication at the fuse is found to be

$$\frac{V(0)}{V_i} = R(0) f (C/L)^{1/2} \quad (7)$$

where

$V(0)$ is the voltage across the fuse

V_i is the initial voltage of the system

$R(0)$ is the value of the resistance step

C is system capacitance

L is system inductance

f is some fraction of the initial energy of the system

Pulse compression can be related by the energy transfer times. The compression can be found to be related to the voltage multiplication in this idealized case by:

$$\frac{V(0)}{V_i} = \frac{2}{\pi} \frac{t(t)}{t_0} \quad (8)$$

where

$t(t)/t_0$ = Time compression

$t(t) = (\pi/2) (LC)^{1/2}$

$t_0 = L/R(0)$

Therefore, a foil fuse will not only effect a transfer of energy to a load it will also multiply the applied voltage and compress the time in which the energy can be transferred to the load. Both these factors have proven very important in plasma physics experiments currently being conducted at Kirtland Air Force Base (Ref 11).

Extension of Fuses to Higher Energies

Fuses are routinely used to switch up to 1.9 MJ at the Air Force Weapons Laboratory (Ref 2, 12). A question arises as to whether fuses will perform satisfactorily at higher energies. That question is one of the major reasons for this thesis.

In order to investigate the effect of higher energies on fuse performance one must realize there are two ways to increase the energy transferred from the capacitive storage system. The first is to increase the system storage capacitance. The second is to increase the charge voltage on the capacitors. The changing of these two parameters is examined through a first order investigation using Masionnier's criteria for the cross sectional area. The assumption is made that the factor k in Masionnier's area criteria does not change from one energy system to the next. Other assumptions are stated when they are made.

One question about fuse scaling that can be asked is the effect on the electric field along the fuse due to increased energy. Too high electric fields can lead to restrike. The voltage drop along the fuse, is found to be $V_f = RI + L \frac{di}{dt}$. Since the $L \frac{di}{dt}$ portion is negative as the fuse opens and the current decreases it may be neglected for worst case analysis. The voltage across the fuse in terms of the resistivity and the maximum current value is

$$V_f = \frac{\rho h}{s} V(0) (C/L)^{1/2} \quad (9)$$

Substituting for s from Eq(4) yields:

$$E_f = \frac{V_f}{h} = K_1 a^{1/2} \rho / (LC)^{1/4} \quad (10)$$

where $K_1 = 2^{3/4} k^{1/2}$.

Thus the electric field is independent of the applied voltage and only weakly dependent on the period of the device. So one may surmise that if the same time constant is kept for high energy systems then the electric field would present no problems.

Earlier it was noted that a high fuse resistance was desireable to maintain good energy transfer. Therefore, the

effects of increasing energy on the resistance of the fuse will be considered. Using $R = \rho h/s$ and assuming ρ is not changing from case to case we find that, from Eq 4, s is proportional to the applied voltage. If one assumes that the same proportion of available energy is consumed in the fuse then

$$W_f = \xi h s \quad \text{and} \quad W_f = \frac{1}{2} C V^2 \quad (11, 12)$$

where ξ is the energy per unit volume needed to raise the material to vaporization temperature. Substituting the dependence of s on V and equating eq 11 & 12 shows that h is also directly proportional to V . Resistance is, therefore, independent of the applied voltage.

Looking at the resistance from another viewpoint, (the variation of the system capacitance and inductance), leads to another dependence. Following the same procedure as above, it can be shown that the resistance varies with the system capacitance and inductance as

$$R \propto (L/C)^{1/2} \quad (13)$$

From Eq(13) it can be seen that increasing the capacitance to increase energy and decreasing inductance to maintain the same time constant will result in reduced resistance. Looking back at voltage multiplication and time

compression, Eqs(7) and (8), we can see little effect on voltage multiplication or time compression.

In summary it appears that higher energy systems using foil fuses should function properly. If the energy increase could be obtained by increasing voltage then neither the electric field nor the resistance should be affected. Changing the capacitance or inductance changes the resistance adversely as energy is increased using increased capacitance but has no affect on the electric field if the time constant does not change.

Thermal Considerations

The following discussion applies directly to the SHIVA-STAR system. The information was obtained in an interview with Maj W. McCullough (Ref 13) and reflects the methodology used in projecting fuse interaction and design with an imploding inductive load. In order for the reader to understand the thermal arguments given it is necessary for the reader to be given a background dealing with the constraints of the fuse and load used on the SHIVA-STAR.

Background: In general there are two desireable aspects that a fuse should posess. One is a large resistance change and the other is a small time in which this resistance change takes place or a large dR/dt . These parameters are

further constrained by the desire to transfer maximum kinetic energy to the load. Maisonnier's first assumption does not fit this application since maximum energy transfer does not occur at maximum current through the inductive store due to the nature of the load. The load inductance varies with time so the maximum energy transfer function also varies with time.

Along with the need to transfer maximum kinetic energy are other constraints. These are to provide energy over a load implosion time on the order of 300 nanoseconds, to give the load a final velocity of 40 to 45 centimeters per microsecond, and to provide load stability.

In order to meet the above constraints the designer has four parameters that can be adjusted. They are the fuse cross sectional area, the fuse length, the load mass, and the load initial radius (the load is cylindrical). These parameters are highly coupled so they are solved iteratively on a computer using an optimizing routine developed at the Air Force Weapons Laboratory.

Effects of cooling the fuse: In general the most direct and beneficial effects of cooling the fuse are to reduce the cross sectional area and to increase the length. These changes lead to increased final resistance and dR/dt improving both desirable characteristics of the fuse. If

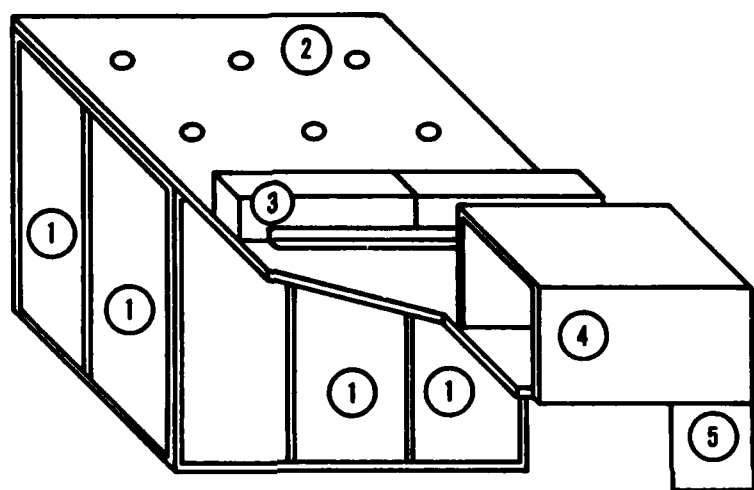
the fuse is further provided with a high thermal conductivity environment the cross sectional area can be further reduced and the length correspondingly increased. This benefit arises from the removal of heat from the fuse keeping the temperature dependent resistivity low for a longer time. Simulations indicate that up to 20 percent of the total energy delivered to the fuse before the load is connected can be absorbed in the surrounding heat sink. These improvements in fuse behavior may be significant contributions to the performance of the SHIVA-STAR system.

III. EQUIPMENT

The equipment used in this experiment consisted of an energy storage medium (capacitors) connected through triggerable switches and a transmission line to an inductive energy store and then the fuse. Figure 5 is a representation of the experimental device. Current and voltage measurements were recorded on a set of transient digitizers. The digitized data sets were then processed and fuse resistance, fuse resistivity, and other related data were generated.

Capacitor Storage Bank

The prime energy storage medium consisted of six high capacity, high energy density Maxwell #32184 capacitors connected in parallel. Each capacitor was nominally 6 microfarads with a 60 kilovolt operating voltage and 2 nanohenries intrinsic inductance. The system capacitance was measured with a capacitance bridge by a previous researcher and found to be 36.25 microfarads. This figure includes all stray capacitance and the capacitance of the transmission line that is charged before bank discharge. Attempts to measure the capacitance with an available bridge proved unsuccessful, so the previously



- ① STORAGE CAPACITORS
- ② TRANSMISSION LINE
- ③ TRIGGERABLE RAIL GAP SWITCHES
- ④ PRIMARY INDUCTIVE STORE
- ⑤ FUSE MOUNTING FIXTURE

Fig 5. Experimental Device

obtained figure was used throughout this study. Although two capacitors were changed during the course of this study, short circuit tests indicated no change in the period of oscillation; hence it was concluded that there was no change in capacitance since the inductance of the system was fixed.

Inductive Store

The primary inductive store consisted of 1/2 inch thick aluminum sheet. Figure 10 is an extended drawing of the store. The system inductance was determined by short circuit test (explained in further detail later in this report) to be approximately 300 nanohenries.

Closing Switches

The closing switches used were pressurized triggered rail gap switches of a type in common use at the AFWL. A pair of switches was connected to a pulse triggering device which is in turn connected to the master trigger. The switches were pressurized to between 40 and 53 psig depending upon the charge voltage. The gas used to pressurize the switches was a mixture of 17 1/2 percent sulfurhexafluoride (SF₆) and 82 1/2 percent argon.

Triggering

Triggering of the system was accomplished with a master time delay signal generator. The timing arrangement is shown in Figure 6. A delayed signal was sent to the trigger pulse generator and a zero prompt signal was sent to the instrumentation system. The delay used was 0.1 microseconds for fuse experiments and 10 microseconds for short circuit tests.

Transmission Line

A power transmission line consisting of 1/2 inch thick aluminum sheets separated by 12 sheets of 5 mil mylar was used to connect the components of the experiment. This transmission line system was similar to other transmission line arrangements used within the AFWL.

Fuse Fixture, Fuse Mounting

The fuses were attached to the inductive store by a fixture as indicated in Figure 5. Except for the initial series of aluminum fuses the general fuse geometry shown in Figure 7 was used.

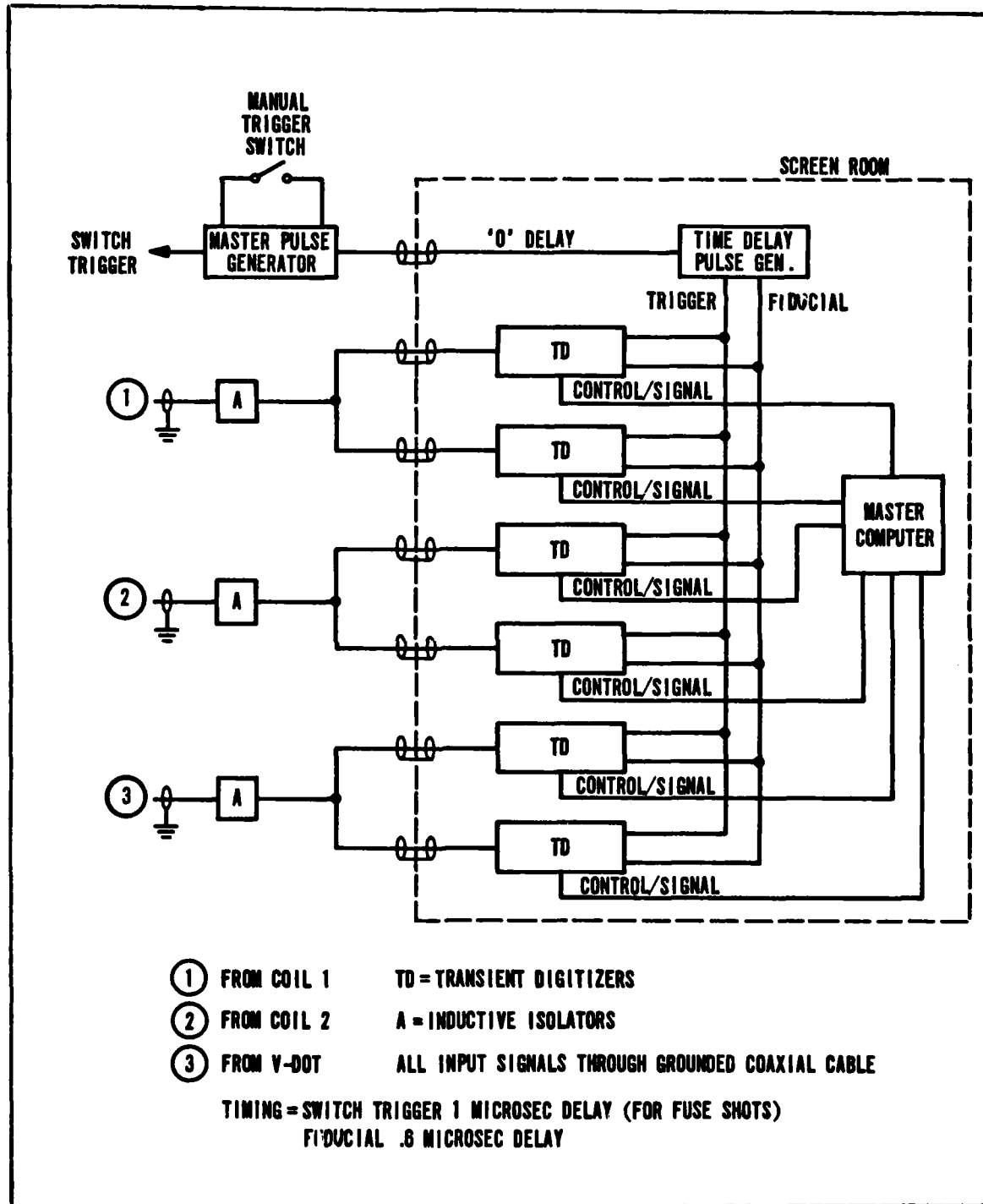
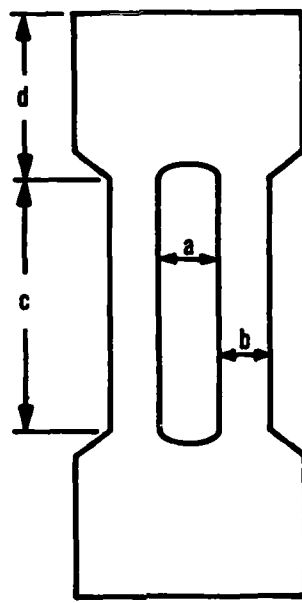


Fig 6. Instrumentation Arrangement



a = SEPARATION BETWEEN STRIPS
b = WIDTH OF FUSE STRIP
c = LENGTH OF FUSE
**d = LONG ENOUGH TO ALLOW EASY
FUSE MOUNTING**

Fig 7. General Fuse Geometry

Three basic mounting procedures were used. These were for fuses in sand (glass beads) at room temperature, fuses in sand cooled to cryogenic temperatures, and fuses in a liquid bath. For the first case an envelope of 5 mil mylar was folded to make an enclosure for the fuse and the sand. Sand was poured into the envelope so that at least one millimeter of sand surrounded the fuse metal. Figure 8 shows how the fuse was mounted on the fuse fixture. In the second case the fuse was packaged as just described but a styrofoam chest (see Figure 9) was placed around the fuse package. Liquid nitrogen was placed in the chest and the fuse and sand cooled. For the fuse in the liquid bath no envelope was used. The fuse was mounted on the inside of the mylar separator of the chest, and the liquid bath, either deionized water or liquid nitrogen, was poured into the container in direct contact with the fuse. A reasonable effort was made to avoid kinks in the fuse especially at the lower bend in order to reduce localized heating due to field distortion. Kinks were a problem because the fuse package, being made of rather stiff mylar, tended to bend sharply.

A sheet of 1/8 inch thick lexan was inserted between the fuse plates. The lexan was approximately four feet by three feet, a size found to be large enough to prevent tracking around the fuse mounting plates. Around the lexan was wrapped 5 layers of 5 mill mylar which increased the total dielectric breakdown strength to prevent punchthrough.

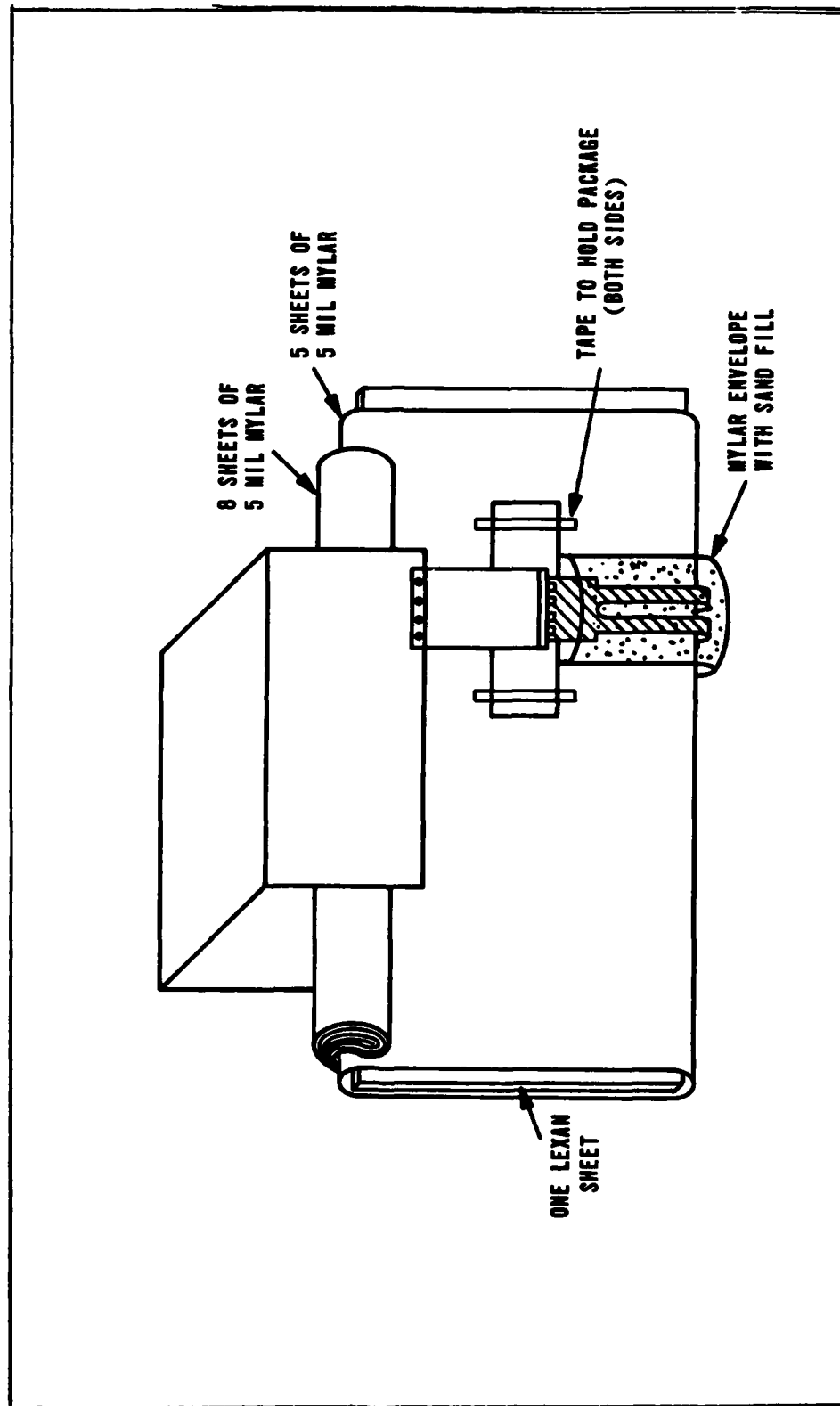


Fig 8. Fuse Mounting, Sand Quench

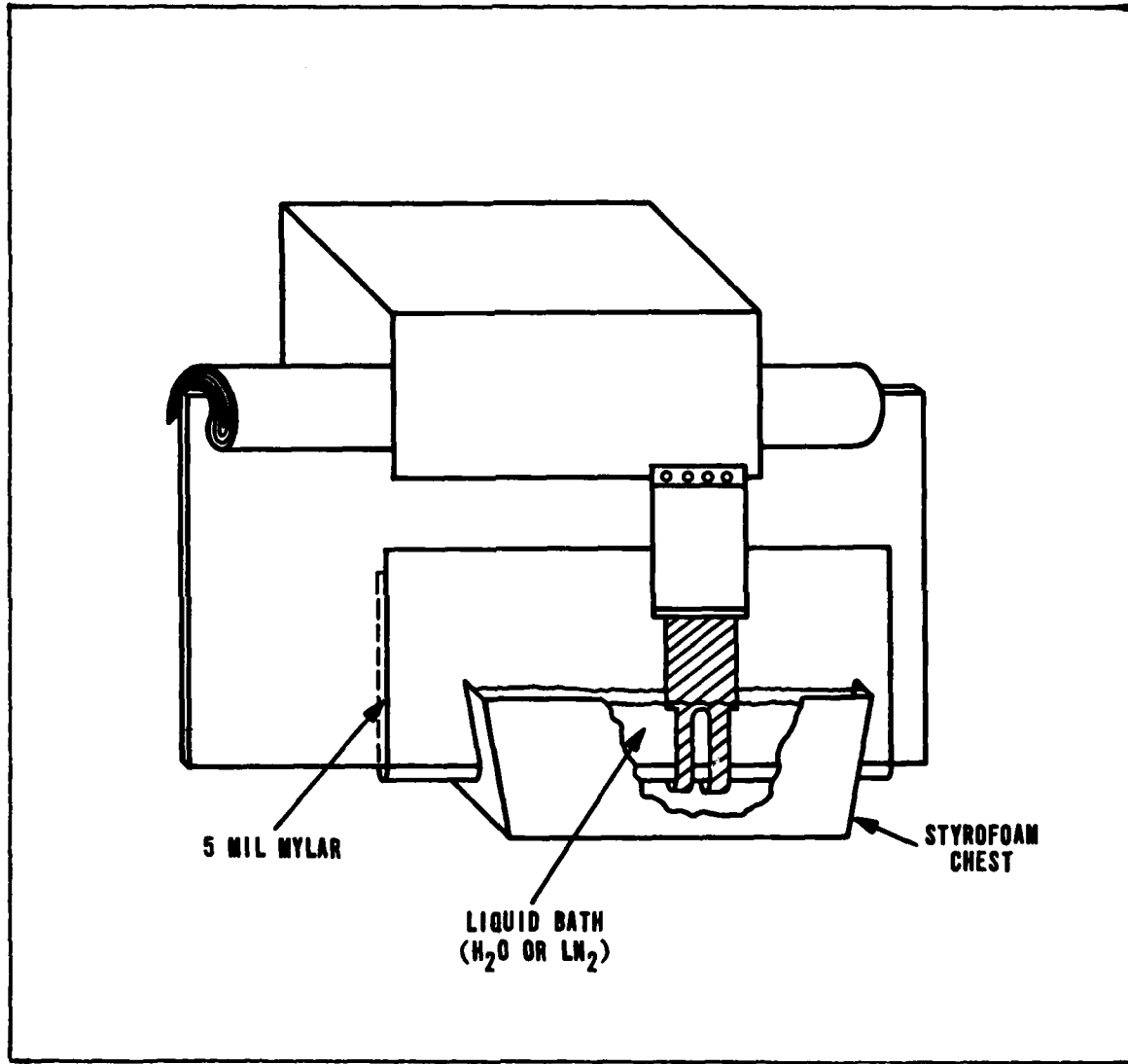


Fig 9. Cold Soaking Device

Above the lexan sheet 8 layers of 5 mil mylar were inserted as indicated in Figure 8 to prevent flashover from the fuse mounting assembly to the inductive store.

Current and Voltage Sensors

Three sensors were used to collect the current and voltage information. Two Rogowski coils were used to measure the bank current and the fuse current (actually the derivative of the current is measured by the coil). A V-dot sensor was used to acquire the voltage information. Figure 10 shows where the sensors were mounted.

The bank coil was laid across the conductor instead of encircling the conductor as had been done on other fuse experiments (Ref 14). This was done to keep the coil from being too long to easily manufacture. The fuse coil was initially only laid across the portion of the transmission line immediately adjacent to the fuse mounting fixture. This procedure proved to be unsatisfactory and the coil was rerouted to encircle the conductor going into the fuse fixture. Since there was no load all the current passed through both the bank area and the fuse area. The use of the two current sensors was redundant and provided a cross-check and a backup. Future experiments anticipate the inclusion of a load in which the two current measurements will be necessary to analyze the experiment.

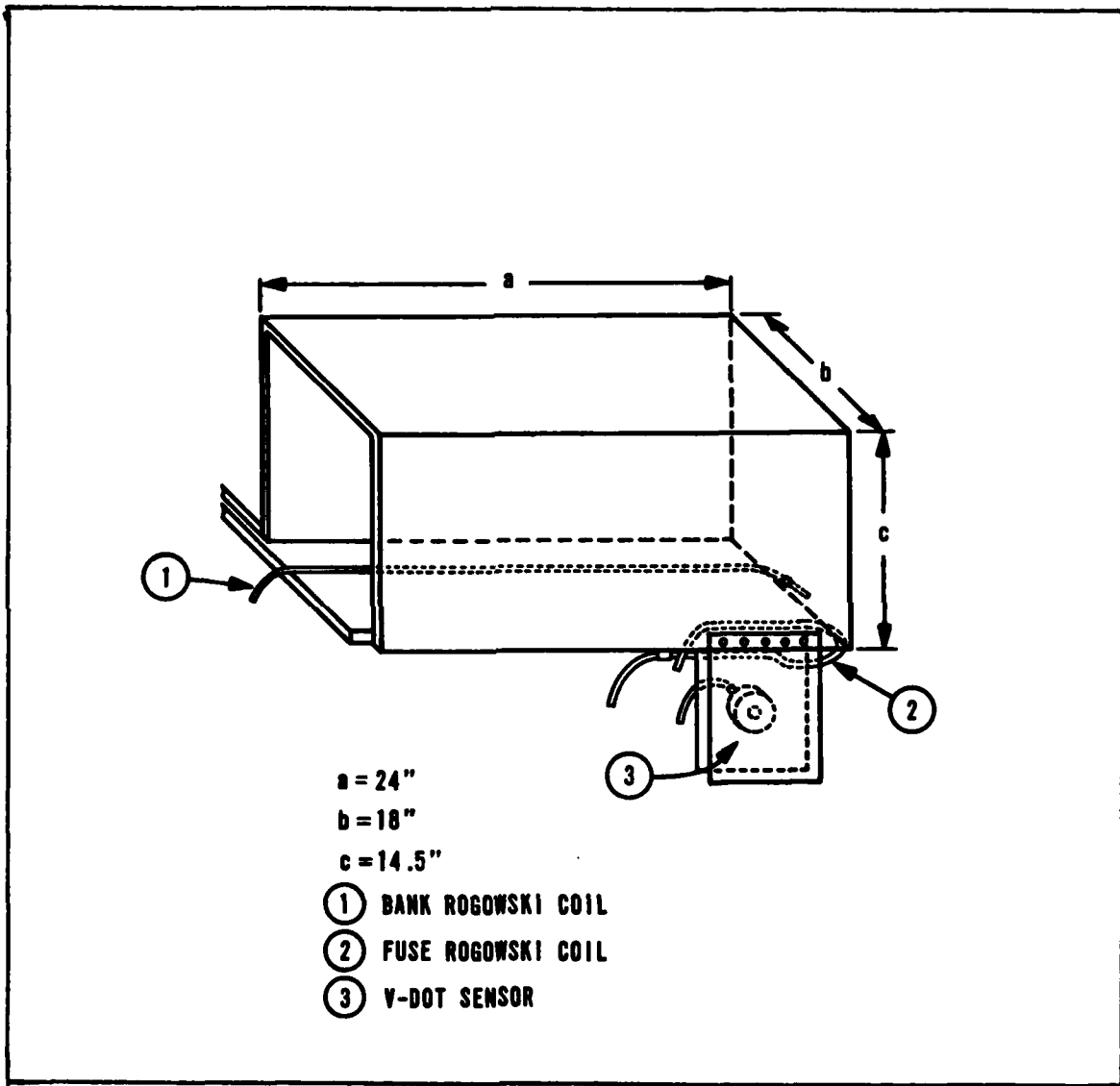


Fig 10. Sensor Mounting and Location

The V-dot sensor was mounted on one side of the fuse mounting fixture. In this location it sensed not only the fuse electric field but the field generated by the fuse mounting fixture inductance. This effect was accounted for in the analysis of the data. V-dot sensors have been successfully used for measuring rapidly changing voltages (Ref 15).

Signal Recorders

Transient digitizers were used to record the sensor data. Both Tektronix R7912 and 7912AD units were used. These units were controlled by a compatible Tektronix computer system under the program control of data acquisition and processing programs written by R. L. Henderson (see Appendix A). A typical instrumentation and timing setup is shown in Figure 6. System calibration was performed as recommended by the manufacturered by personnel assigned to the laboratory. The transient digitizers were located in a instrumentation screen room more than 100 feet away from the experimental site. Signals were transmitted to the screen room over identical runs of RG214 coaxial cable.

Initial data processing was performed on the Tektronix system. This processing included data formating for further analysis on a larger computer system and correction of the droop introduced when passive integrators were used to

obtain currents and voltages from the derivative sensors. The droop correction was accomplished using the relationship

$$\text{True Signal} = \text{Measured Signal} + \text{Droop Correction}$$

Droop correction is defined as the inverse of the integrator time constant times the integration over the time of observance with respect to time of the measured signal.

The passive integrators used were coaxial integrators built and calibrated by laboratory personnel. Their coaxial feature improved their frequency response over more common passive integrators (Ref 16). Average time constants were on the order of 22 microseconds.

Final signal processing was accomplished by Lt Steve Payne, a computational physicist assigned to the section where the experiment was performed. The program used for this analysis is flow charted in Appendix A and is discussed in the Final Calibrations section of this report.

Calibration

Initial system calibration was accomplished using a short circuit test where the fuse was replaced by a shorting bar and a ringing discharge was obtained when the capacitor bank was fired. The resulting sinusoid was recorded and

analyzed. A program written by Capt C. L. Starke and modified by the writer was run on the data (see Appendix A). Figure 11 shows typical sinusoidal data taken from the I-dot signals of the Rogowski coils.

The principle behind the calibration procedure is based on simple circuit analysis of a much underdamped RLC circuit. The current is found to be

$$I(t) = V (C/L)^{1/2} e^{-\frac{R}{2L} t} \sin \omega t \quad (14)$$

where

$\omega = (1/(LC))^{1/2}$ (assumes negligible resistance)

C is systems capacitance

L is systems inductance

V is charged voltage of the capacitor

R is systems resistance

Looking at the derivative of this current and only evaluating it at relative maximum and minimum points, ie. where it touches the exponential envelope, I-dot is found to be:

$$I\text{-dot} = \frac{V}{L} e^{-\frac{R}{2L} t} \quad (15)$$

RAW DATA

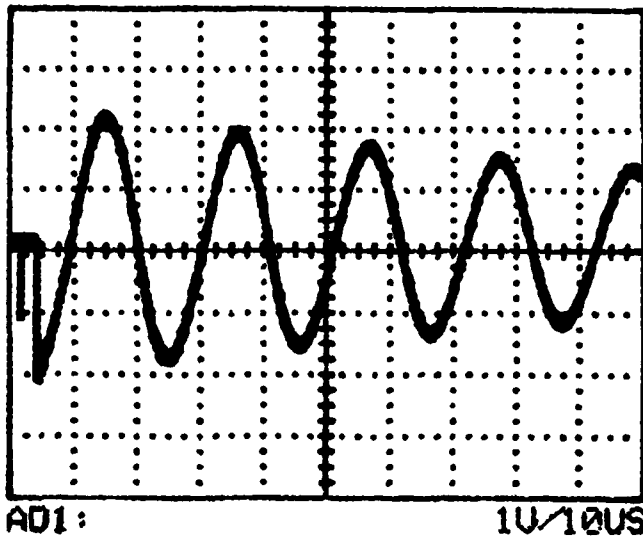


Fig 11. Short Circuit I-Dot Coil Signal

DATA FOR WAVEFORM
 THE VOLTAGE READING AT T=0 IS: 1
 THE COEFFICIENT OF DETERMINATION IS: 47. 0287
 THE NUMBER OF POINTS USED IS: .998413
 8

PERIOD < T > IS: 2. 08048E-05
 LC= 1. 09639E-11

BANK CAPACITANCE? 3. 02453E-07
 ?36. 25E-6

L= ATTENUATION/ MULTIPLIERS OF SHOT.DAT ?
 ?1

BANK CHARGE VOLTAGE
 ?32500

ROGOWSKI COIL CALIBRATION CONST IS: 2. 28468E+09
 THE SYSTEM RESISTANCE IS : 2. 41669E-09
 3 OHMS

Fig 13, Typical Calibration Output

WAVEFORM 1
DATA FROM SHORT U
SHOW FIT TO DATA? WAIT FOR ? THEN (Y/N)

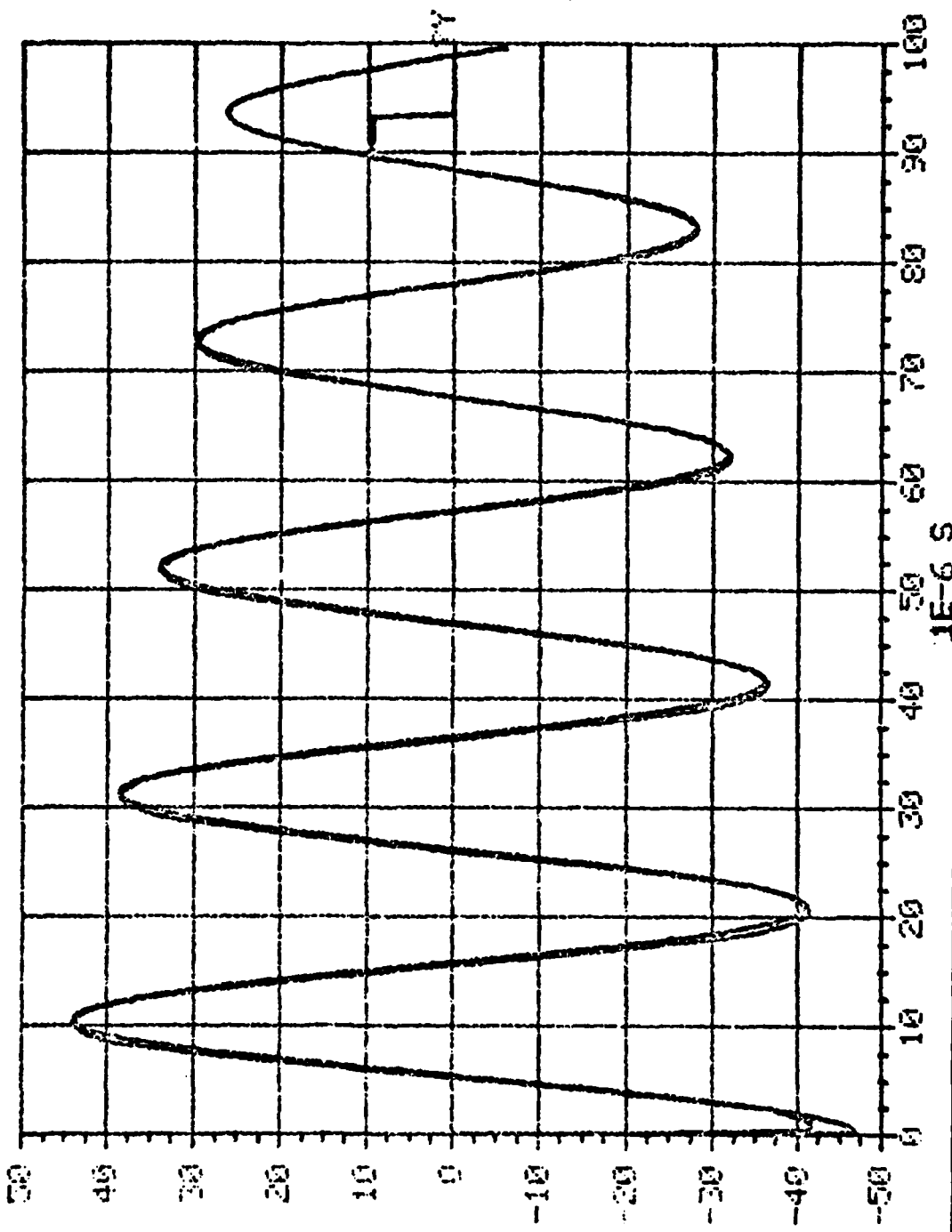


Fig 12. Calculated Signal Overlay of Measured Signal

A least squares fit is made using the natural logarithms of the relative maximum and minimum values of the I-dot signal. The initial charge voltage, $V(0)$ is known and the systems inductance is found from measuring the period. Knowing the capacitance and the period one calculates the inductance and uses the least squares data evaluated at $t=0$ to find the calibration constant. As a visual confirmation, the measured signal and a signal trace generated from the calculated values are overlaid in Figure 12. System resistance then can be calculated by evaluating the function at a maximum or minimum knowing the time of this occurrence and the value of the function. This resistance calculation gives a small figure and verifies the assumption of negligible resistance. Figure 13 shows typical calibration routine output.

Voltage probe calibration can be accomplished in one or more ways. The method used here was performed in tests done by previous experimenters using this system. Voltage readings were taken using both the V-dot probe and a resistive divider. The ratio of the integrated V-dot signal and the better known voltage divider signal divided by the integrator time constant provided the desired calibration constant. Another method of calibrating the system is described in Ref 5.

These calibrations provided basic system measurements and are used in basic resistance calculations found in Appendix C. Final calibrations are described in detail in the following paragraphs.

Final Calibrations

The final system calibration and data processing was performed by the computational physics section. The procedure is described below and a flowchart including this procedure and the final data processing is included in Appendix A.

The procedure used is predicated on applying the most well known parameters of the circuit and of the measurement process. These parameters are time, system inductance without the fuse, system capacitance, and charge voltage. The fuse voltage provides the information needed to calculate the fuse inductance. The characteristic step on the voltage waveform is taken to be the result of the inductive voltage division at time $t=0+$. If this is true then the fuse inductance is

$$L_f = \frac{V_f L_s}{V - V_f} \quad (16)$$

where V and V_f are the applied voltage and fuse voltage and L_s is the systems inductance.

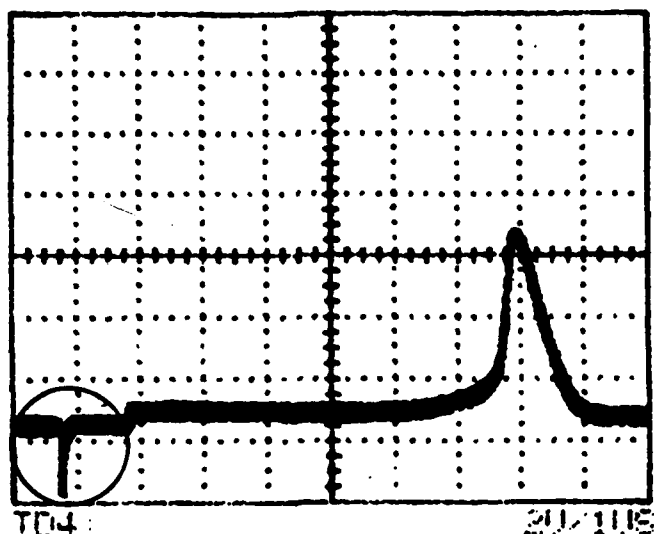
Since the fuse inductance is usually only a fraction of the systems inductance, the error in fuse voltage calibration is minimized in terms of total systems calibration.

The next step is to calculate the total systems inductance, L_t , as the sum of L_s and L_f . Knowing the capacitance and inductance the ideal systems response excluding the fuse resistance is a sinusoid. This current sinusoid is generated from Eq (14) with the resistance being set equal to zero.

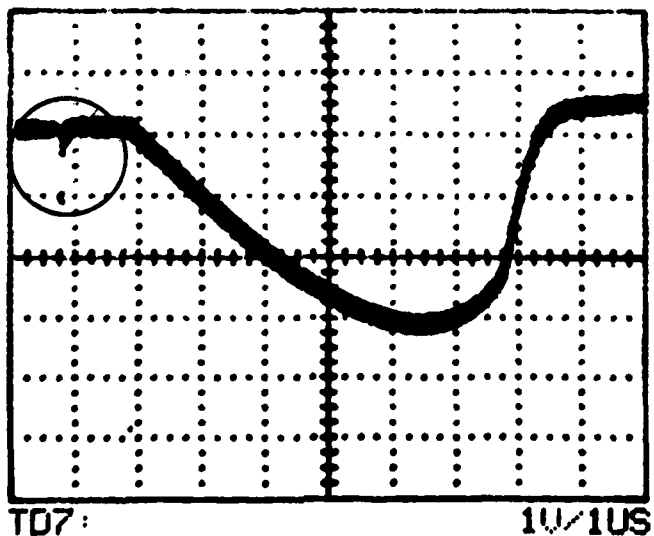
The measured current is fit via a scale factor to the ideal response for the initial portion of the curve. The measured current is adjusted to fit the generated curve and this is the basis for the new calibration of the current. Using the adjusted current value the total systems inductance is recalculated using the $t=0+$ value of the slope of the ideal curve. From this the total systems inductance is found to be

$$L_t = \frac{V}{dI/dt} \quad (17)$$

Using this value of L_t and knowing L_s , L_f is recomputed and the value of the voltage step is found. The new value



Raw Voltage Signal



Raw Current Signal

Fig 14. Typical Raw Voltage and Current Data
(Fiducial is Circled)

for the voltage step is used to recompute L_f and the system parameters are recomputed until the values agree within some tolerance specified by the programmer. Resistance data is then generated and a circuit model is solved using the resistance data as a look up table. New response curves are generated and energy balance is observed. The system is iterated until the measured and calculated values are self consistent with the known circuit parameters.

Time Correlation

Since the purpose of making the voltage and current measurements is to find the ratio of the two, the resistance, the relative timing of the signals is very important. Two methods for time correlation were used. In processing the basic data a fiducial was inserted into the signal. This fiducial can be noted on the raw data in Figure 14. The fiducial is a common time point for all the recorded signals.

A second method is used in the computer processing of the data. Both the voltage and current signals have easily determined starting points. The current zero is found by fitting an ideal response to the measured signal and then noting the zero crossing. The voltage zero is found by the characteristic step that is due to inductive voltage dividing as is shown in Figure 15. These two points provide

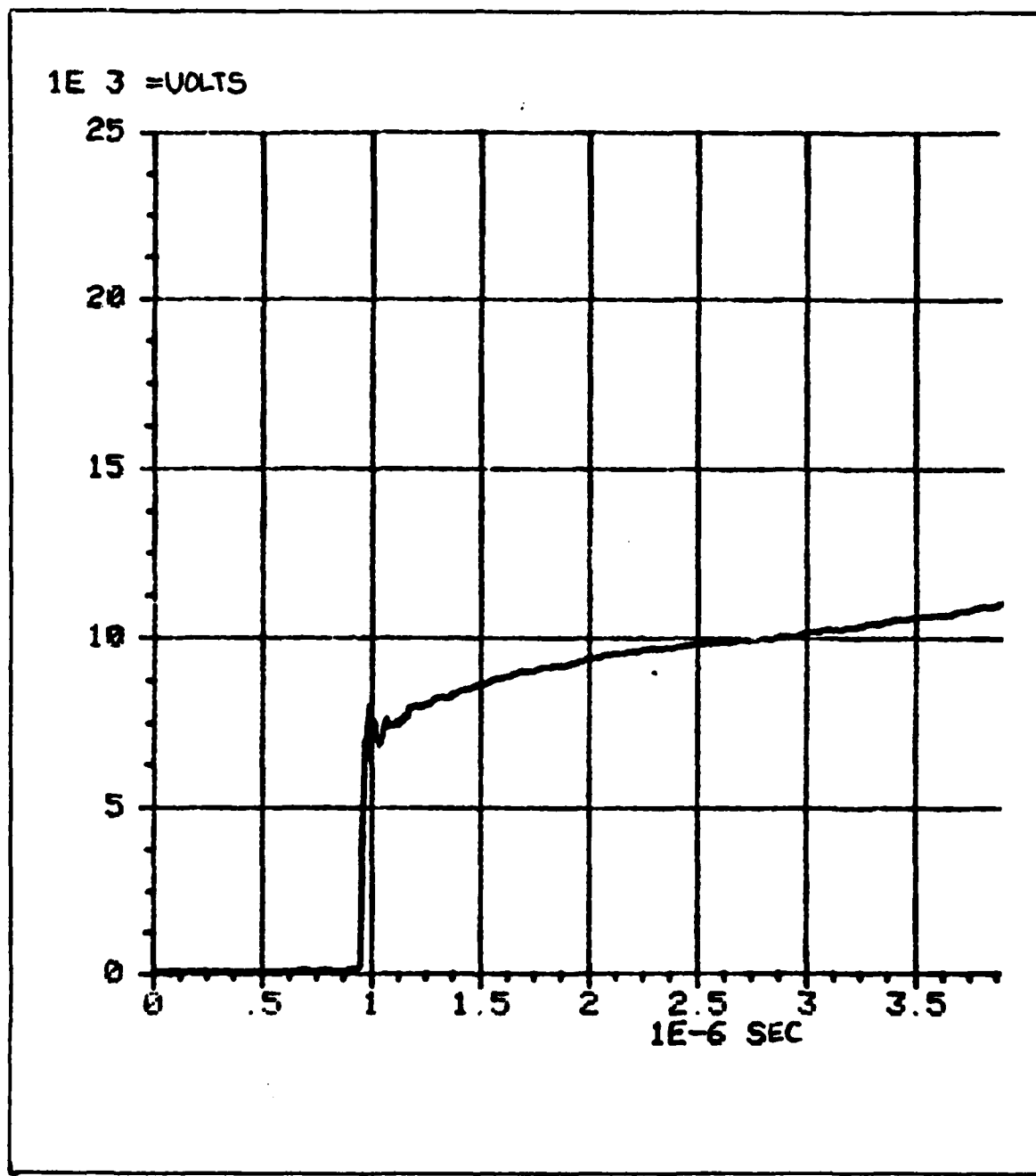


Fig 15. Characteristic Voltage Step On Fuse Signal

the time correlation used to determine the resistive values. Backward processing of the resistive data into the circuit model shows good time correlation using this method (Ref 17).

IV RESULTS

This chapter contains the results of many of the experiments listed in Tables I and II. The chapter begins with a discussion of the various data processing techniques applied to the experimental data and attempts to point out some critical drawbacks associated with using the preprocessed data. Following this section are five sections which deal with the experiments directly. These sections are grouped as fuses in room temperature sand, fuses in cold sand, fuses in liquid nitrogen, fuses in deionized water, and other copper fuse configurations.

Data Processing

The results are displayed in graphical form using the plots of the current and voltage vs. time, resistivity vs. time, and resistivity vs. specific energy. Specific energy is defined as:

$$\text{Specific Energy} = \frac{1}{\gamma} \int_0^t \rho(t') J^2(t') dt' \quad (18)$$

where

$$J = I/S$$

The use of specific energy is common in the fuse literature; however, there are problems in data interpretation. The specific energy increases most near the

Table I
Aluminum Fuse Shots

THIS FILE CONTAINS THE LIST OF SHOTS PERFORMED IN CHRONOLOGICAL ORDER ALUMINUM FUSES				
DATE	SHOT NAME	VOLTAGE	SIZE	REMARKS
1 30/6	Al in sand	47kv	8x44	
2 2/7	Al in sand	47kv	8x44	Flashover at inductive store
3 15/7	Al in sand	47kv	8x44	Flashover at inductive store Rogowski coil at fuse rerouted
4 16/7	Al in sand	47kv	8x44	Restrike
5 26/7	Al in cold sand	>47	8x44	Cold soaked in LN2 for 45 min.
6 27/7	Al in cold sand	>47kv	8x44	Cold soaked for about 30 min evidence of flashover
7 28/7	Al in LN2 bath	**	8x44	Prefire at about 40kv
8 29/7	Al in LN2 bath	**	8x44	Prefire at about 35kv data lost
9 30/7	Fuse inductance determination	**	8x44	Prefire at about 25kv, 10mill fuse shape
10 3/8	Al in LN2 bath	47kv	8x44	Difficulty in maintaining LN2 level due to excessive leaks
11 5/8	Al in sand	42kv	8x44	Charge voltage reduced to try to avoid restrike
12 6/8	Al in H2O bath	47kv	8x44	
13 13/8	Al in Sand	42kv	8x44	
14 13/9	Al in Sand	47kv	8x44	
15 13/9	Al in Sand	42kv	8x44	
16 14/9	Al in Sand	42kv	8x44	

Table II
Copper Fuse Shots

COPPER FUSE SHOTS IN CHRONOLOGICAL ORDER				
DATE	SHOT NAME	VOLTAGE	SIZE	REMARKS
1 9/8	SAND	42KV	5X20	RAPID RESTRIKE DUE TO INSUFFICIENT LENGTH OF FUSE
2 9/8	SAND	42KV	5X40	
3 10/8	SAND	42KV	5X40	FLASHOVER
4 10/8	SAND	42KV	5X40	ALL DATA LOST DUE TO COMPUTER DISK MALFUNCTION
5 11/8	SAND	42KV	6X40	CROSS SECTIONAL AREA INCREASED FOR LATER FIRING TIME
6 11/8	COLD SAND	42KV	5.5X40	COLD SOAKED SAND FOR APPROXIMATELY 25 MINUTES DUE TO LN2 LEAKING
7 11/8	SAND	42KV	5.5X40	
8 11/8	SAND	42KV	6X40	SHOT #2
9 12/8	COLD SAND	47KV	5.5X40	COLD SOAKED FOR ABOUT 30 MINUTES
10 12/8	SAND (3 MILL CU)	42KV	1.84X40	FUSE SURFACE AREA REDUCED BY ABOUT ONE THIRD
11 13/8	LN2 BATH	47KV	5.5X40	
12 13/8	SAND (3 MILL CU)	47KV	1.84X40	FUSE SURFACE AREA REDUCED
13 16/8	SAND/WATER FROZEN	47KV	5.5X40	SAND AND WATER MIXTURE FROZEN WITH LN2
14 16/8	SAND (*12)	47KV	5.5X40	PREVIOUS SHOTS INADVERTANTLY DONE WITH #8 BEADS
15 17/8	SAND (4 CU STRIPS)	47KV	5.2X40	FOUR STRIPS OF CU FOIL USED TO EXAMINE EFFECTS OF INCREASED SURFACE AREA
16 19/8	LN2 BATH	47KV	5.5X40	
17 19/8	AIR	47KV	5.5X40	BASELINE SHOT FOR EFFECTS OF QUENCHING ENVIRONMENT
18 15/9	H2O BATH	47KV	5.5X40	VOLTAGE AFTER PEAK LOST

time when the fuse begins to open. Therefore the early part of the fuse behavior is highly compressed and is more or less lost in the noise. This drawback is further compounded by the potential errors found in the preprocessed data used in many of the experiments.

As described in Chapter III, the data was initially processed on the Tektronix data acquisition system. The output of this processing is referred to as preprocessed data. The final processing as described in the final calibrations section of Chapter II was accomplished on a PDP 11/70. Due to variations in sensor calibration, fuse inductance, and other changes from shot to shot, the final processing has proved to be essential to analyze the results. Unfortunately due to the large amount of data acquired during the study, not all of it could be fully processed in time for this thesis.

Figure 16 shows a comparison of computed and scale factor corrected curves. These corrected curves are used in the first part of the fuses in room temperature and found in the next section. Only one set of data was thus processed due to the extreme time in developing and applying this process.

Except for the first set of shots already mentioned, the preprocessed data was used to generate the curves displayed. The reader is cautioned to take this into account when analyzing the results of these experiments.

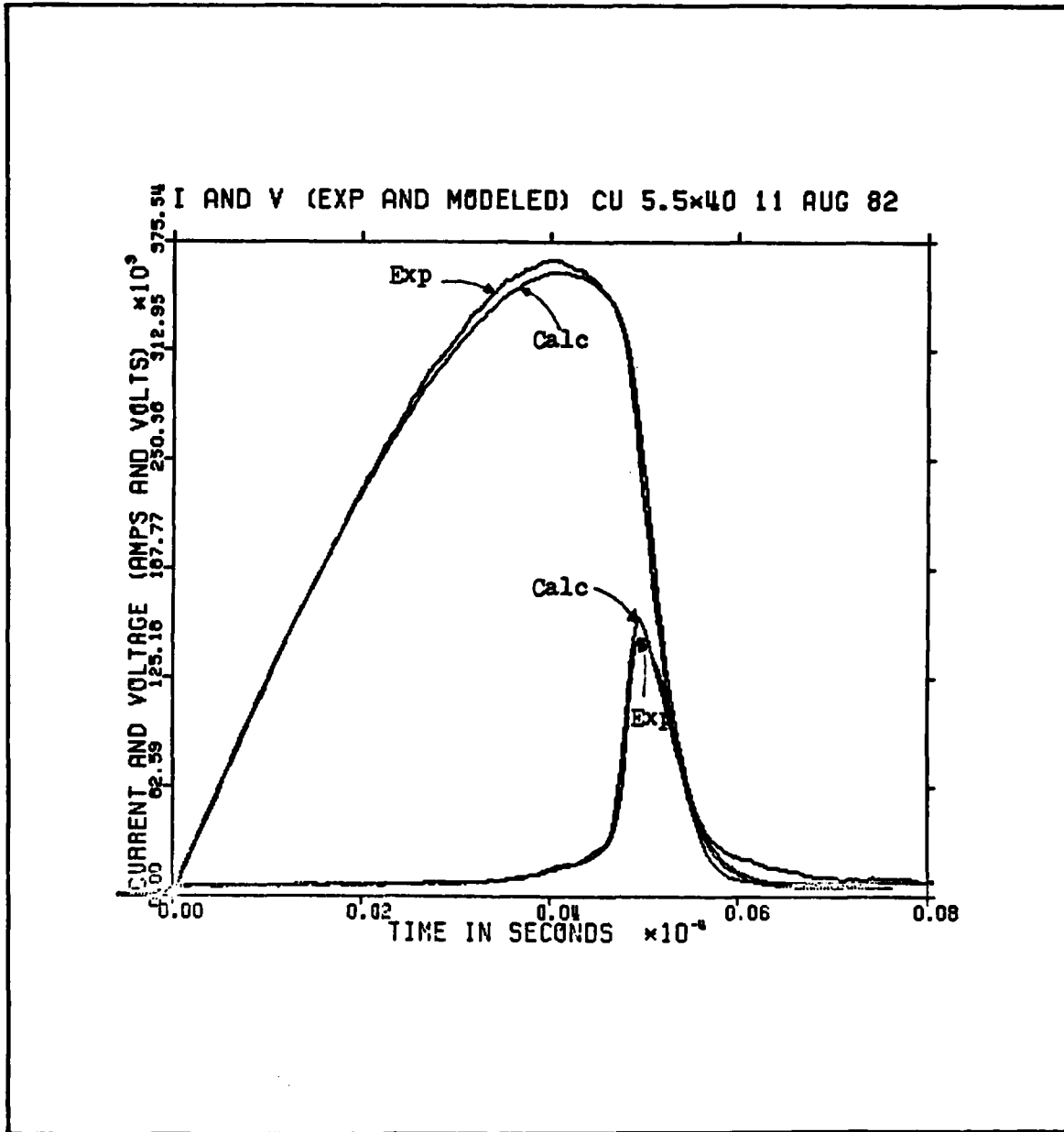


Fig 16. Experimental and Computed Voltage and Current

Fuses in Sand at Room Temperature

This series of experiments was obtained using a sand quench at room temperature. Shots were done at 42 and 47 KV. The 42 KV shots for both the copper fuse and aluminum fuse were fully processed as previously described. The measurements for the aluminum fuse were 8 x 44 cm and for the copper fuse the measurements were 5.5 x 40 cm. Both fuses were one mil thick.

A full range of graphical analysis is presented for the fully processed fuse experiments. The fully processed data is also compared with the preprocessed data to give the reader an idea of the variation to be expected from one set of processing to the other.

Figures 17 and 18 are the current and voltage traces for the processed and preprocessed experiments respectively. Note the significant difference in the voltage magnitudes and the shift in the current levels. Figure 19 shows the resistivity vs. specific energy obtained from the processed data. Figures 20 and 21 compare the resistivity vs. specific energy using the processed and preprocessed data.

Figures 22 and 23 show the resistivity vs. time for both the processed and preprocessed data. Note that similarity of shape is easier to see than in the case of the specific energy graphs.

Figures 24, 25, and 26 show resistance, power, and energy vs. time respectively using the processed data. Note

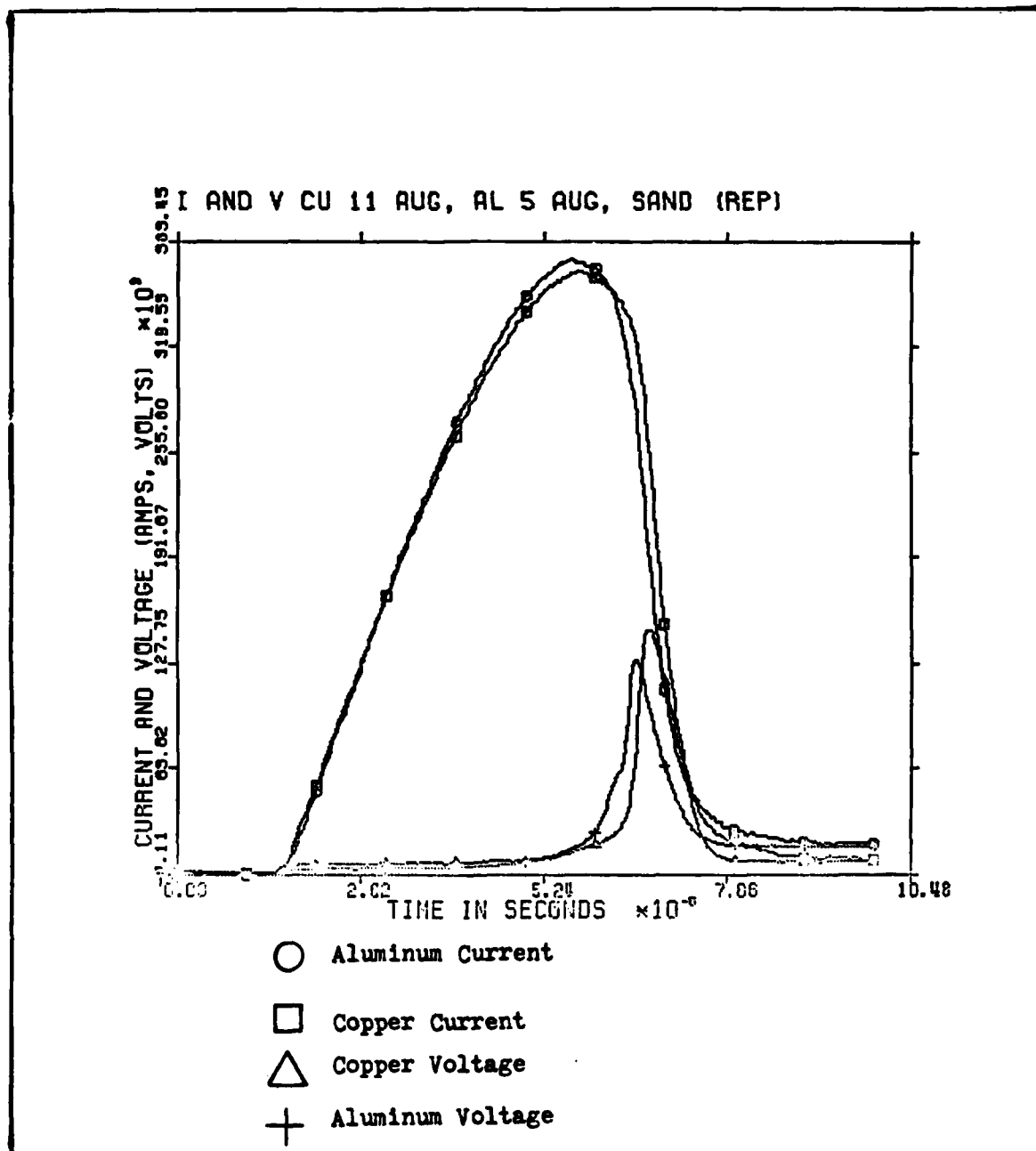


Fig 17. Processed Voltage and Current
Aluminum and Copper Fuse in Sand at 42 KV

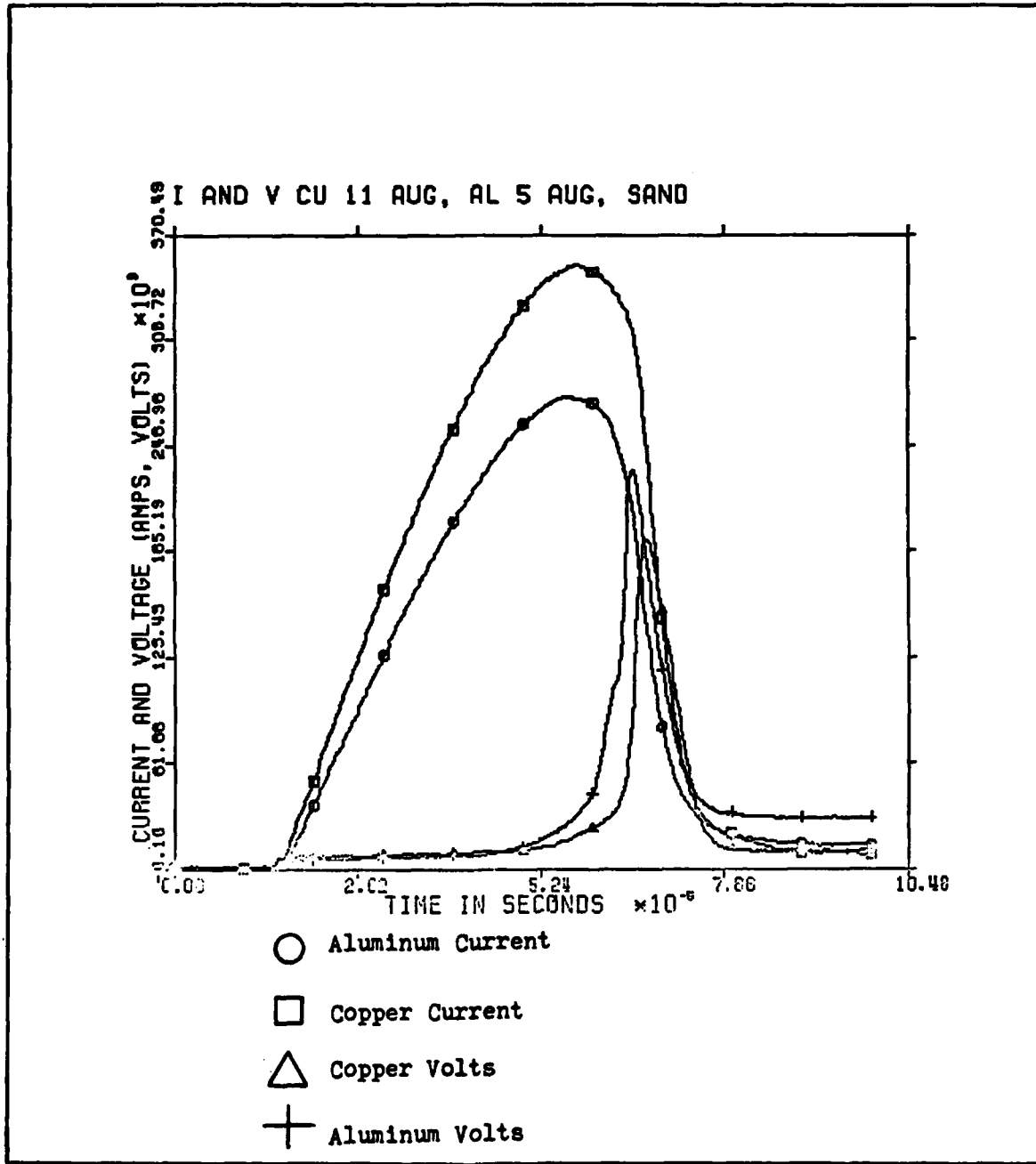


Fig 18. Preprocessed Voltage and Current
Aluminum and Copper Fuse in Sand at 42 KV

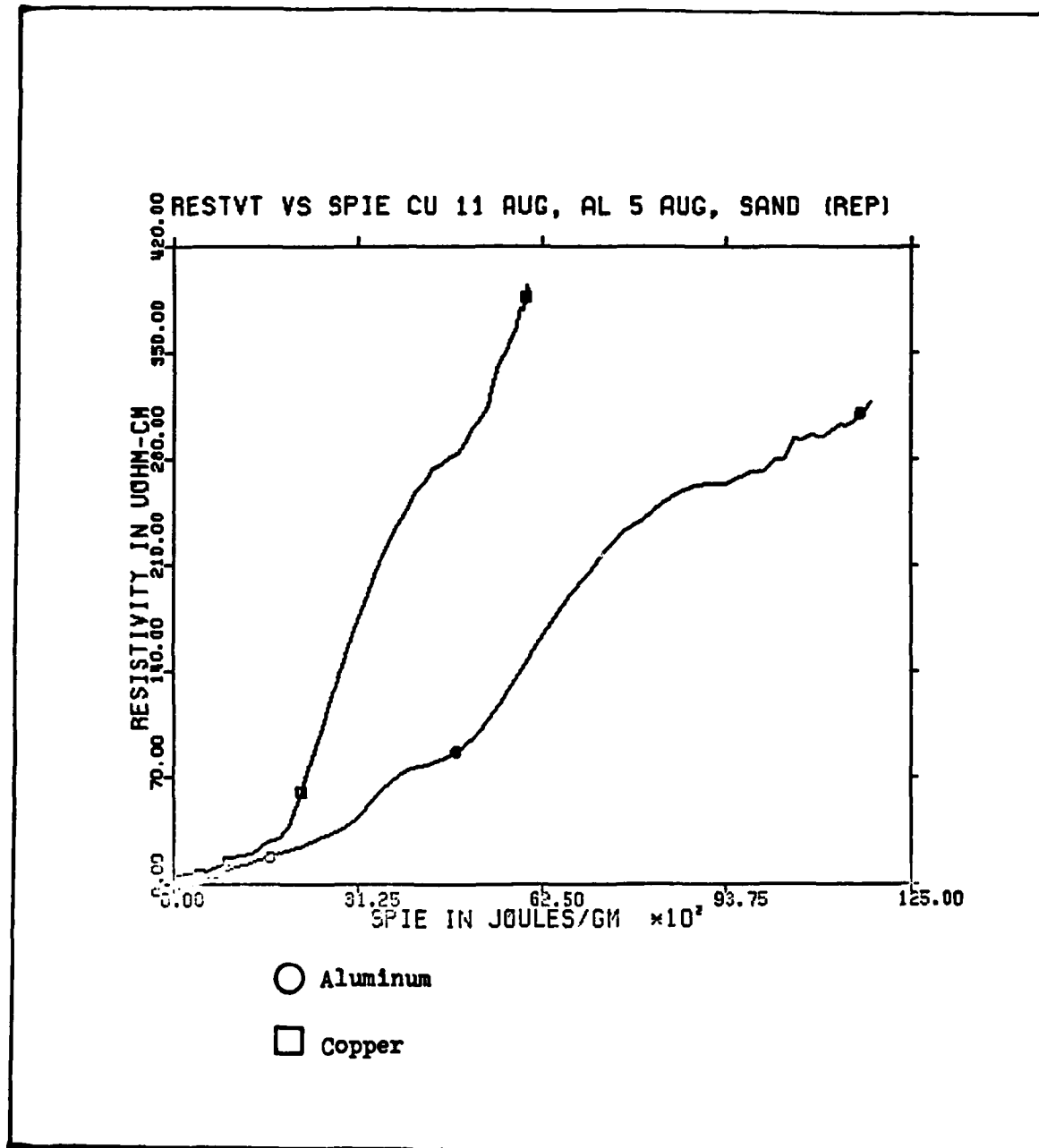


Fig 19. Processed Resistivity Vs. Specific Energy
Sand Quench at 42 KV

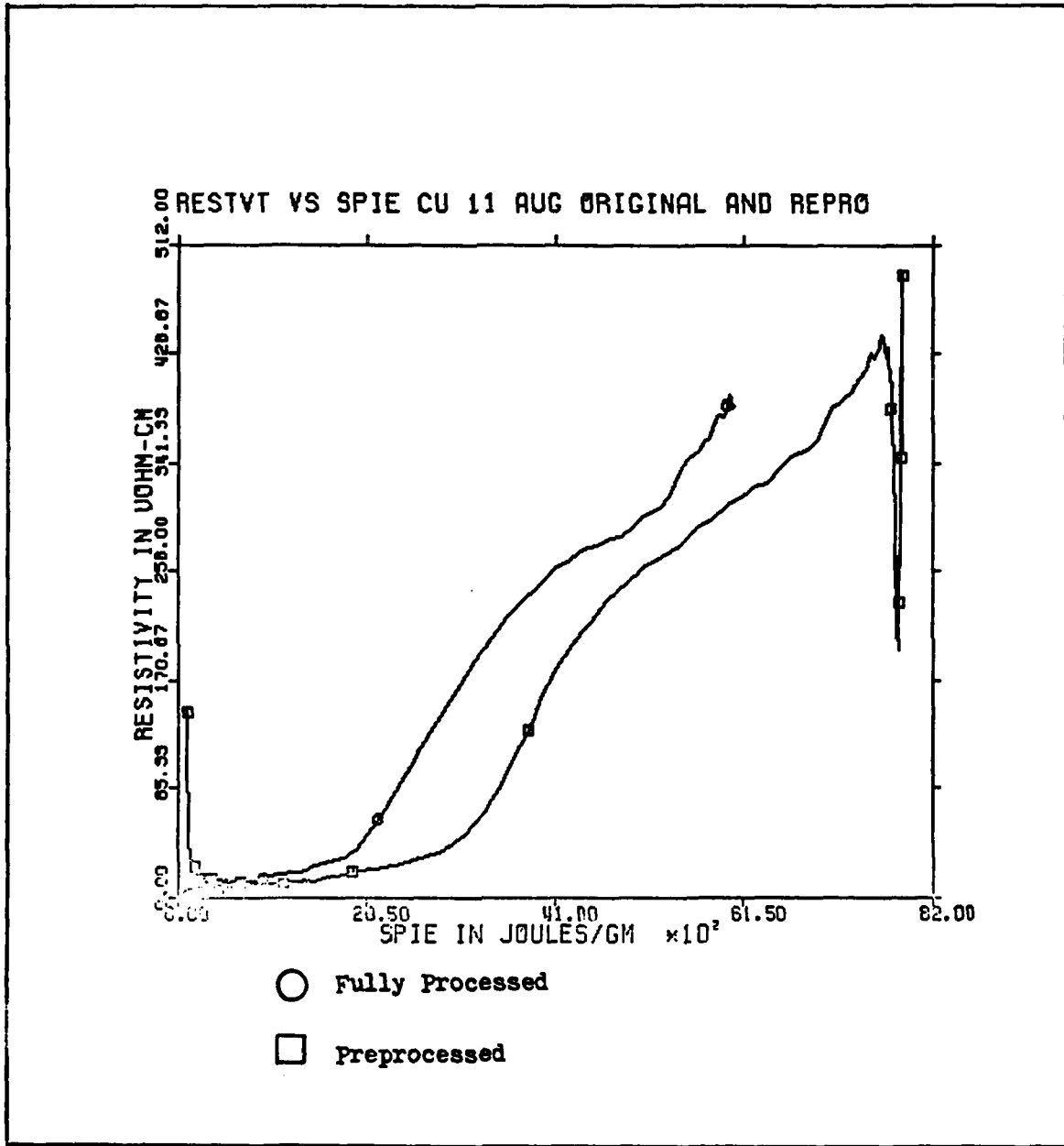


Fig 20. Processed and Preprocessed Resistivity Vs. Specific Energy
Copper Fuse at 42 KV

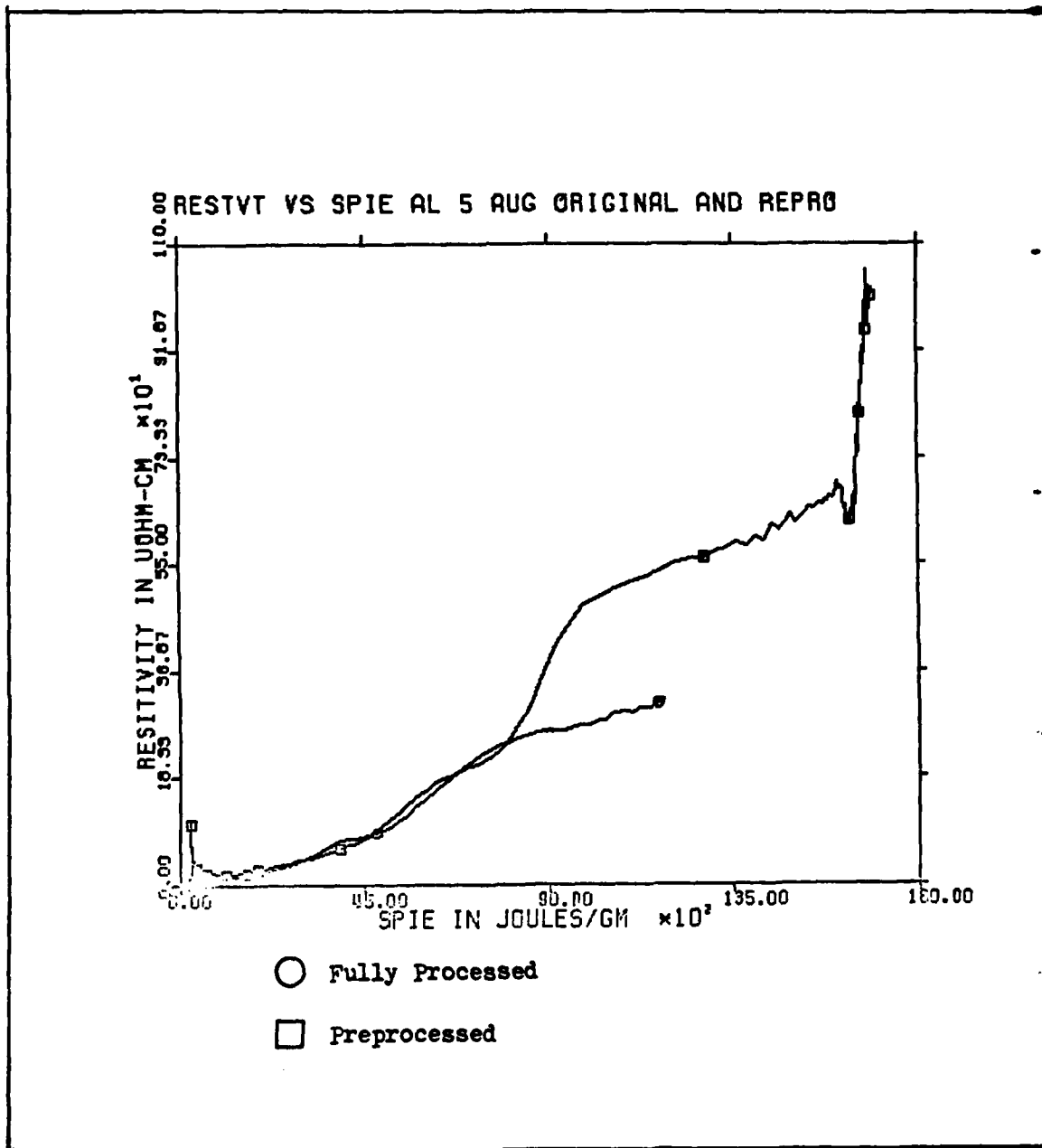


Fig 21. Processed and Preprocessed Resistivity Vs. Specific Energy

Aluminum Fuse at 42 KV

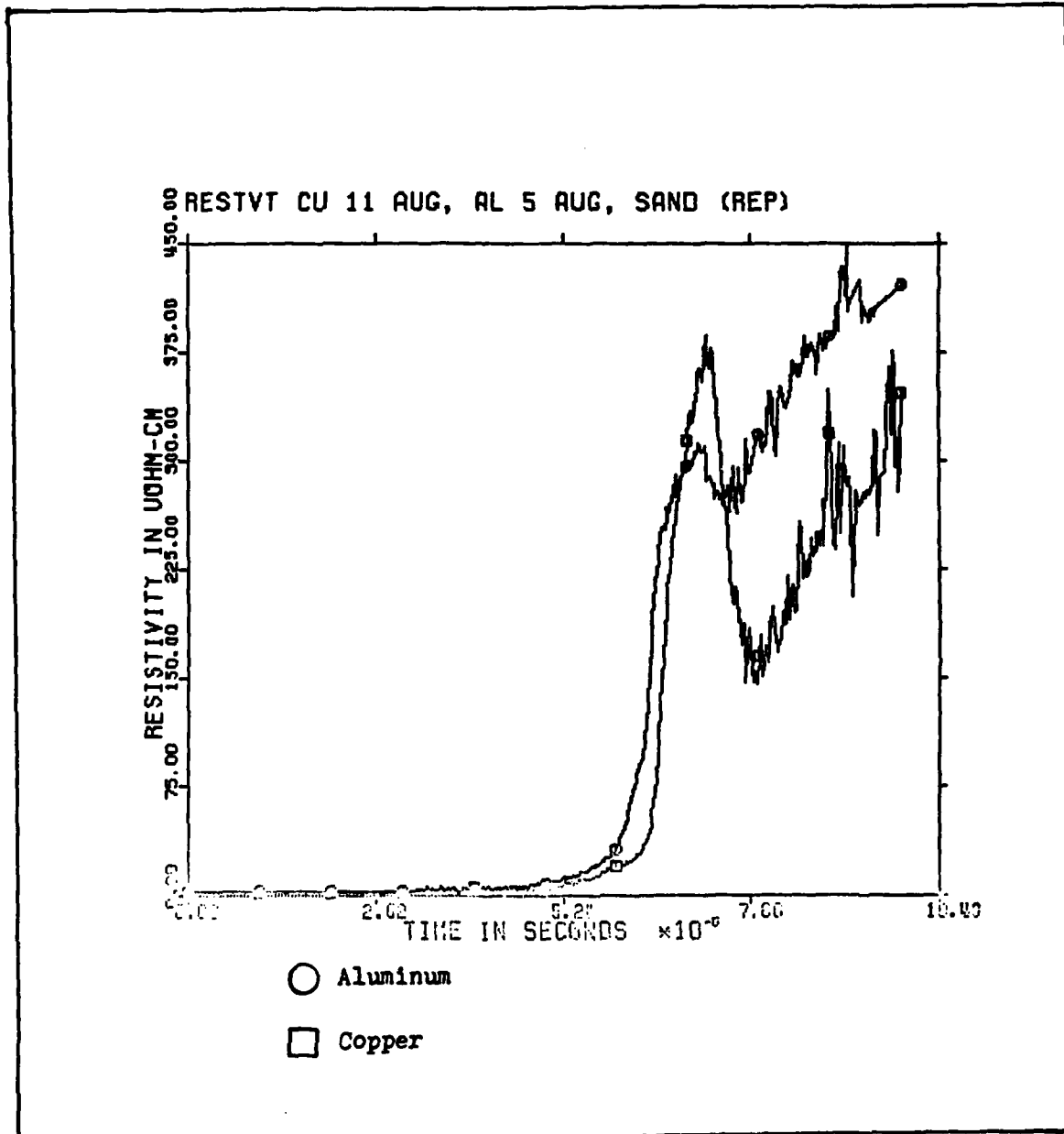


Fig 22. Processed Resistivity

Aluminum and Copper Fuse at 42 KV

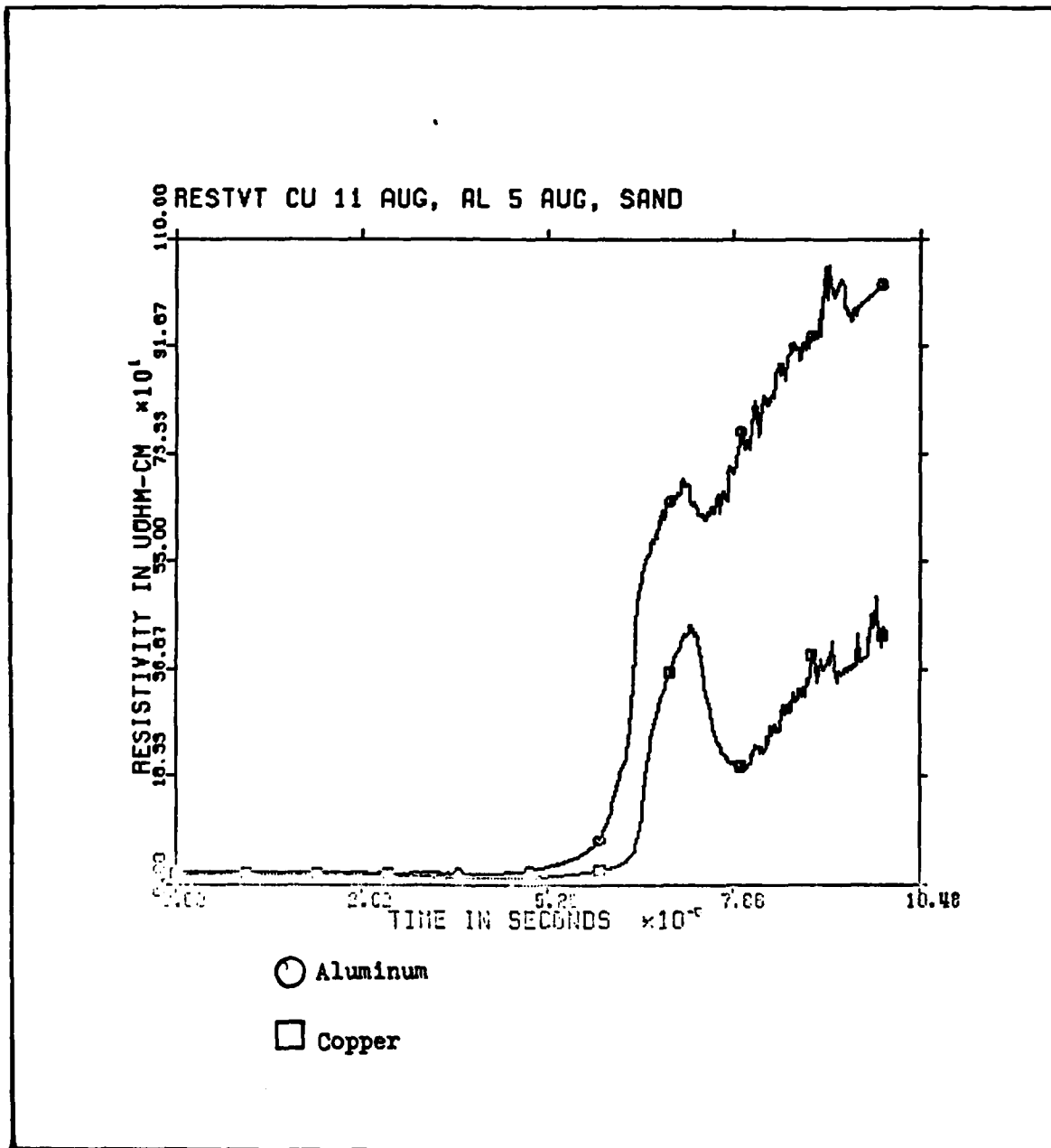


Fig 23. Preprocessed Resistivity
Aluminum and Copper Fuse at 42 KV

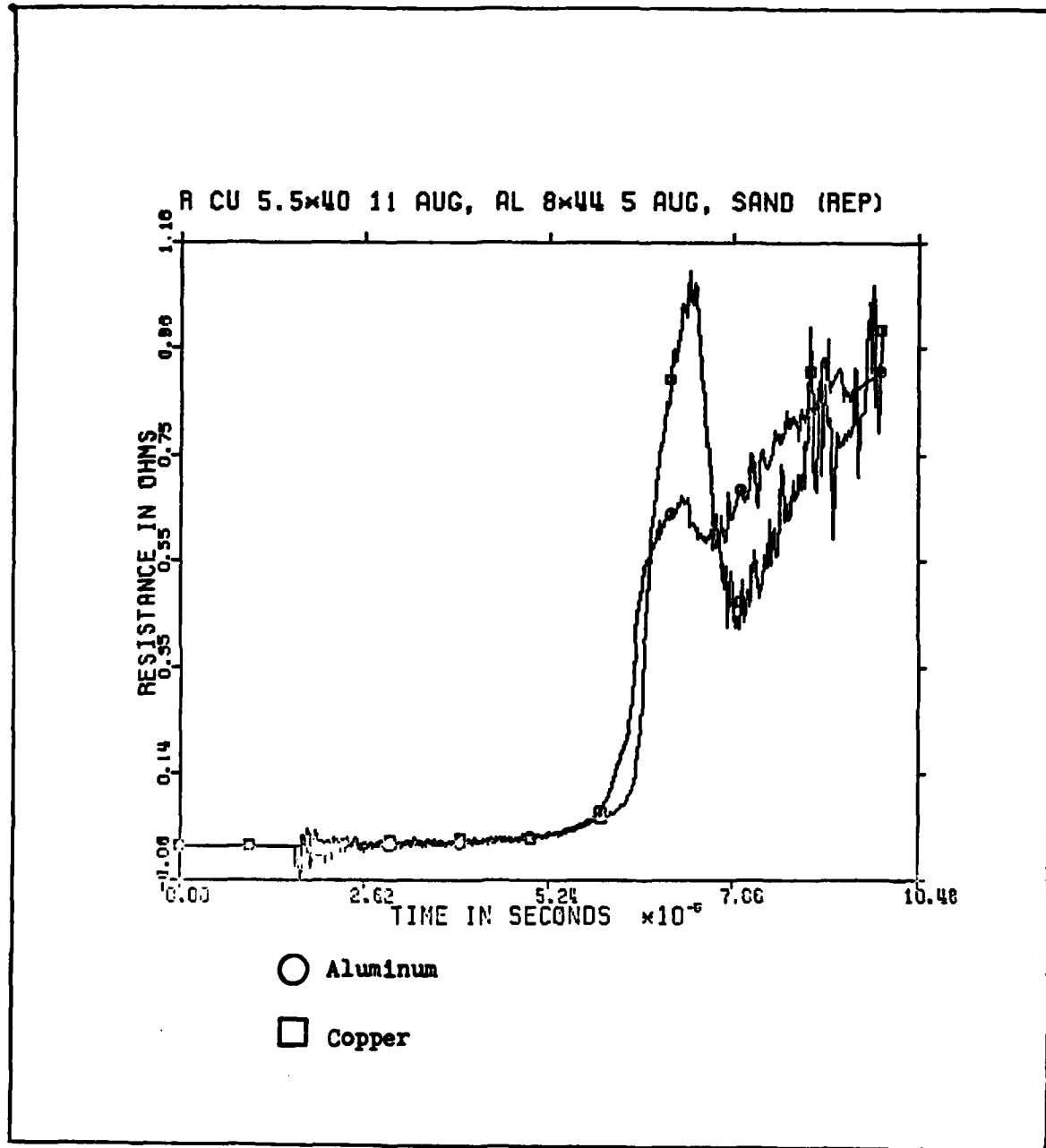


Fig 24. Processed Resistance
Aluminum and Copper Fuse at 42 KV

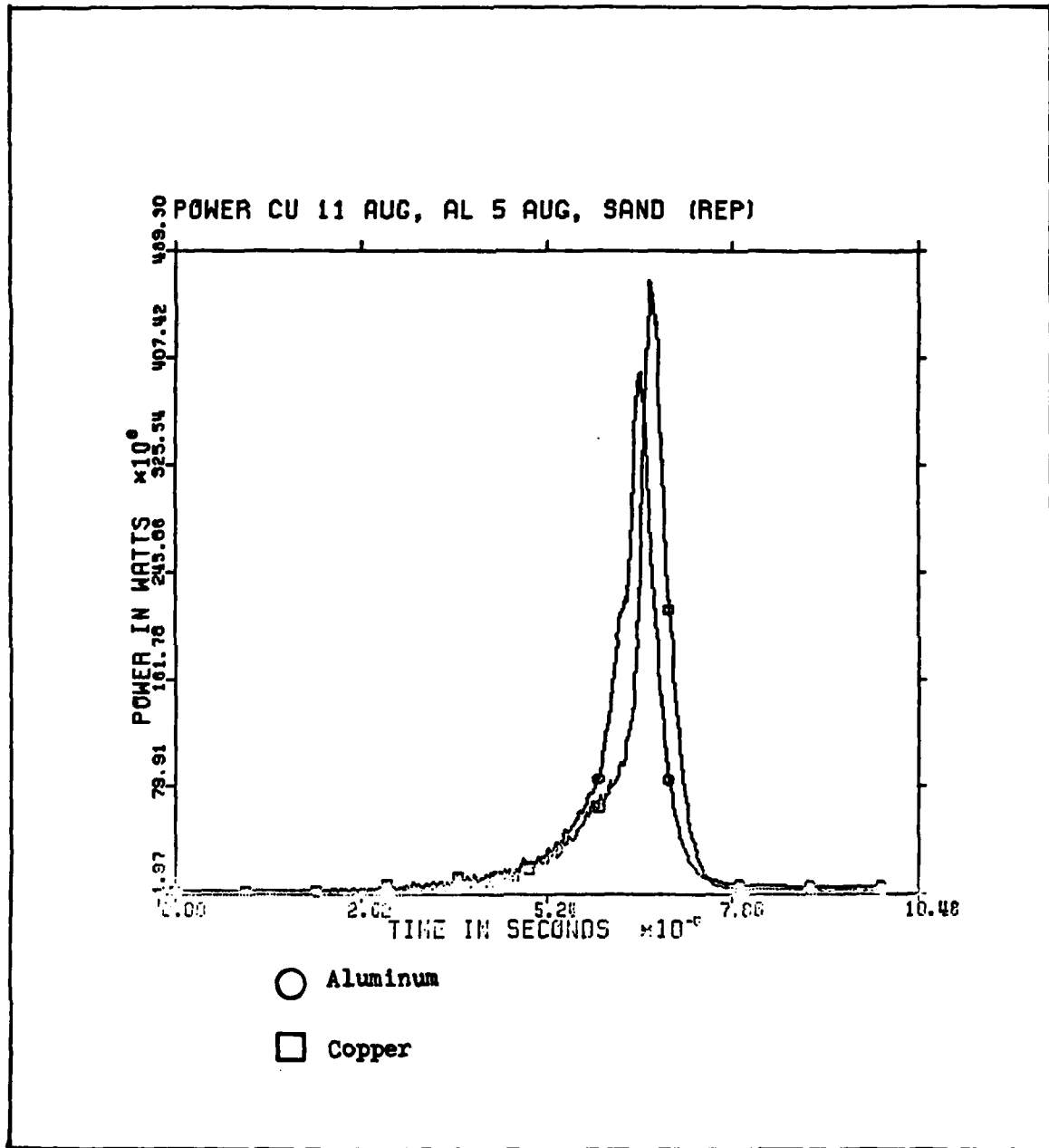


Fig 25. Processed Power
Aluminum and Copper Fuse at 42 KV

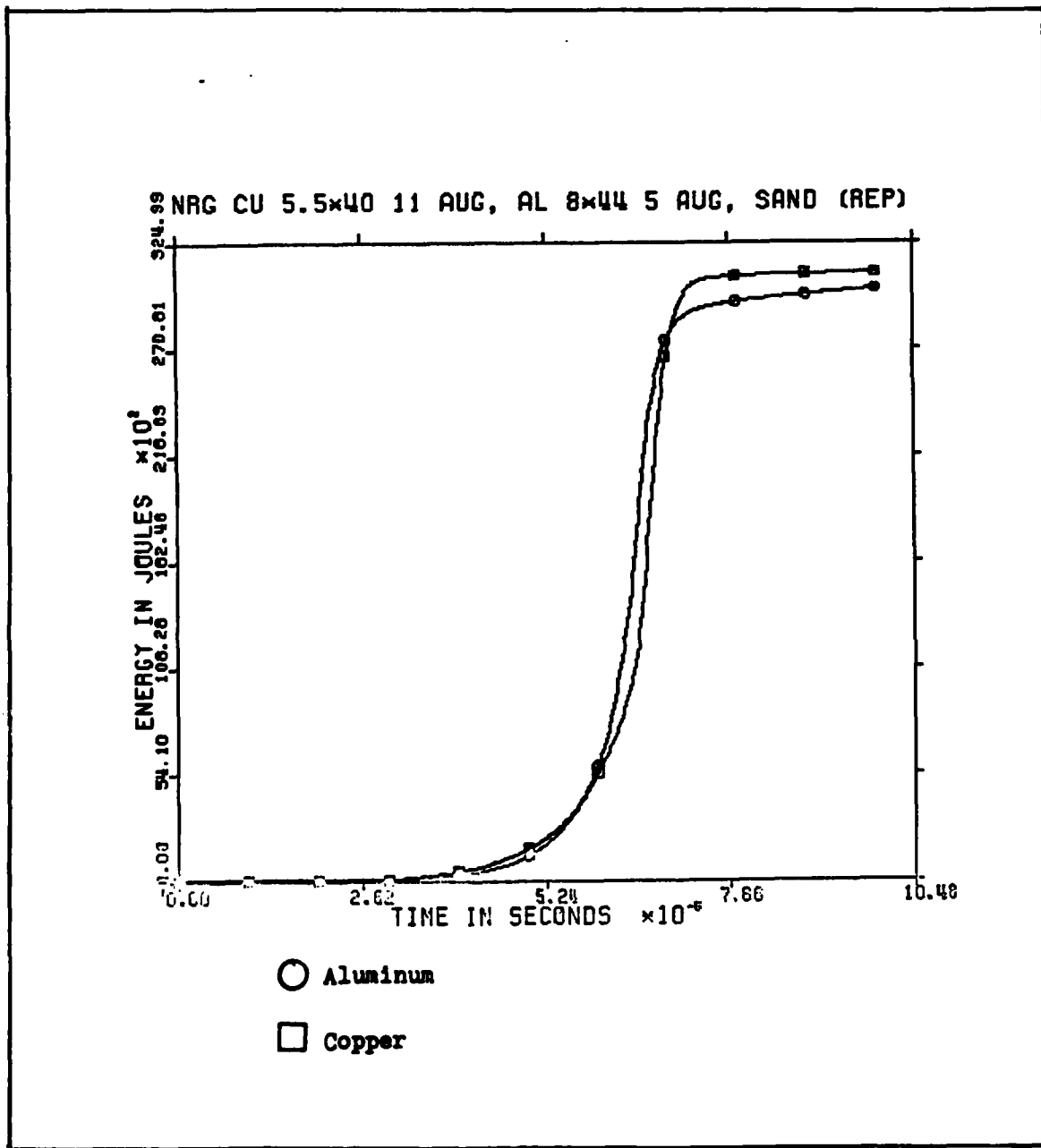


Fig 26. Processed Energy
Aluminum and Copper Fuse at 42 KV

that the energy is just short of the 32KJ available indicating that most of the energy is used within the time of observance and is consumed in the fuse.

The next set of figures deal with the same copper and aluminum fuses operated at 47 KV. Figures 27, 28, and 29 show the current and voltage traces, the resistivity vs. specific energy, and the resistivity vs. time. A greater time difference in reaching peak voltage is apparent in this case than in the 42 KV case.

Figure 30 is a comparison of three shots performed under the same conditions. It baselines the system for repeatability of the preprocessed data. Note the significant differences in shape. Using the specific energy relationship enhances any differences between the curves of each experiment.

Fuses in Cold Sand

This series of experiments also used sand as the quench medium; however, the sand was cooled with liquid nitrogen as described in the Equipment chapter. The liquid nitrogen was not allowed to come into direct contact with the sand. Cooling times are indicated in Tables 1 and 2. Simulations performed after the experiments indicate that cooling times of up to two hours were necessary to insure that the sand temperature was within a few percent of the liquid nitrogen temperature. The cooling times used were able to reduce the sand temperature adjacent to the fuse to about -77C degrees

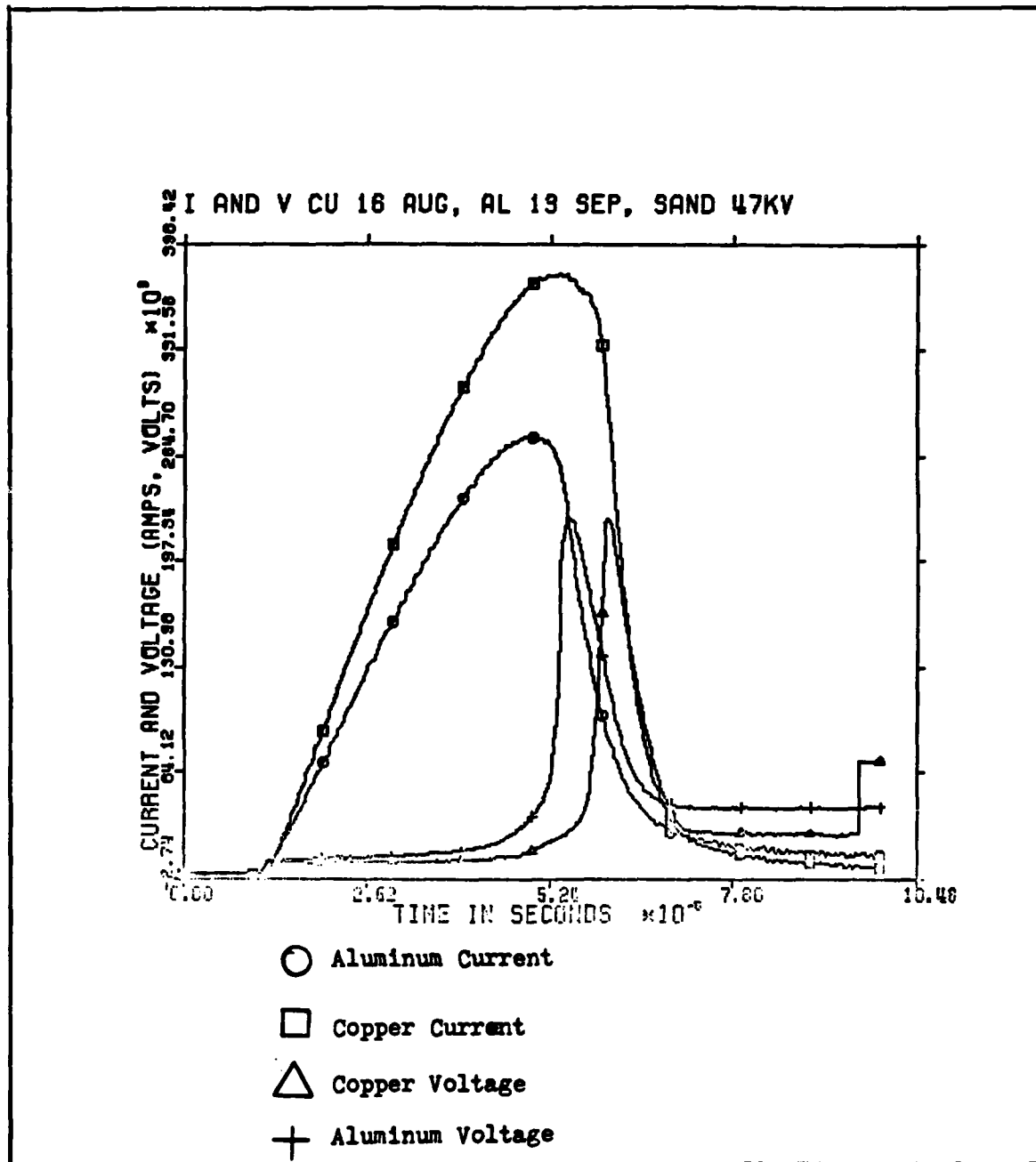


Fig 27. Preprocessed Voltage and Current
Aluminum and Copper Fuse at 47 KV, Sand Quench

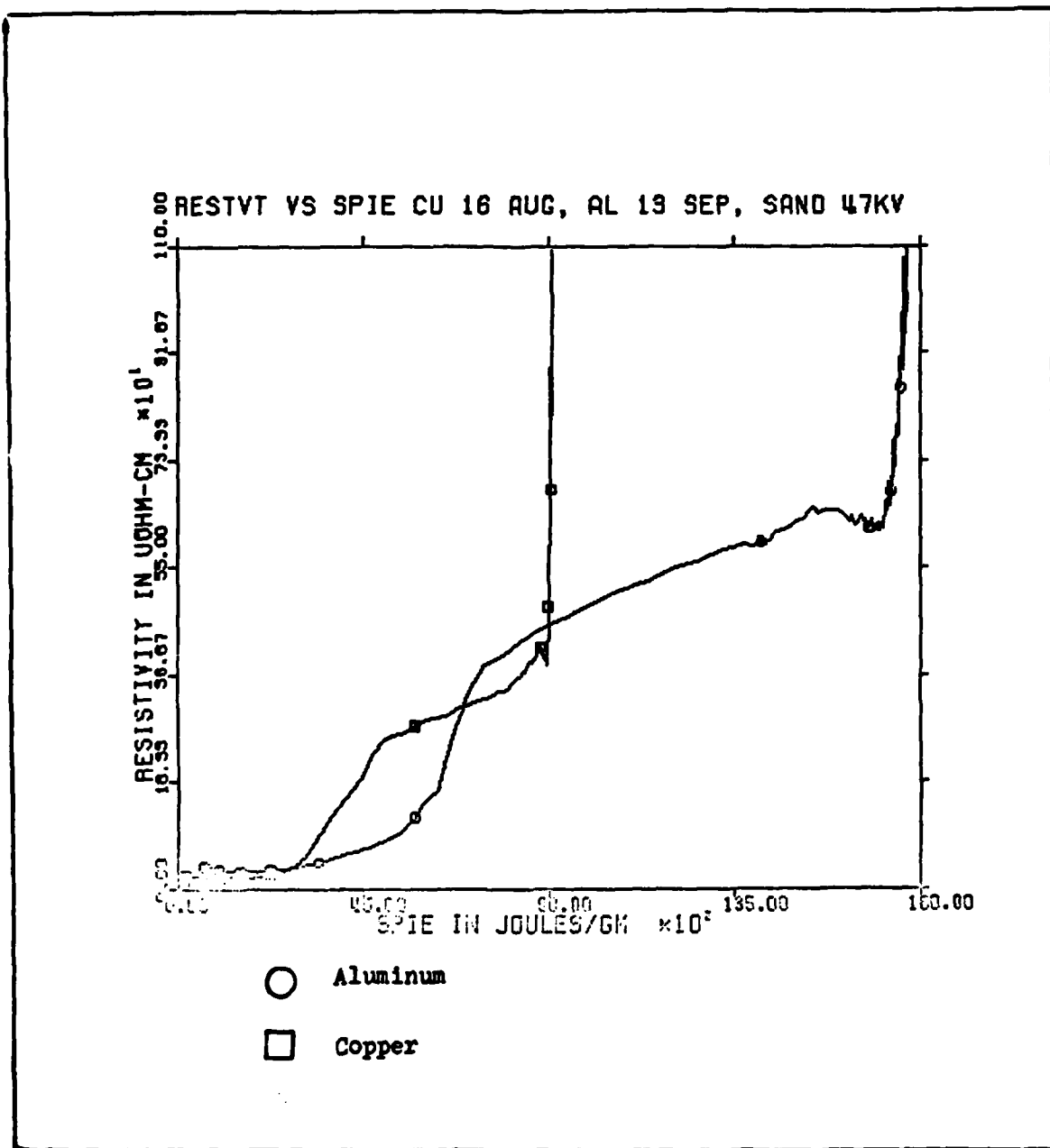


Fig 28. Preprocessed Resistivity Vs. Specific Energy
 Aluminum and Copper Fuse at 47 KV, Sand Quench

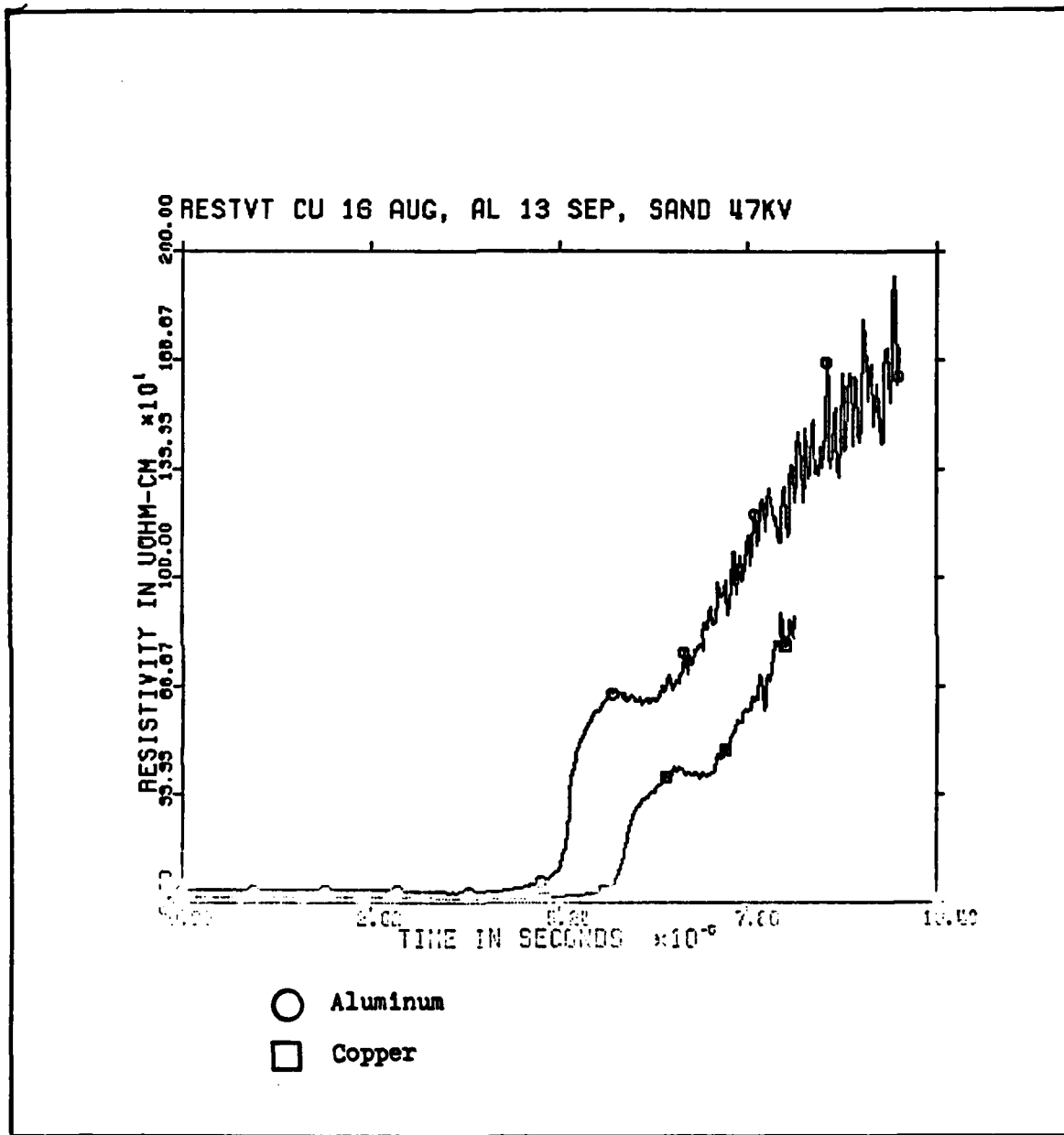


Fig 29. Preprocessed Resistivity

Aluminum and Copper Fuse at 47 KV, Sand Quench

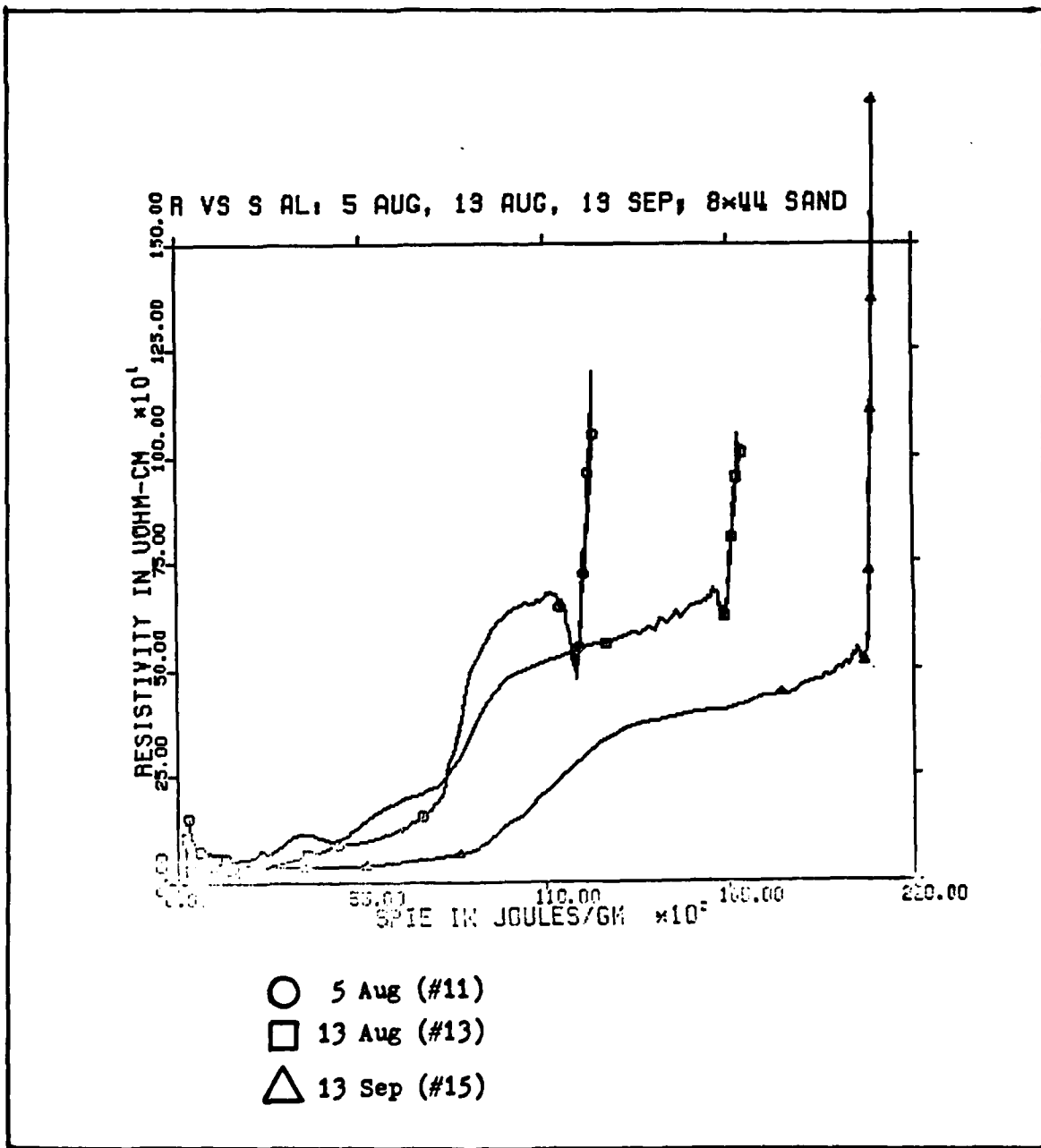


Fig 30. Baseline Proprocessed Resistivity Vs. Specific Energy
Aluminum Fuse at 42 KV, Sand Quench

according to the simulation. The time of cooling was limited due to the deterioration of the container holding the liquid nitrogen around the fuse package.

These experiments were conducted using a 47 KV charge voltage. Restrike was not a problem for the aluminum fuse unlike the 47 KV aluminum shots in room temperature sand. This indicates that even in the short time scale of these experiments enough energy transfer takes place at the high energies to inhibit local ionization and prevent restrike.

Figures 31, 32, and 33 show the results of these experiments using the preprocessed data. Note the time shift of the voltage peaks from the room temperature shots. The voltage trace of the aluminum shot is at best questionable beyond the peak value. This problem appeared on many of the non room temperature experiments. No reason for this event was discovered.

Fuses in Liquid Nitrogen

To further assess the effects of cryogenic temperatures on the behavior of copper and aluminum fuses the fuses were fired in a liquid nitrogen bath. The fuse was in direct contact with the liquid nitrogen thereby insuring the fuse was at liquid nitrogen temperatures as opposed to the low temperature of the cooled sand experiments.

Again a charge voltage of 47 KV was used for both fuses. Figures 34, 35, and 36 show the results using preprocessed data. The most obvious features are the time

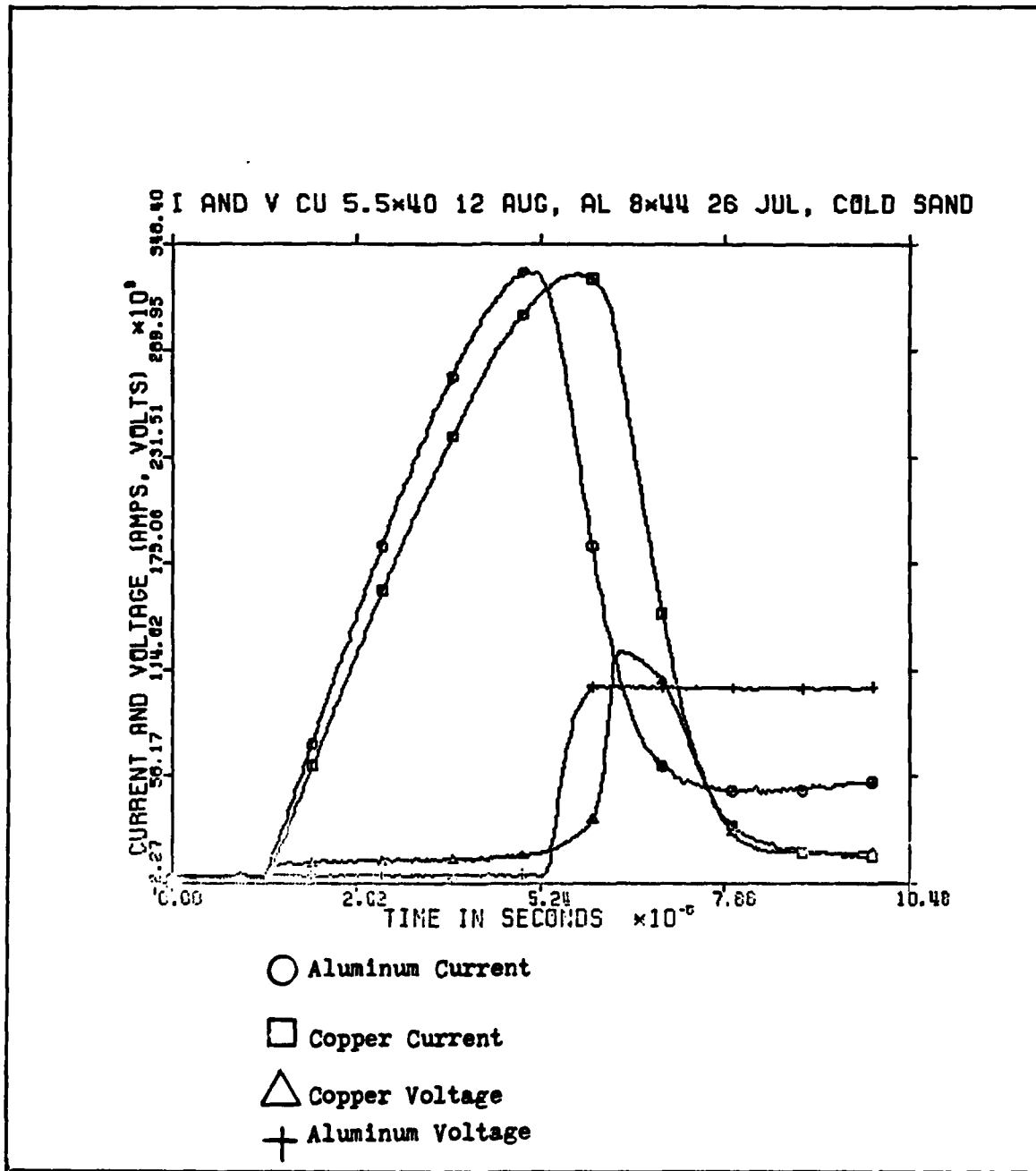


Figure 31. Preprocessed Voltage and Current

Aluminum and Copper Fuse at 47 KV, Cold Sand Quench

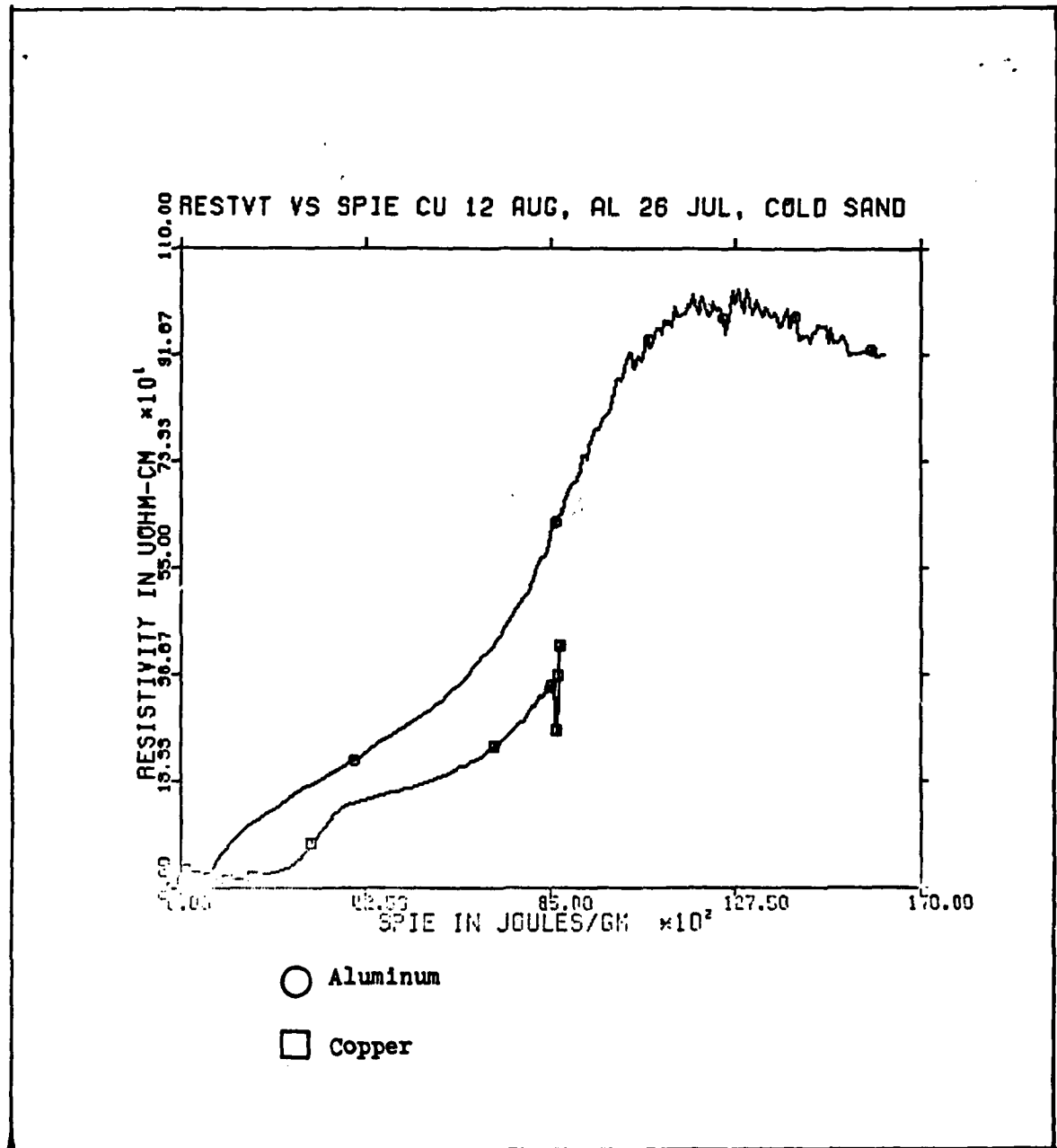


Fig 32. Preprocessed Resistivity Vs. Specific Energy
 Aluminum and Copper Fuse at 47 KV, Cold Sand Quench

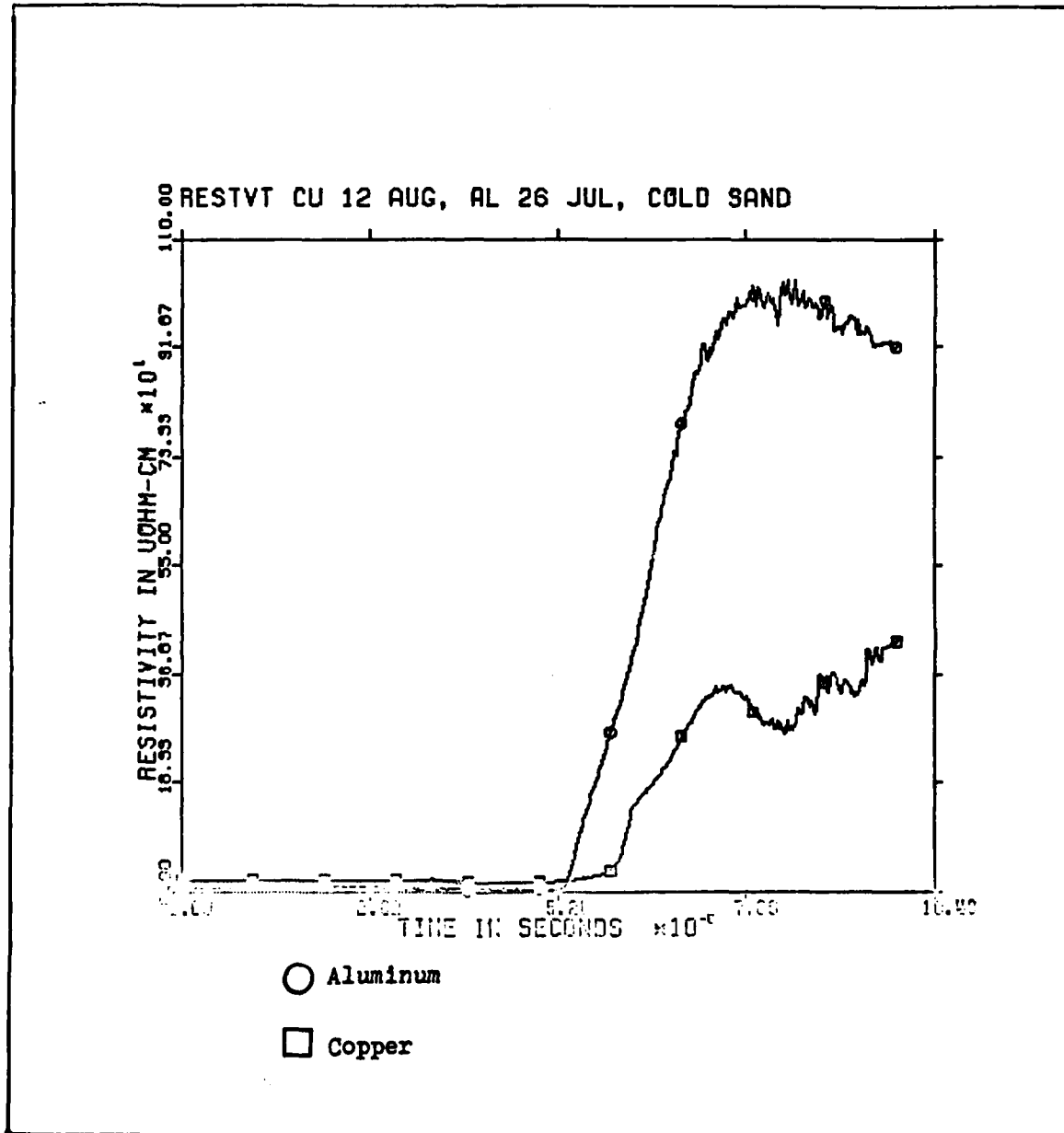


Fig 33. Preprocessed Resistivity
Aluminum and Copper Fuse at 47 KV, Cold Sand Quench

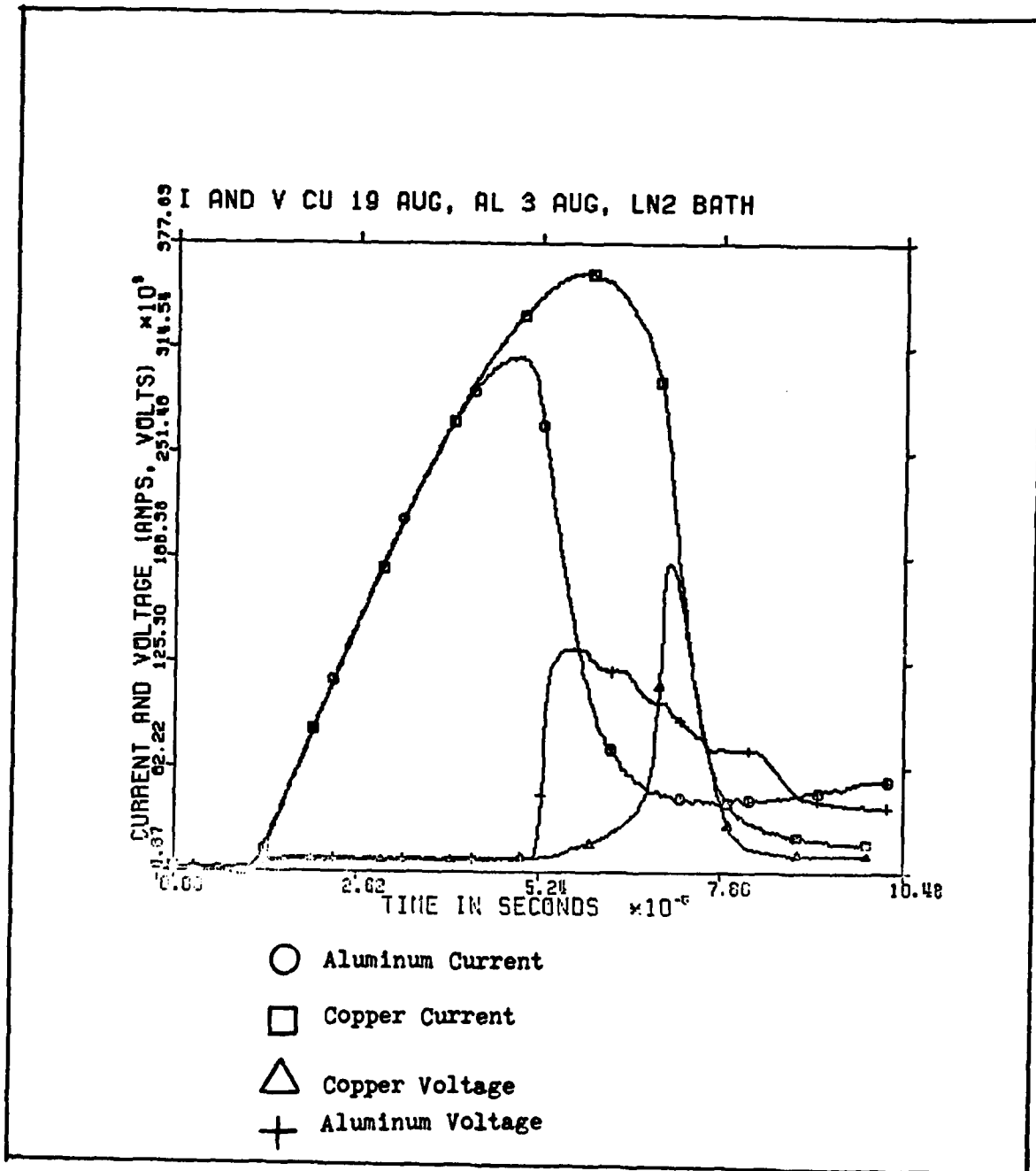


Fig 34. Preprocessed Voltage and Current

Aluminum and Copper Fuse at 47 KV, Liquid Nitrogen Bath

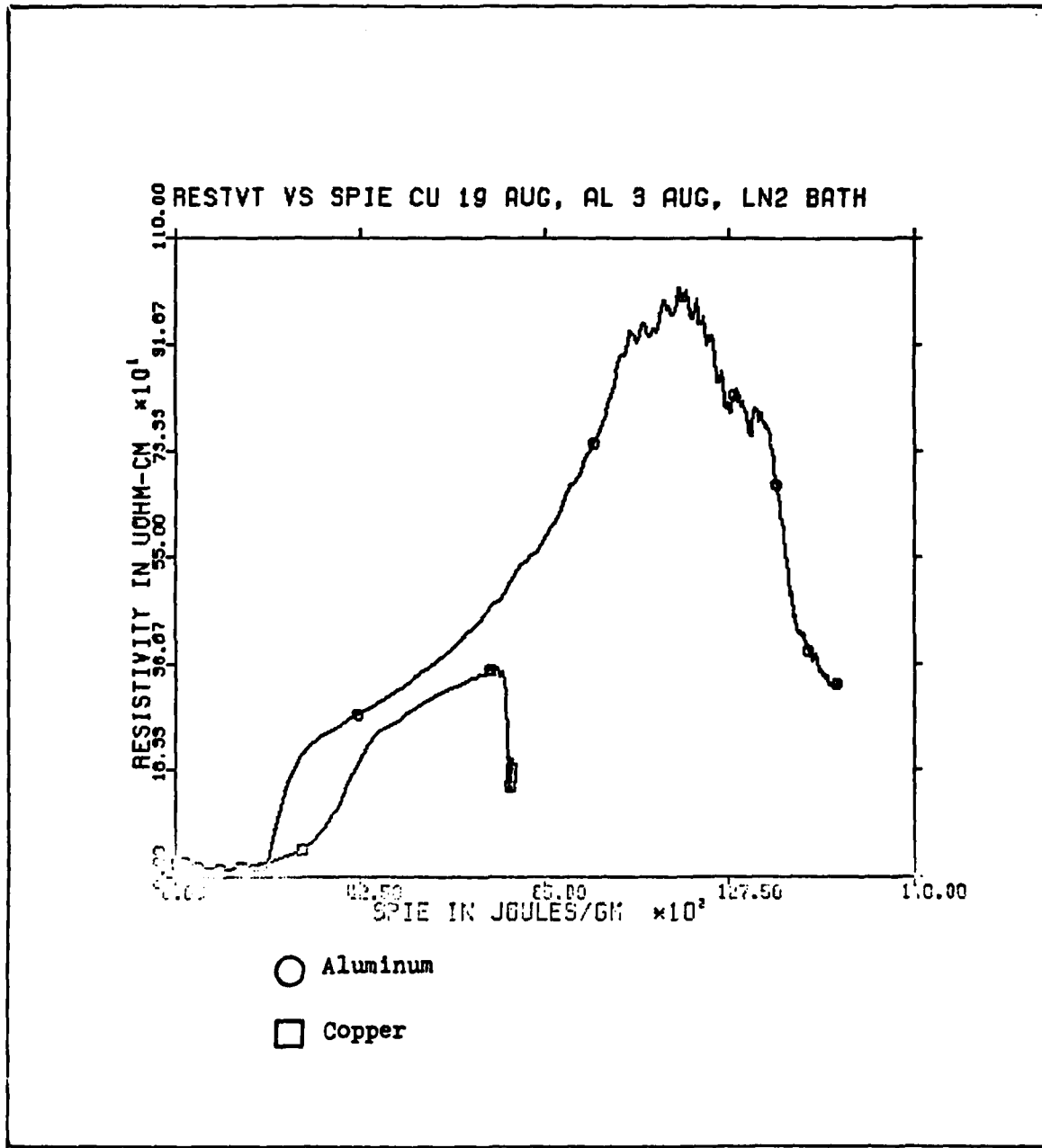


Fig 35. Preprocessed Resistivity Vs. Specific Energy
 Aluminum and Copper Fuse at 47 KV, Liquid Nitrogen Bath

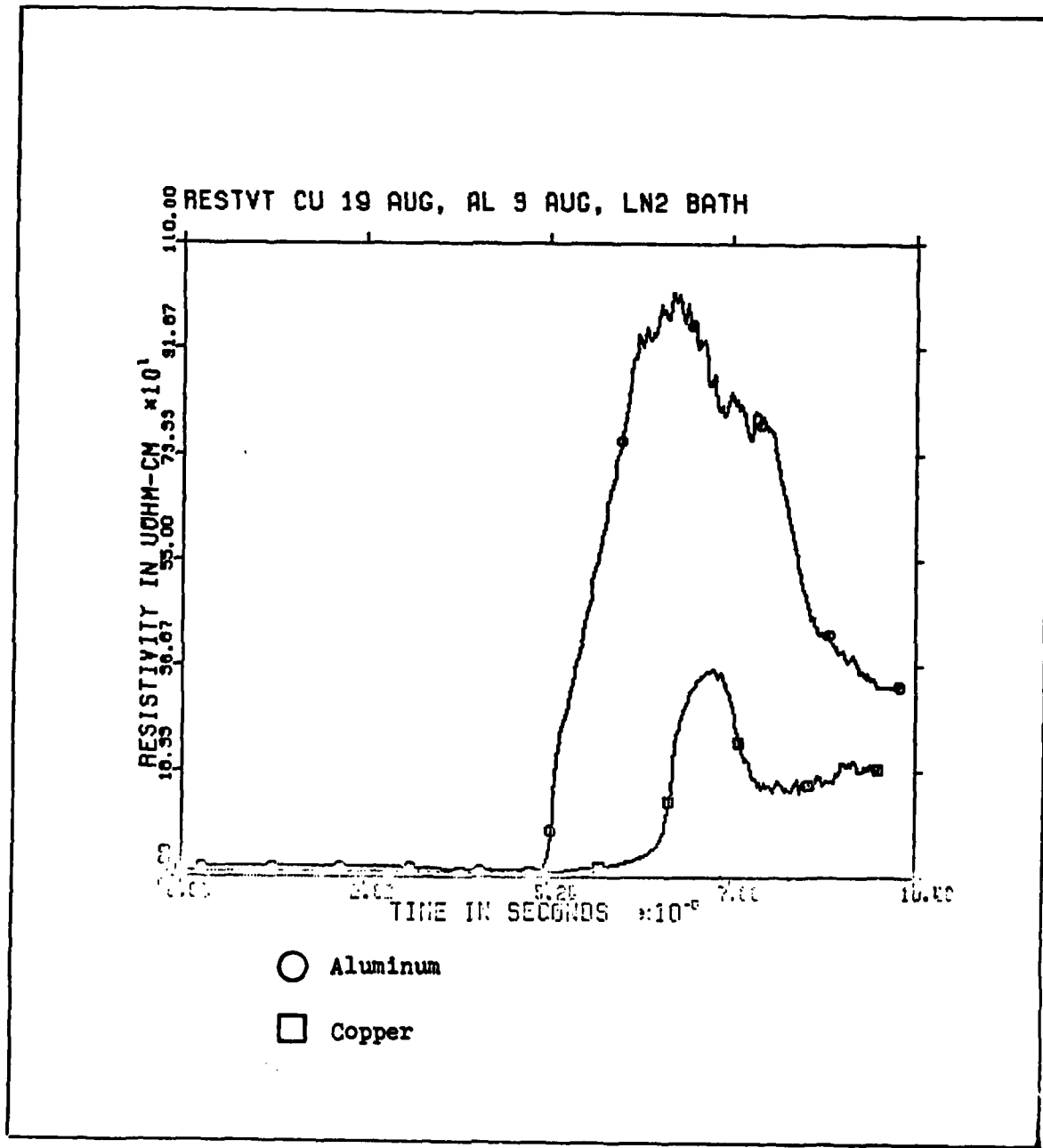


Fig 36. Preprocessed Resistivity
Aluminum and Copper Fuse at 47 KV, Liquid Nitrogen Bath

shift of the voltage peaks from the room temperature sand experiment. The cryogenic environment seems to have more effect on the aluminum fuse than the copper fuse. The voltage traces beyond the peak are again suspect.

Fuses in Deionized Water

Deionized water was used as a quench medium in order to better assess the contribution to fuse behavior from temperature changes. Both water and liquid nitrogen are incompressible fluids and chemical effects on fuse behavior are assumed insignificant. Therefore, any changes between the liquid nitrogen environment and deionized water environment should be due to temperature alone.

Figures 37, 38, and 39 show the preprocessed data from these experiments. Most obvious is the time of voltage peak change for the aluminum fuse. Again the voltage beyond the peak must be disregarded for the copper fuse.

Other Copper Fuse Configurations:

Several other copper fuse configurations were tested in order to assess the possible effect of thermal transfer to the quench medium.

In one case the surface area exposed to the medium was reduced by about one third by using three mil copper foil. In another, the surface area affected by the quench was increased by dividing the fuse into four sections instead of the two shown in Figure 7. This increase of surface area

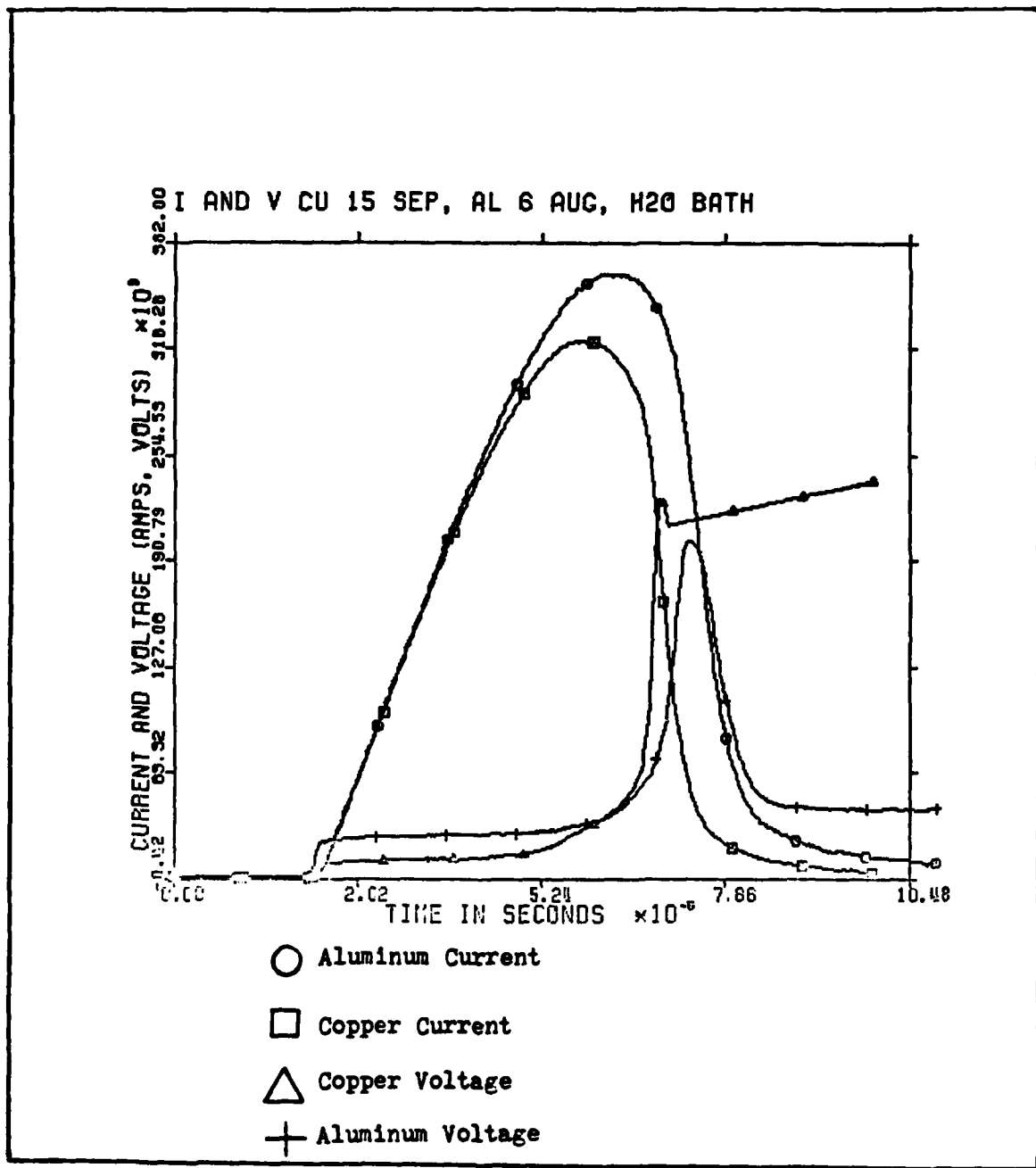


Fig 37. Preprocessed Voltage and Current

Aluminum and Copper Fuse at 47 KV, Deionized Water Bath

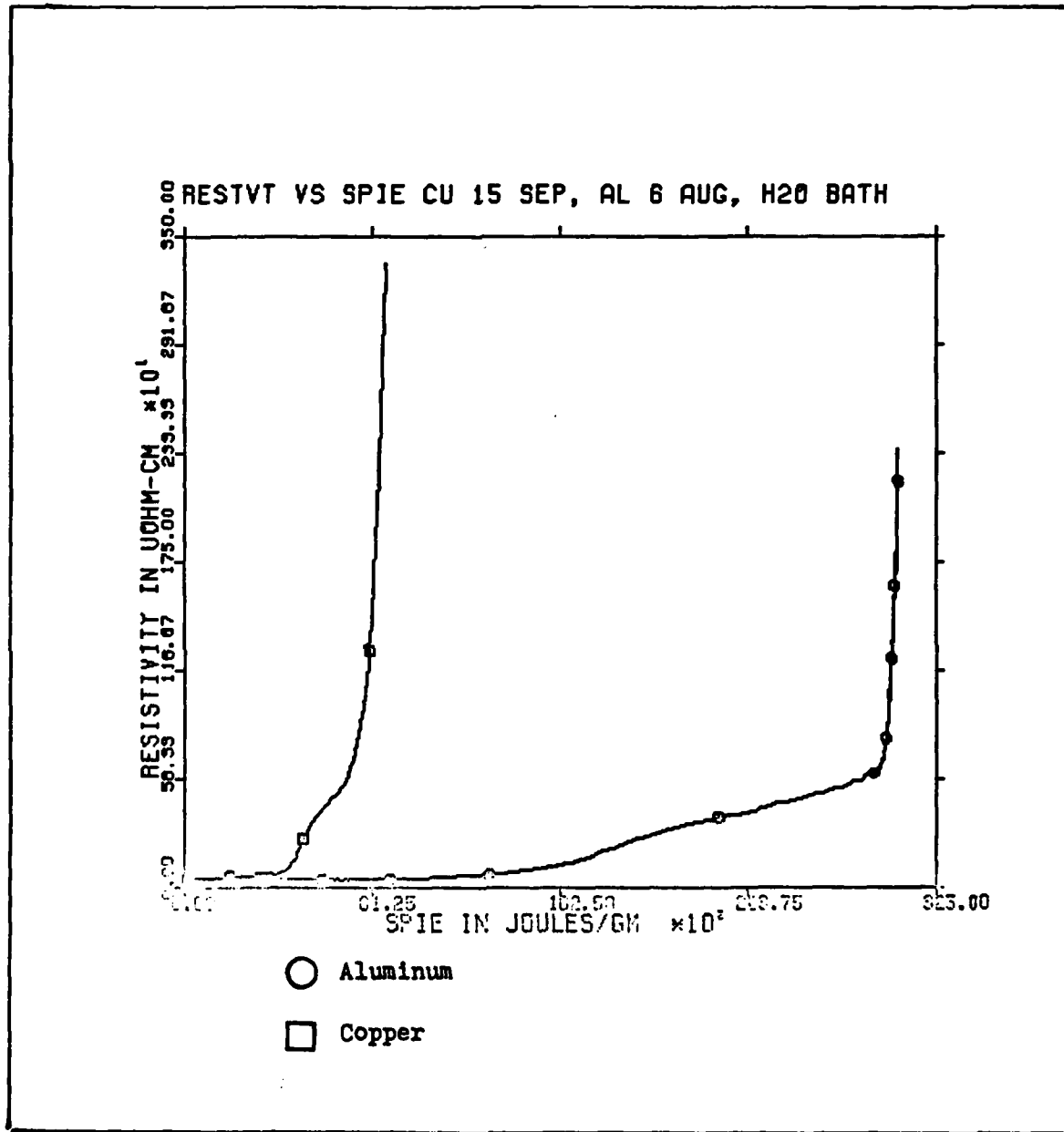


Fig 38. Preprocessed Resistivity Vs. Specific Energy

Aluminum and Copper Fuse at 47 KV, Deionized Water Bath

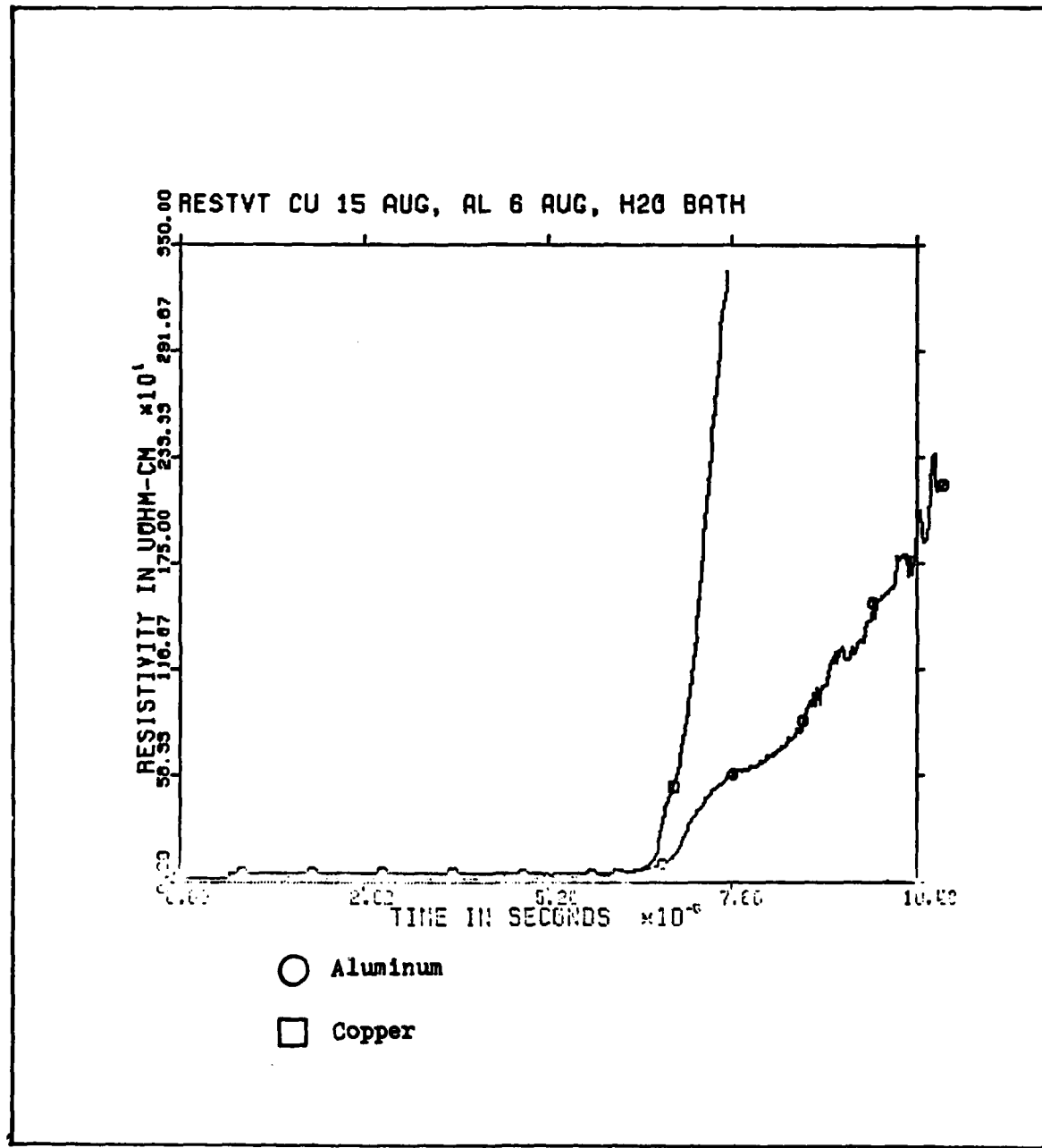


Fig 39. Preprocessed Resistivity
Aluminum and Copper Fuse at 47 KV, Deionized Water Bath

was effective if we assume that edge effects produce more heat so increasing the number of edges increases the opportunity for heat transfer to the medium.

Finally, a fuse was tested in a relatively solid environment made of sand and frozen water. This was done to see if the pressure increase of vaporization in a solid had any effect on the rate of phase change (Ref 20). All shots were at 47 KV.

Figure 40 shows the results of these shots. There could possibly be some relationship between the effective surface area and fuse behavior. It is not clear what the mechanisms causing the changes are.

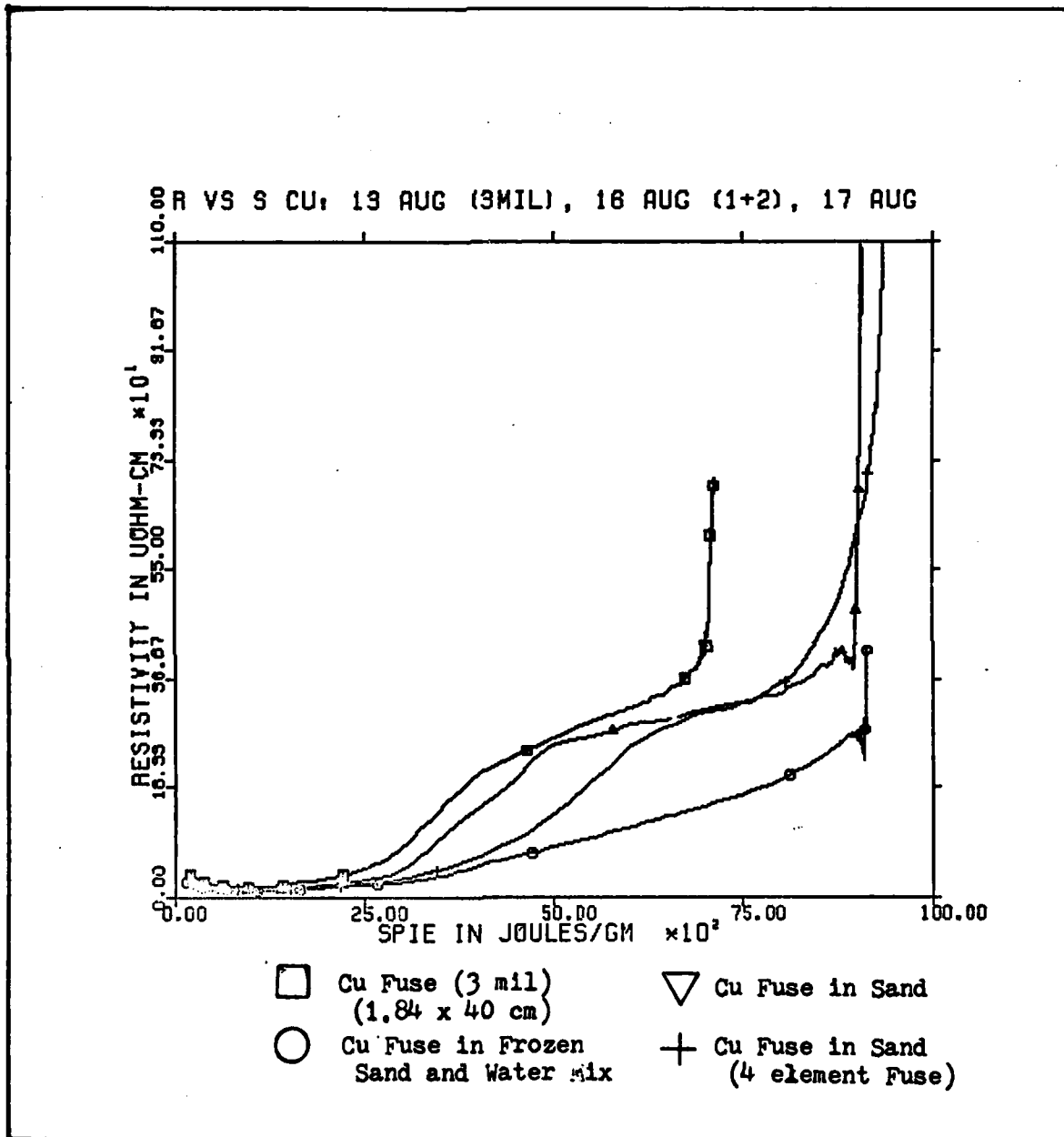


Fig 40. Preprocessed Resistivity Vs. Specific Energy

Other Copper Fuse Configurations at 47 KV

V. SUMMARY, CONCLUSIONS, AND RECOMMENDATIONS

Summary

A number of experiments using copper and aluminum foil fuses in several different environments were conducted to assess the effects of temperature on fuse performance. Two processing techniques were used to analyze the data. The first process was merely scale factoring and droop correcting the data before using numerical techniques to find resistivity information. The second method was extensive processing producing a self consistent solution with the experimental data and the circuit model.

Conclusion

The major conclusion that can be drawn from this set of experiments is that temperature and heat transfer have an effect. The results obtained from the two methods produce substantially different results on the behavior of aluminum and copper fuses. Aluminum fuses are affected to a greater extent than are copper fuses. A second conclusion that can be made is that the data must be processed more completely as was done in the fuse in sand at room temperature. The large variations in the graphical evidence from processed and preprocessed leads one to suspect the results obtained from preprocessed data.

Increasing the energy levels of systems using electrically exploded foil fuses should not present problems of electric field breakdown as long as system time constants are not reduced significantly. Increasing the systems energy storage by increasing the system capacitance will result in lower resistance in the open state of the fuse opening switch. Increasing system energy by increasing the charge voltage allows the fuse resistance to stay constant.

Recommendations

The first recommendation is that the data presented in this report be fully processed so as to facilitate comparison of the characteristics of fuse properties. Along with this recommendation, a study of the applicability of the processing method and an automation of the procedure would be advisable.

During the course of this experiment several areas were noted that may deserve further study. First among them is an investigation of the fuse characteristics discussed here with a load connected. Deeper investigation into the effects of cryogenic environments is needed as is development of a more accurate measuring system. Several possible quench materials possessing much higher heat capacities and heat transfer characteristics than sand were identified during the course of this experiment. These materials, such as alumina, should be tested for improvement in fuse performance. Additional experiments to determine

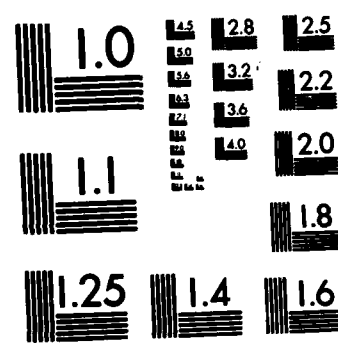
the effect of heat transfer with other fuse materials such as stainless steel or other alloys need to be performed. Almost every set of experiments performed in this experiment could be repeated several times to insure repeatability of fuse performance.

Bibliography

1. Reinovsky, R. E. et al. "Inductive Store Pulse Compression System for Driving High Speed Plasma Implosions", IEEE Transactions on Plasma Science, PS-10 (2): (June 1982).
2. Stuerke, C. et al. "Multi-Megamp, Multi-Terawatt Inductive Pulse Compression System Operation", Digest of Technical Papers, 3rd International Pulsed Power Conference, Albuquerque, NM, (June 1981).
3. Henderson, R. P. et al. "Preliminary Inductive Energy Transfer Experiments" Digest of Technical Papers, 2nd IEEE International Pulsed Power Conference, 347-350, Lubbock, Texas (1979).
4. Andrezen, A. B. et al. "Investigation of a Fast Foil Current Breaker - Electrical Foil Explosion In Pulverized Quartz" NIIEFA Preprint in Russian, Leningrad, 1975. (AD B045 219L)
5. Degnan, J. "Proposal for Exploding Wire/Foil Opening Switch Studies", Memo for the Record, Kirtland AFB, (4 August 1975).
6. Maisonnier, C. et al. "Rapid Transfer of Magnetic Energy by Means of Exploding Foil", Review of Scientific Instrumentation, 37 (10): 1380-1384 (October 1966).
7. DiMarco, J. N., and Burkhardt, L. C. "Characteristics of a Magnetic Energy Storage System Using Exploding Foils", Journal of Applied Physics, 41 (9): 3894-3899 (August 1970).
8. Janes, G.S. and Koritz, H. "High Power Pulse Steepening By Means fo Exploding Wires" Review of Scientific Instruments, 30 (11): 1032-1037 (November 1959).
9. Stuerke, C. Private Communication, Kirtland AFB, NM, (July 1982).

AD-A124 774 COMPARISON OF ALUMINUM AND COPPER FUSE OPENING SWITCHES 2/2
UNDER ROOM AND CR. (U) AIR FORCE INST OF TECH
WRIGHT-PATTERSON AFB OH SCHOOL OF ENGI. J C BUECK
UNCLASSIFIED DEC 82 AFIT/GE/EE/82D-22 F/G 9/1 NL

END
FILED
DTM



MICROCOPY RESOLUTION TEST CHART
NATIONAL BUREAU OF STANDARDS-1963-A

Bibliography

10. Early, H.C. and Martin, F. J. "Method of Producing a Fast Current Rise From Energy Storage Capacitors" Review of Scientific Instrumentation, 36(19): 1000 (1965).
11. Bedford, J. et al. "High-Power Pulse Generation Using Exploding Fuses", Energy Storage, Compression, and Switching, edited by H.W. Bostick, V. Nardi, and O. S. F. Fuekes, New York and London: Plenum Press, 1976.
12. Reinovsky, R. E. and Smith, D. L. "Fuse Switches for High Current Inductive Pulse Compression Systems" Final Report on Procedures, ARO Proceedings Workshop on Repetitive Opening Switches, Durango, CO (January 1981). (DTIC ADA 110770)
13. McCullough, W. Private Communication, Kirtland AFB, NM, (September 1982).
14. McClenahan, C. R., et al. "200 kJ Copper Foil Fuses" AFWL-TR-78-130, Air Force Weapons Laboratory, Kirtland AFB, NM (April 1980).
15. McClenahan, C. R. "A Technique for Calibrating V-Dot Probes", AFWL-TR-80-113, Air Force Weapons Laboratory, Kirtland AFB, NM (January 1981).
16. Henderson, R. P. Private Communication, Kirtland AFB, NM, (July 1982).
17. Payne, S. Private Communication, Kirtland AFB, NM, (July 1982).
18. Berger, T. L. "Effects of Surrounding Medium on Electrically Exploded Aluminum Foil Fuses", IEEE Transactions on Plasma Science, PS-8 (3): 213-216 (September 1980).

Bibliography

19. Conte, D., et al. "A Method for Enhancing Exploding Aluminum Foil Fuses for Inductive Storage Switching" Procedures, First IEEE Pulsed Power Conference Lubbock, TX, II D-7,1-6, (1976).
20. Lesnick, A. G. "A Necessary Condition for Conversion To Vapor of a Wire Exploded by Current" Doklady, 11 (10): 902-903 (April 1967).

APPENDIX A

This Appendix contains the first level flow charts for the programs used in this experiment to process the data. The ~~actual~~ programs used or modified versions of these programs may possibly be obtained by contacting the Applied Physics Division, NYTP, Air Force Weapon's Laboratory.

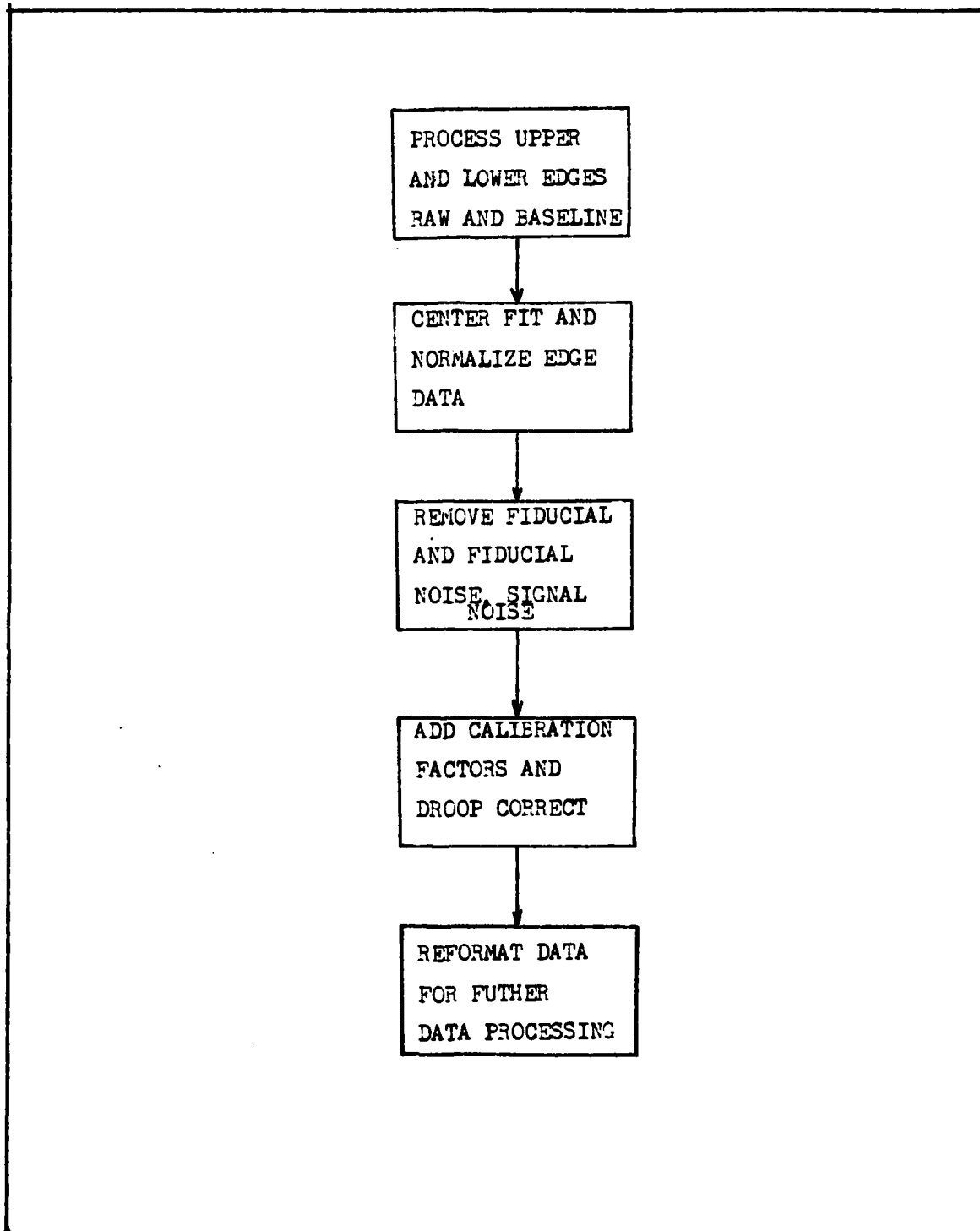


Fig 41. Flow Chart, Initial Signal Processing
A-2

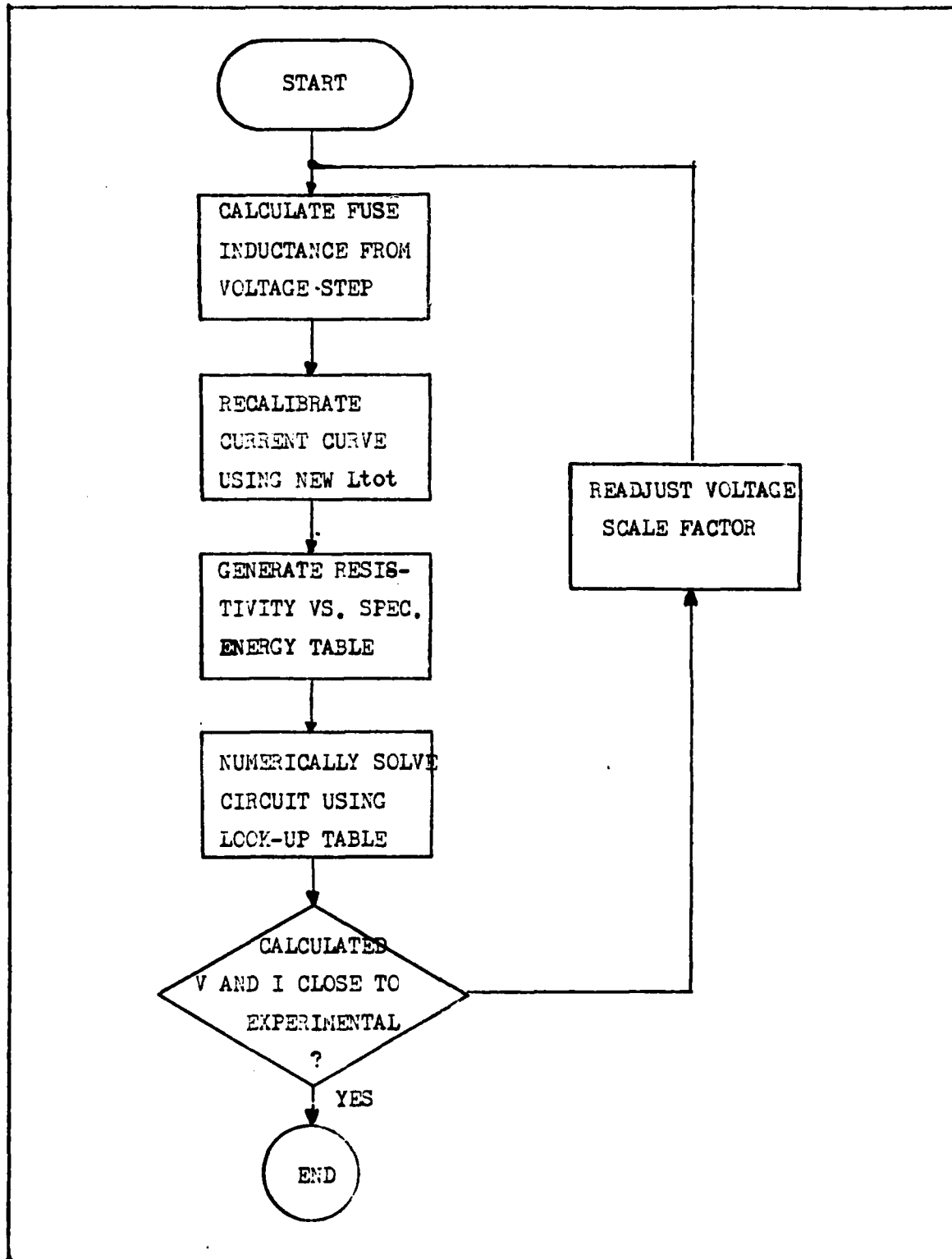
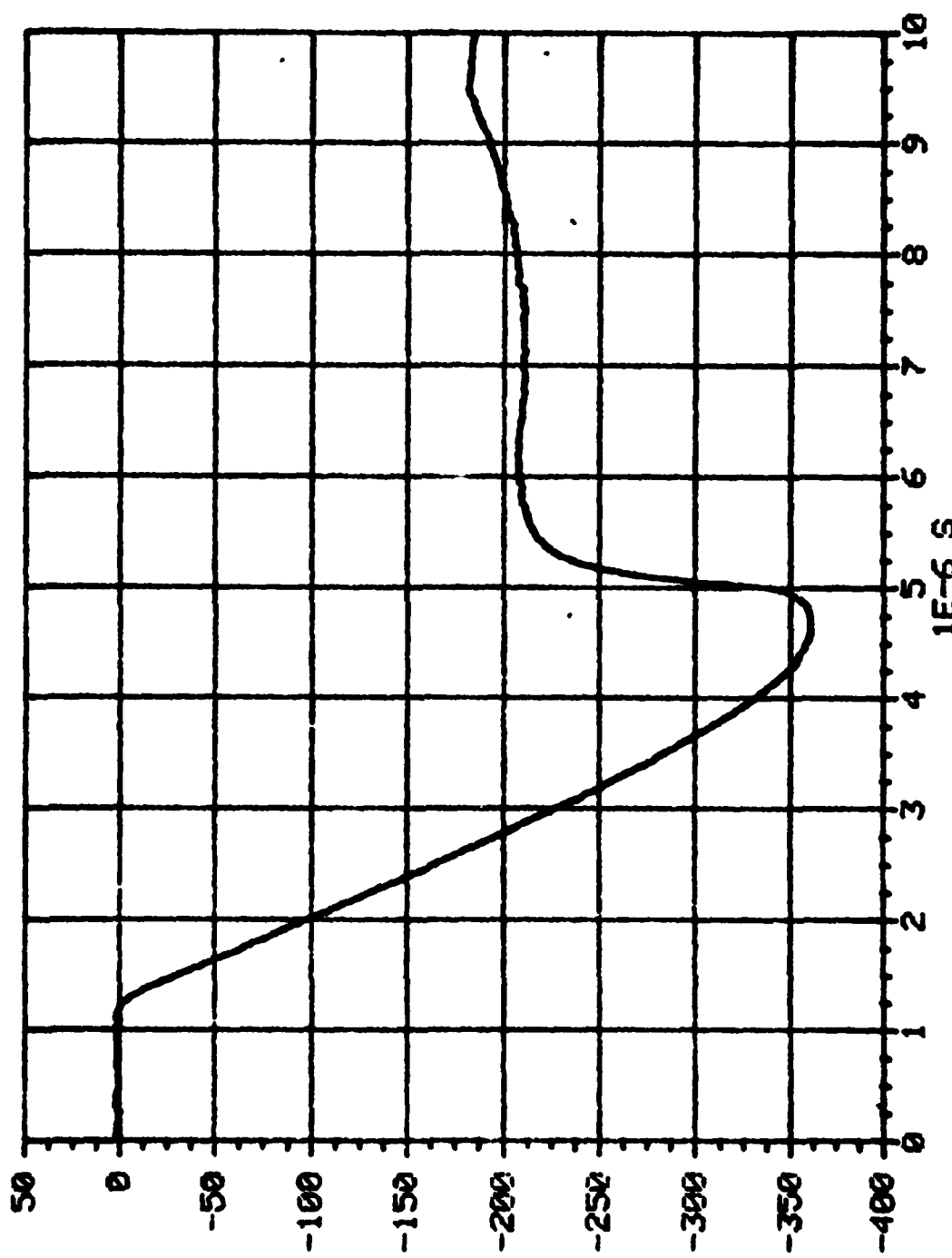


Fig 42. Flow Chart, Full Data Processing

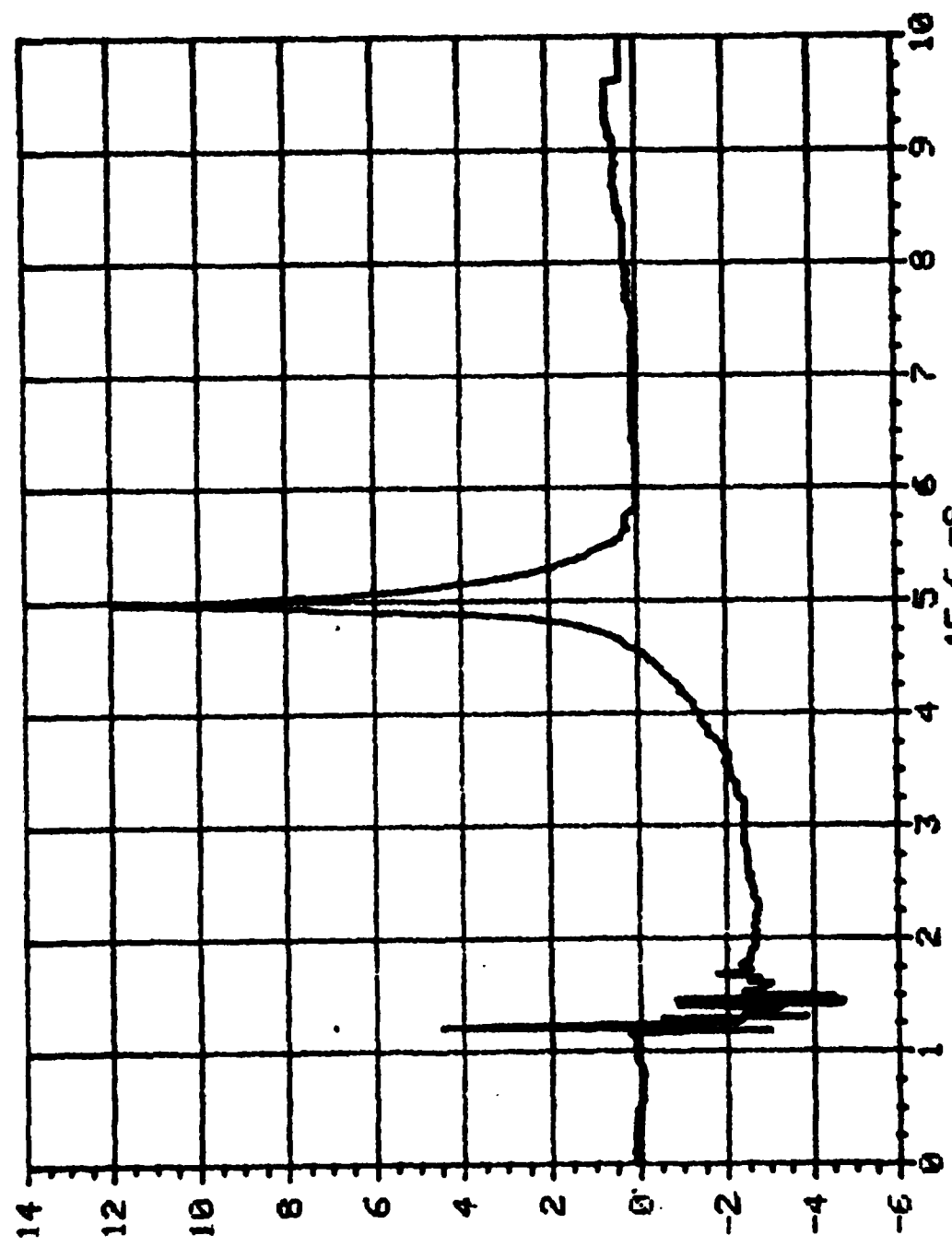
AL FUSE IN SAND, 47KU, 8X44CM, 15 JULY 82
BANK CURRENT $T_{H1} = 2.22 \times 10^{-6}$ A
 $1E-3 = 0.1$



B-2

Fig 43. Bank Current, Restrike

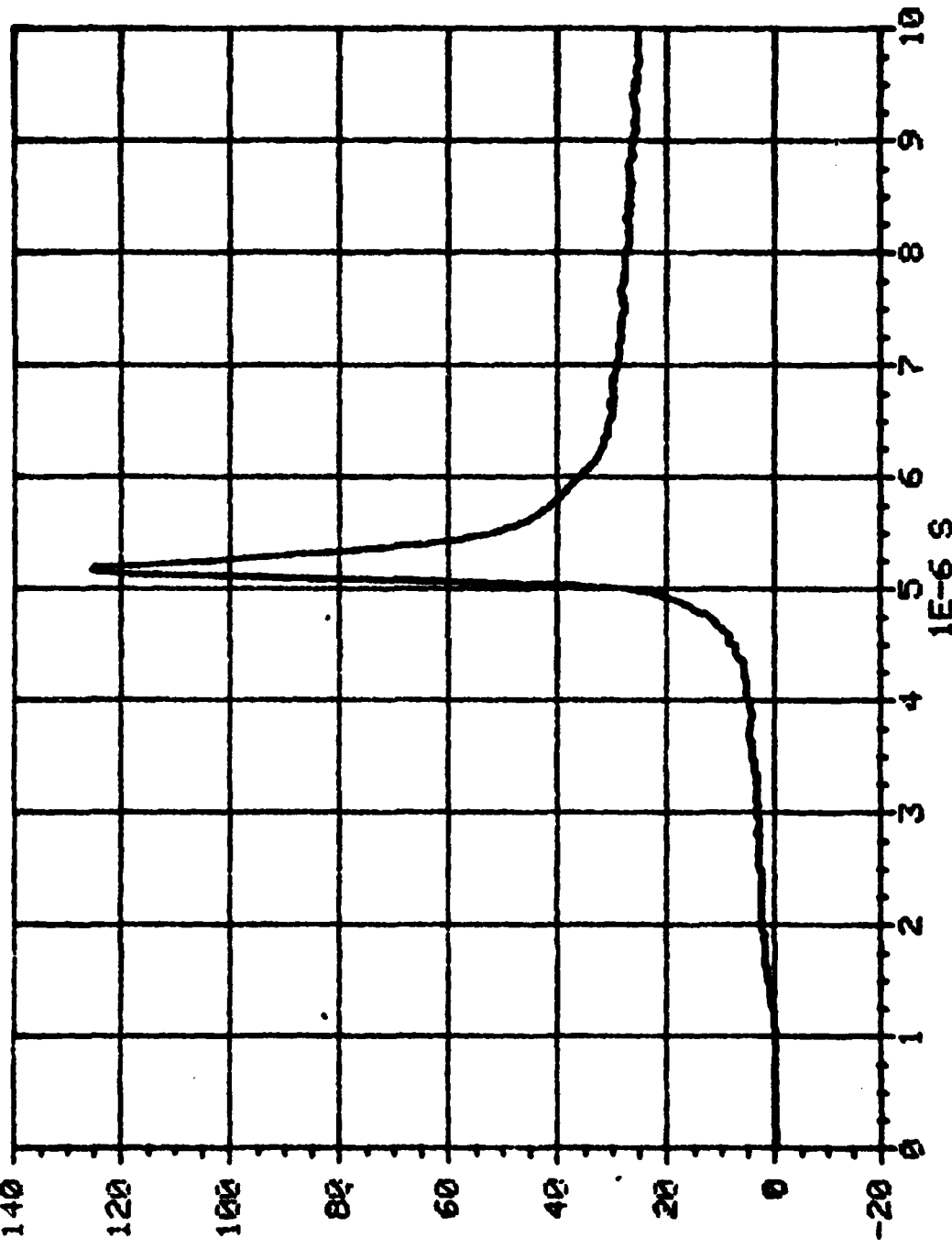
AL FUSE IN SAND, 47KU, 8X44CM, 15 JULY 82
T_{0.5} = 9
1E⁹ = 10
IDOT FUSE



B-3

Fig 44. Fuse dI/dt , Restrike

AL FUSE IN SAND, 47KV, 8X44CM, 15 JULY 82
FUSE VOLTAGE 10^3 =
2. 1000VIE-15



B-4

FIG 45. Fuse Voltage, Restrike

COPPER FUSE IN AIR (5.5X40 CM) AT 45KV, 19 AUG 82, JC BUICK
FUSE VOLTAGE 10^3 THI = 2.1600E-15

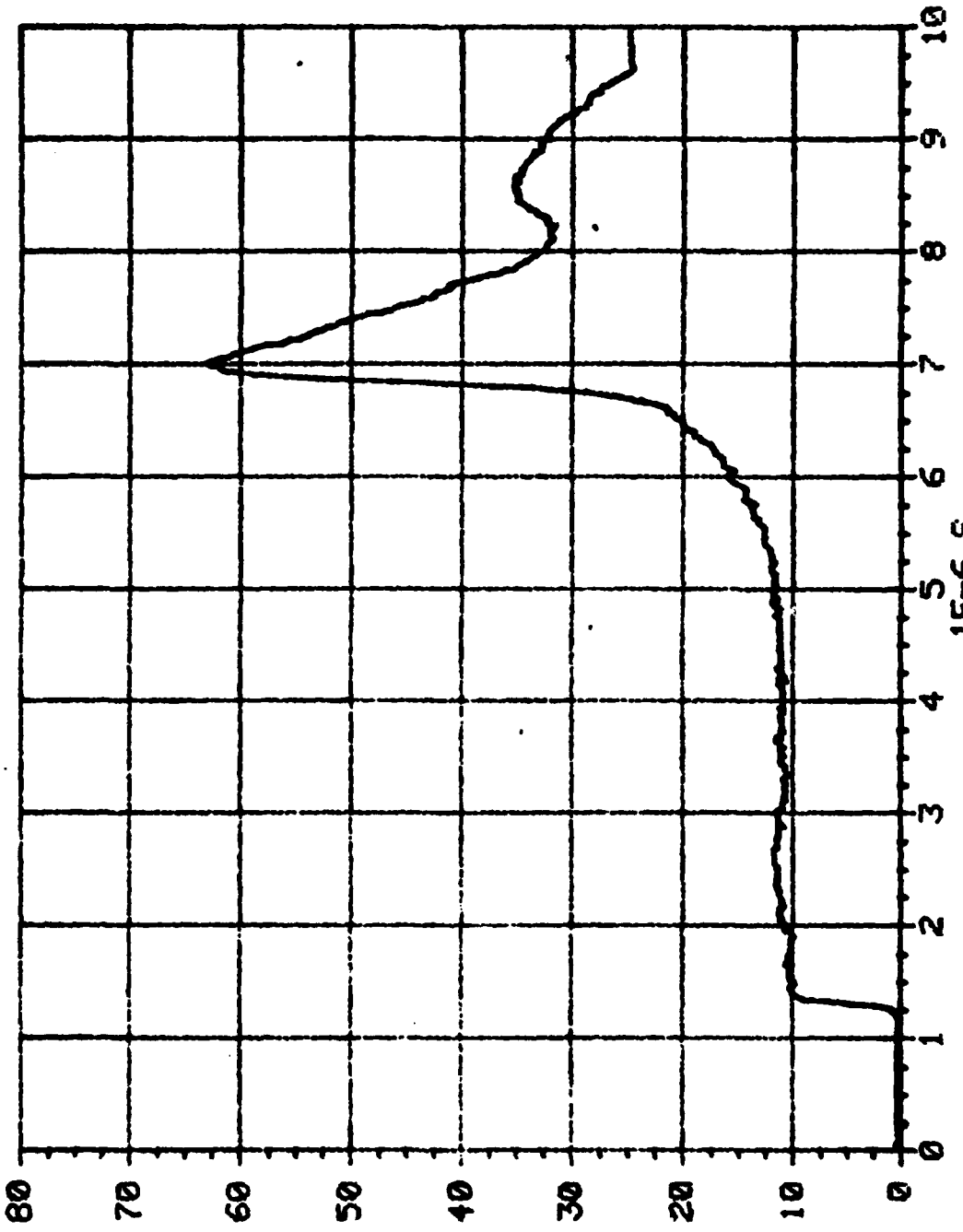


Fig 46. Fuse Voltage, Air Quench

COPPER FUSE IN AIR (5.5x40 CM) AT 45KV, 19 AUG 82, μ C BLOCK
BANK 100T $T_{AL} = 1E-9 s^{-1}$

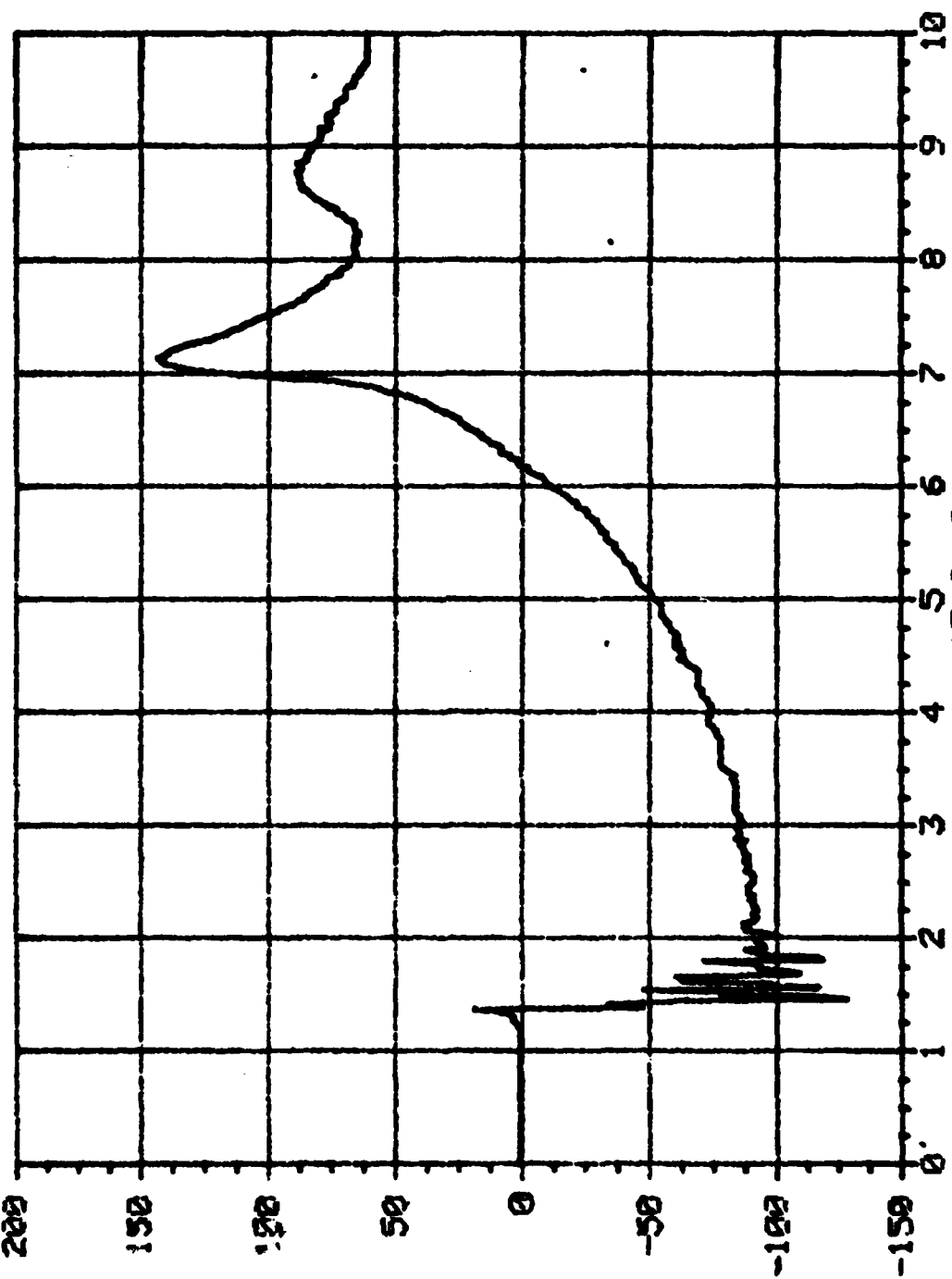
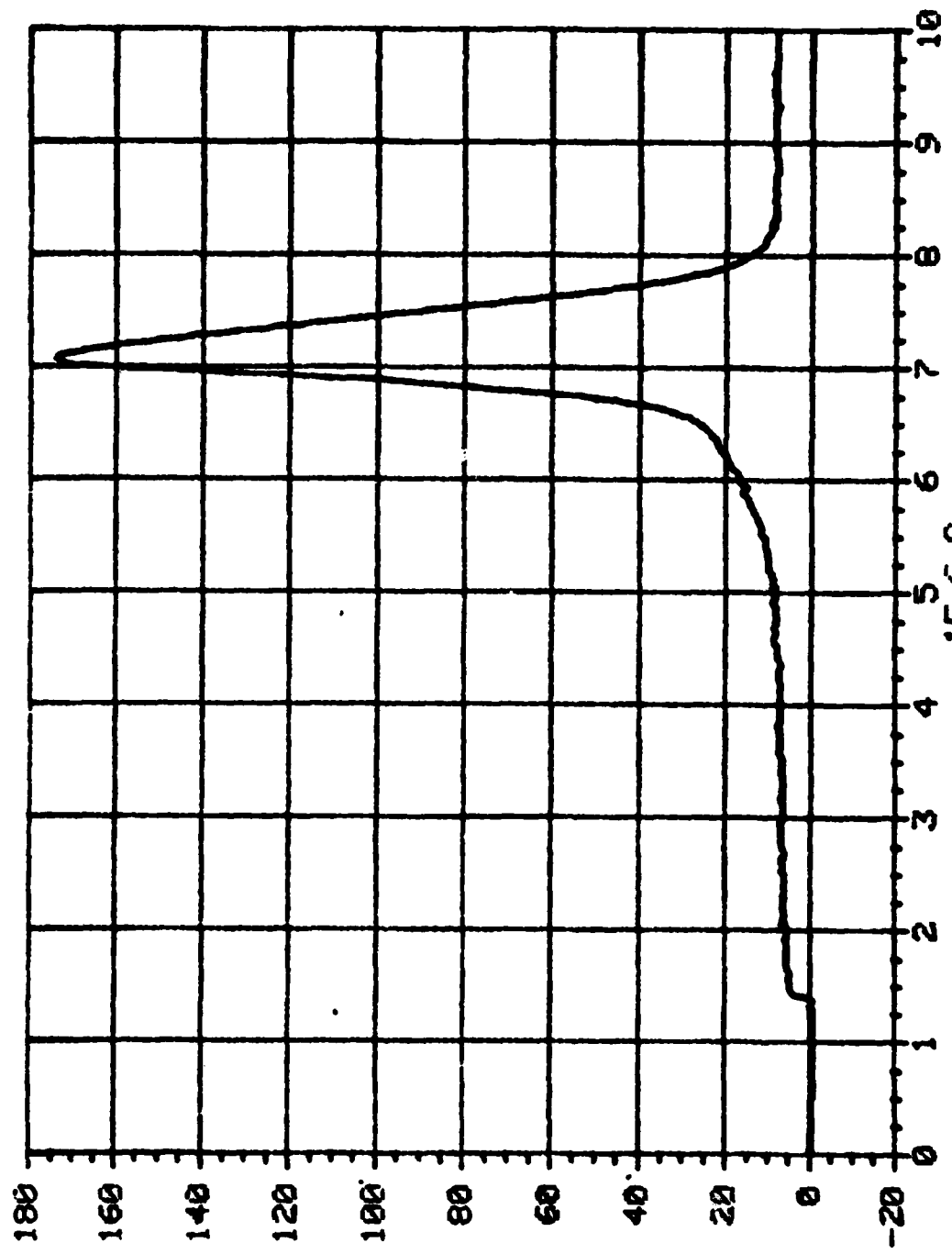


Fig 47. Bank dI/dt , Air Quench

CU FUSE IN SAND, 42 KV, 6X40CM, 11 AUG 82
FUSE VOL TAGE
 $1E^{-3}$ = 1
1E 3 = 1000



CU FUSE IN SAND, 42 KU, 6X40CM, 11 AUG 82
IDOT BANK
 $T_{HJ} = 1$
 $1E-9 = 1$

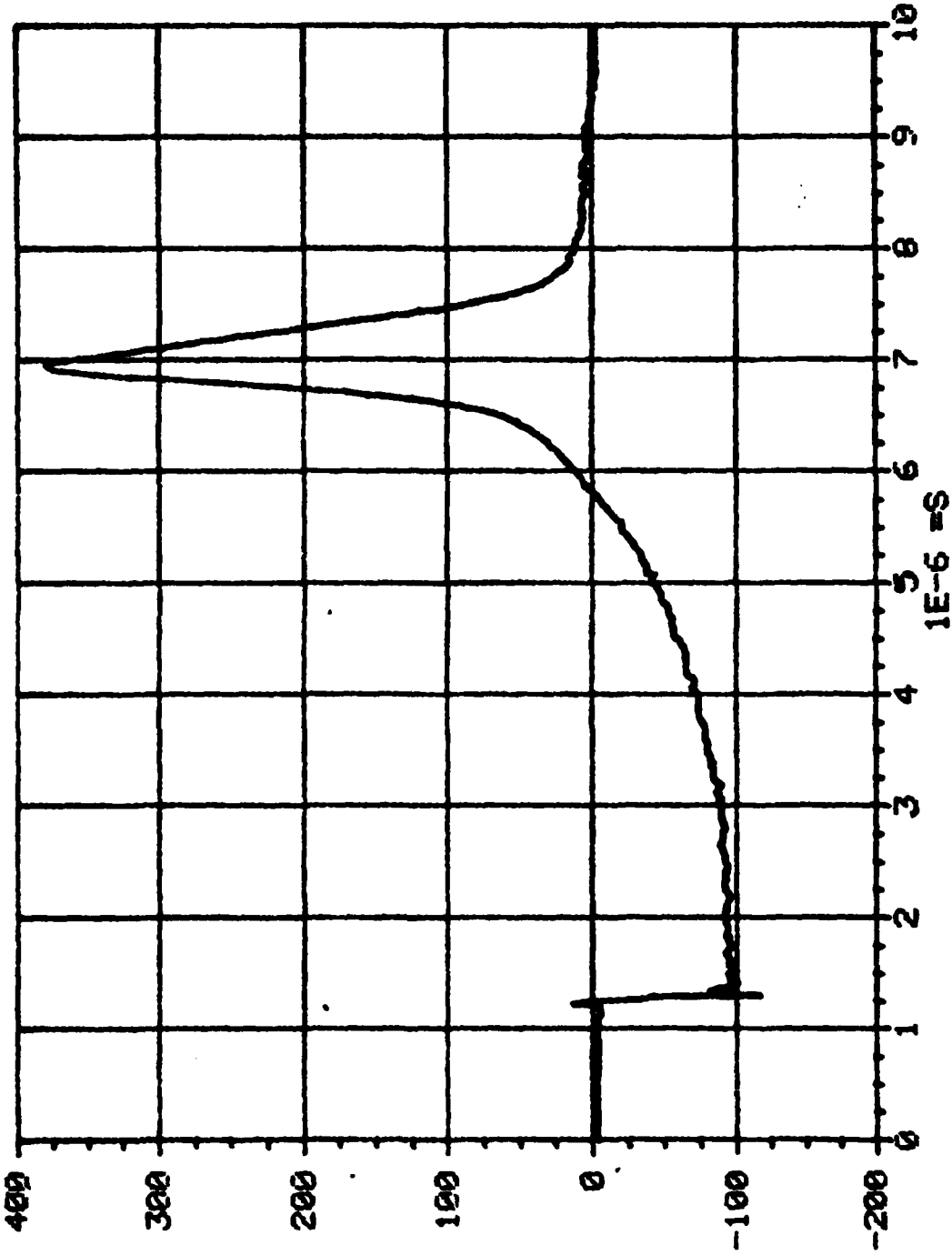


Fig 49. Bank dI/dt

CU FUSE IN SAND, 42 KV, 6X4ACH, 11 AUG 82
BANK CURRENT $1E-3 = 1$

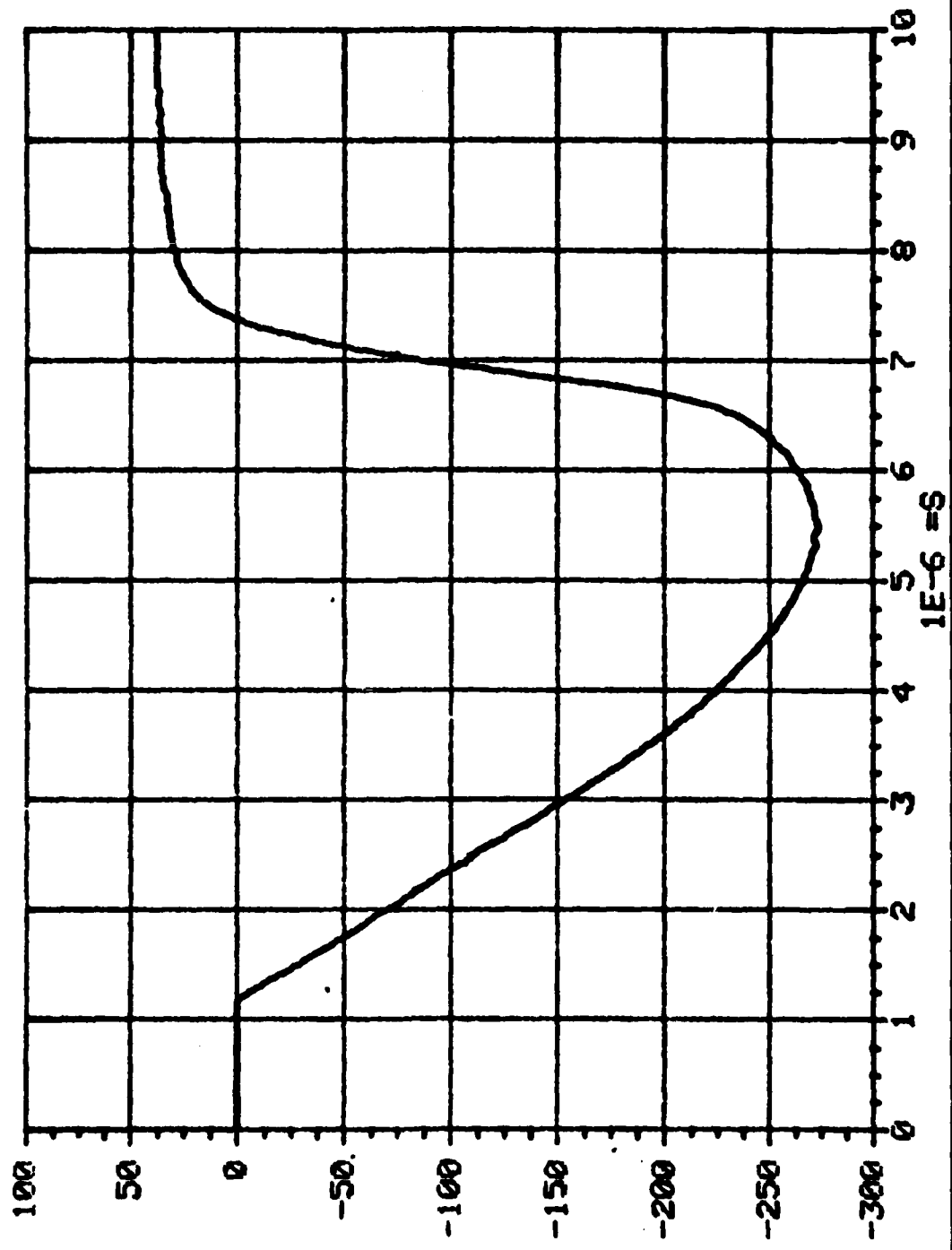


Fig 50. Bank Current, (No Droop Correction)
 $1E-6 = 1$

CU FUSE IN SAND, 42KV, 5X4CM, 9 AUG 82
FUSE VOLTAGE 10^3 = 1
250 200 150 100 50 0

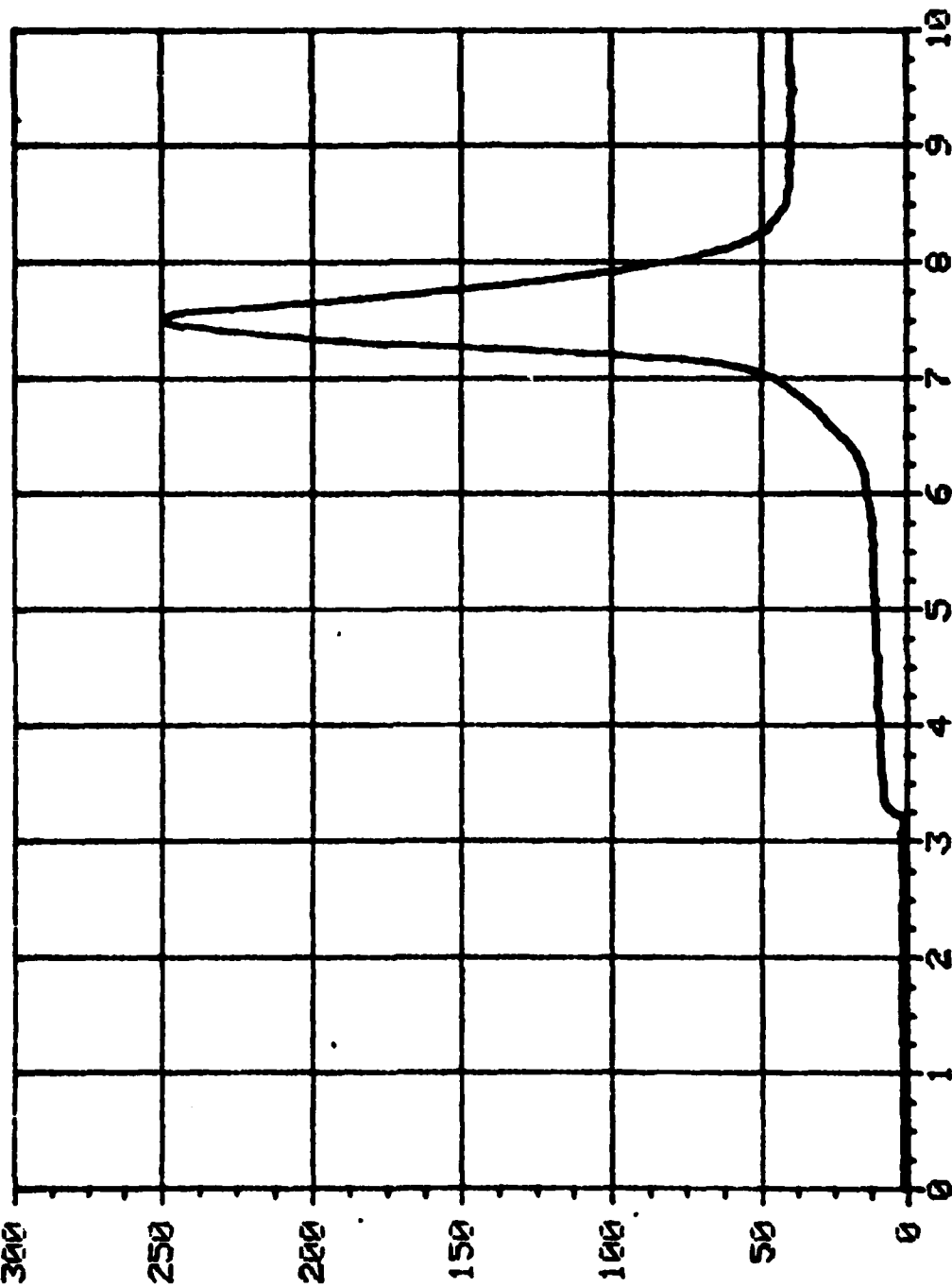


Fig 51. Fuse Voltage

CU FUSE IN SAND, 42KU, 5X40CM, 9 AUG 82
FOOT BANK $10^9 = 1$

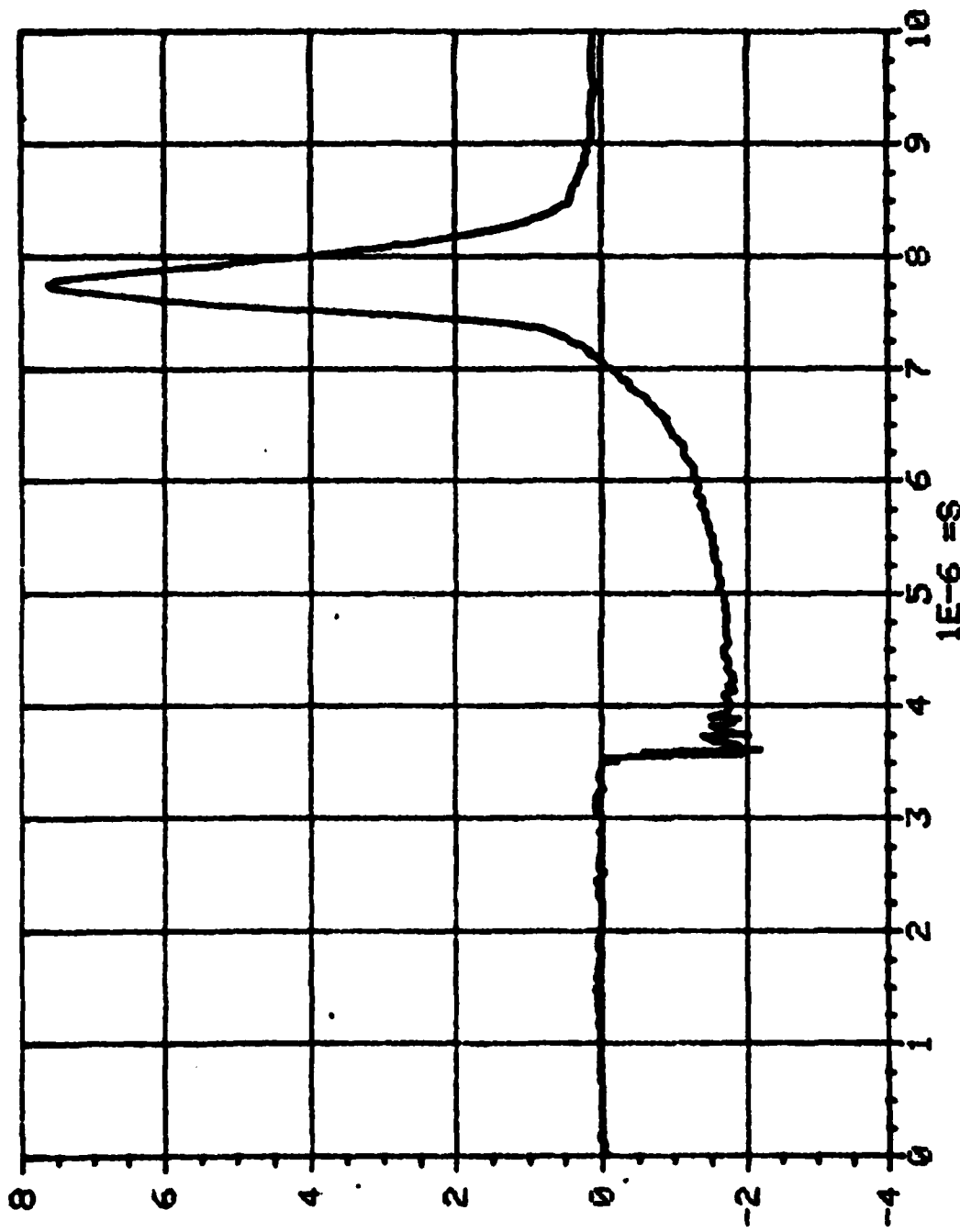


Fig 52. Bank dI/dt

CU FUSE IN SAND, 42KV, 5X40CM, 9 AUG 82
THJL= 2.16E-05
BANK CURRENT 1E-3 A

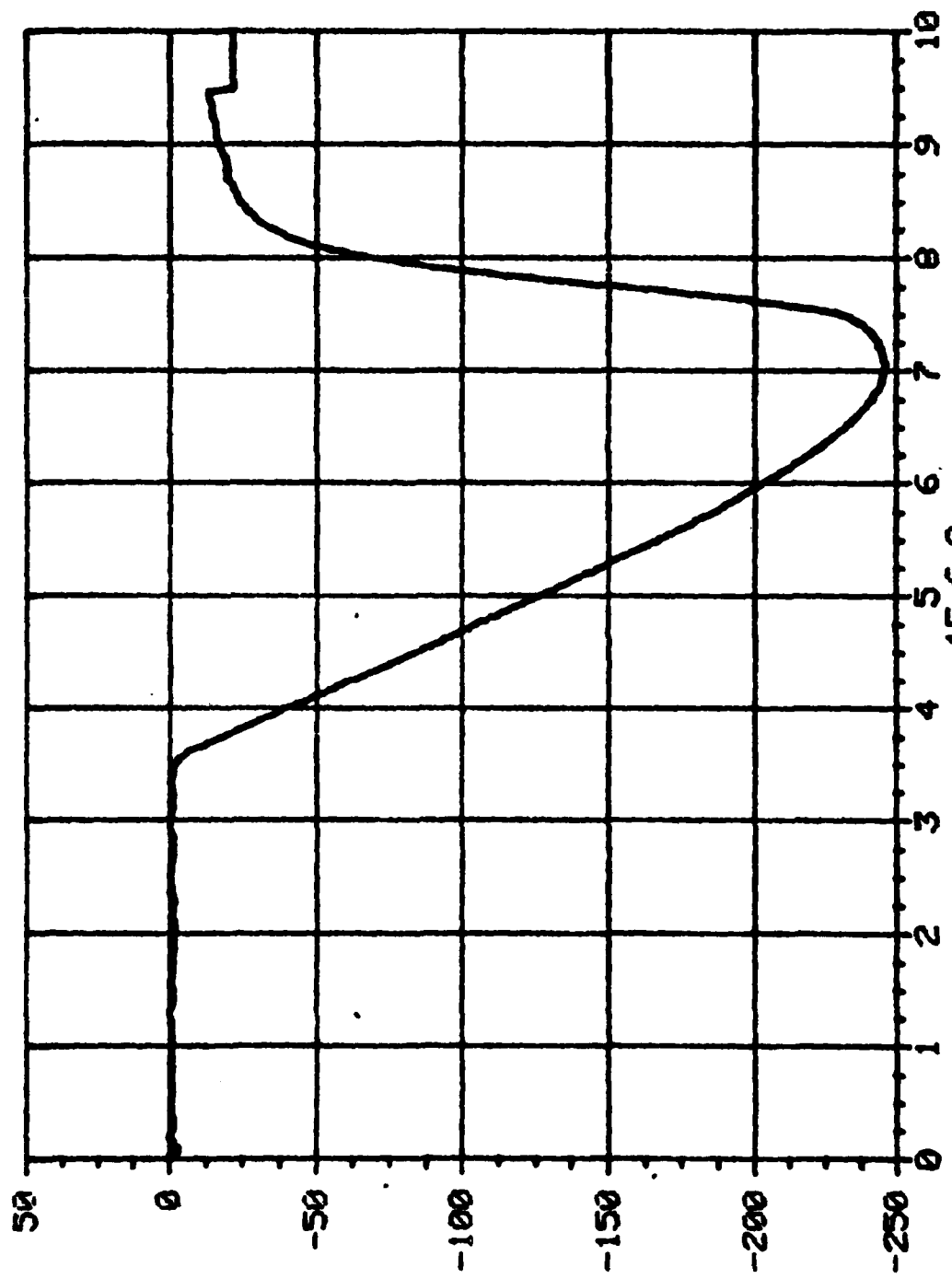
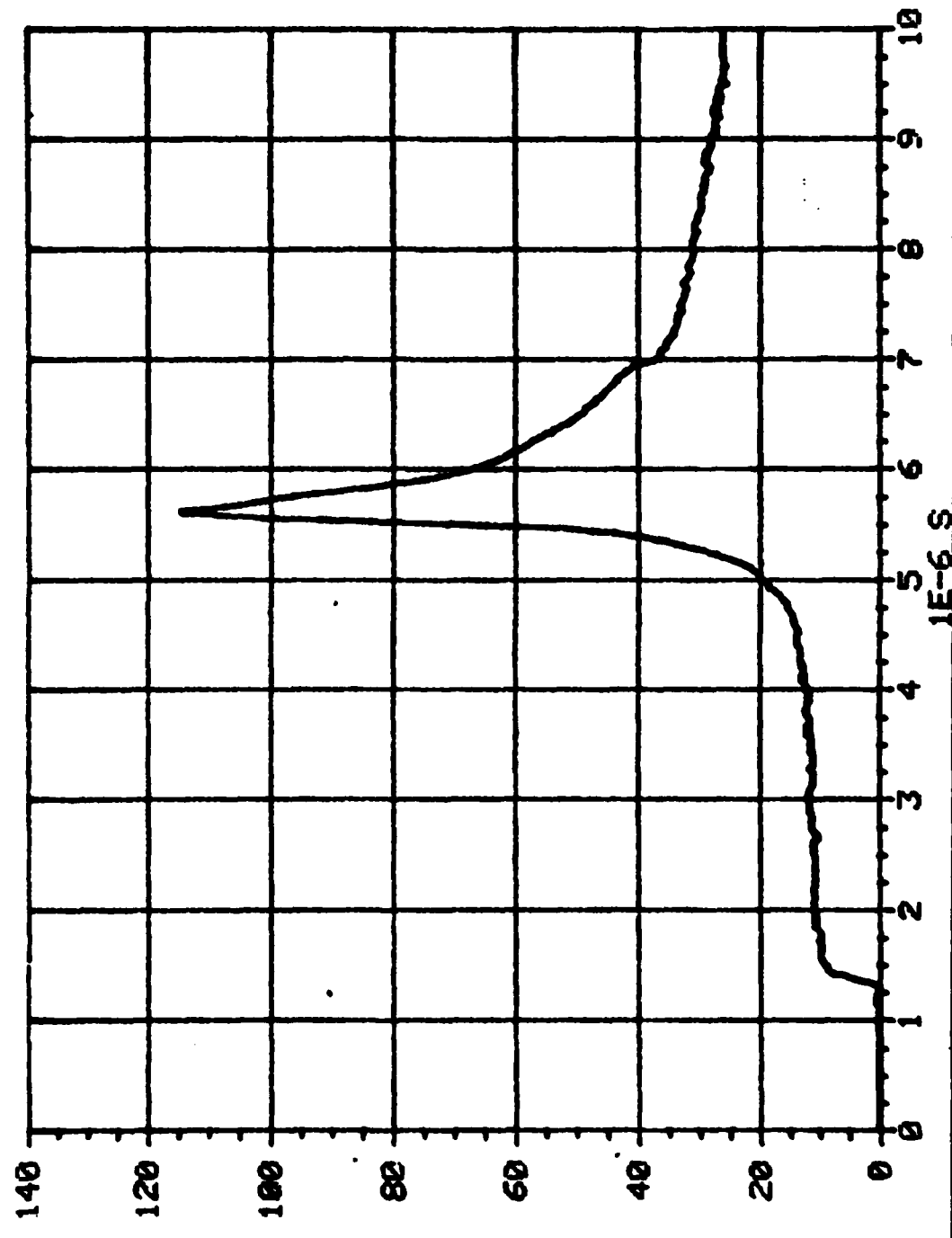


FIG 52. Bank Current

CU FUSE IN SAND, 42KV, 5X20CM, 9AUG 82
FUSE VOLTAGE $1E-3 = 1$
2.20301E-05



CU FUSE IN SAND, 42KU, 5X20CM, 9AUG 82
BANK $\frac{dI}{dt}$ = 1
 $1E9 = 1$

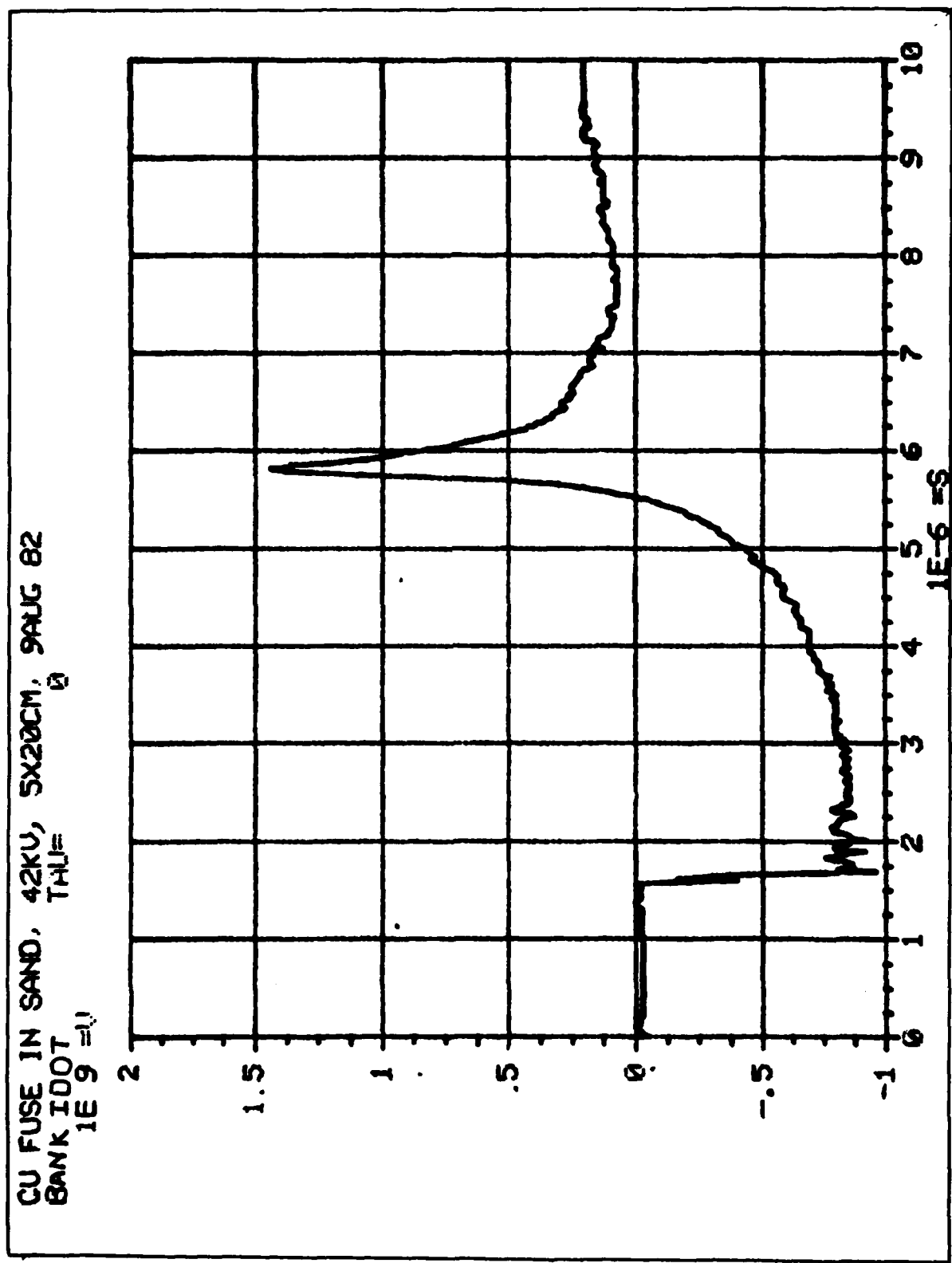


FIG 55. Bank $\frac{dI}{dt}$

CU FUSE IN SAND, 42KV, 5X20CM, 9AUG 82
THU= 2.16801E-05
BANK CURRENT 1E-3

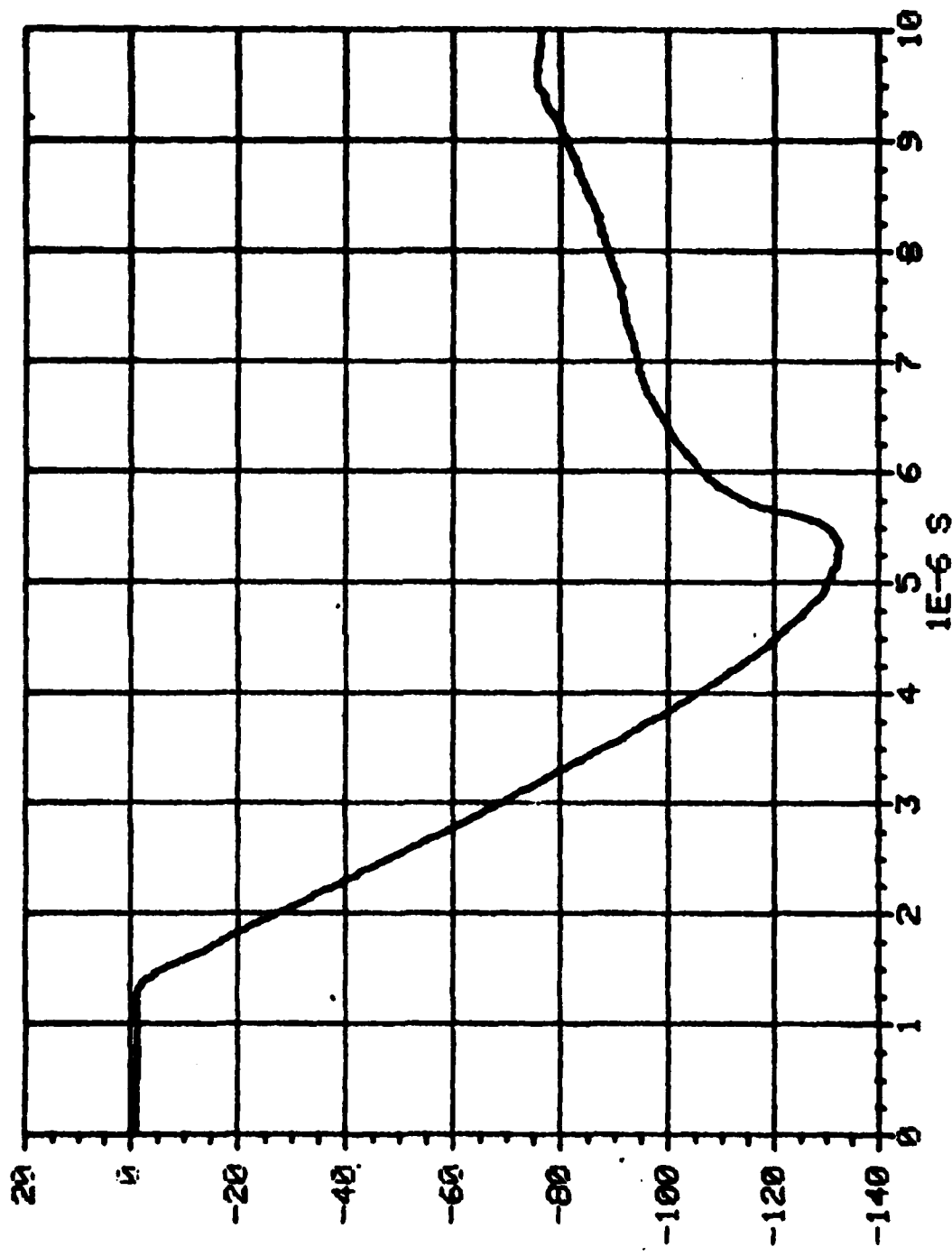


Fig 56. Bank Current

APPENDIX C

This Appendix contains selected processed and preprocessed data that is interesting but not specifically addressed in the text. Several Figures included were processed on the acquisition computer system unlike the data in the Results chapter.

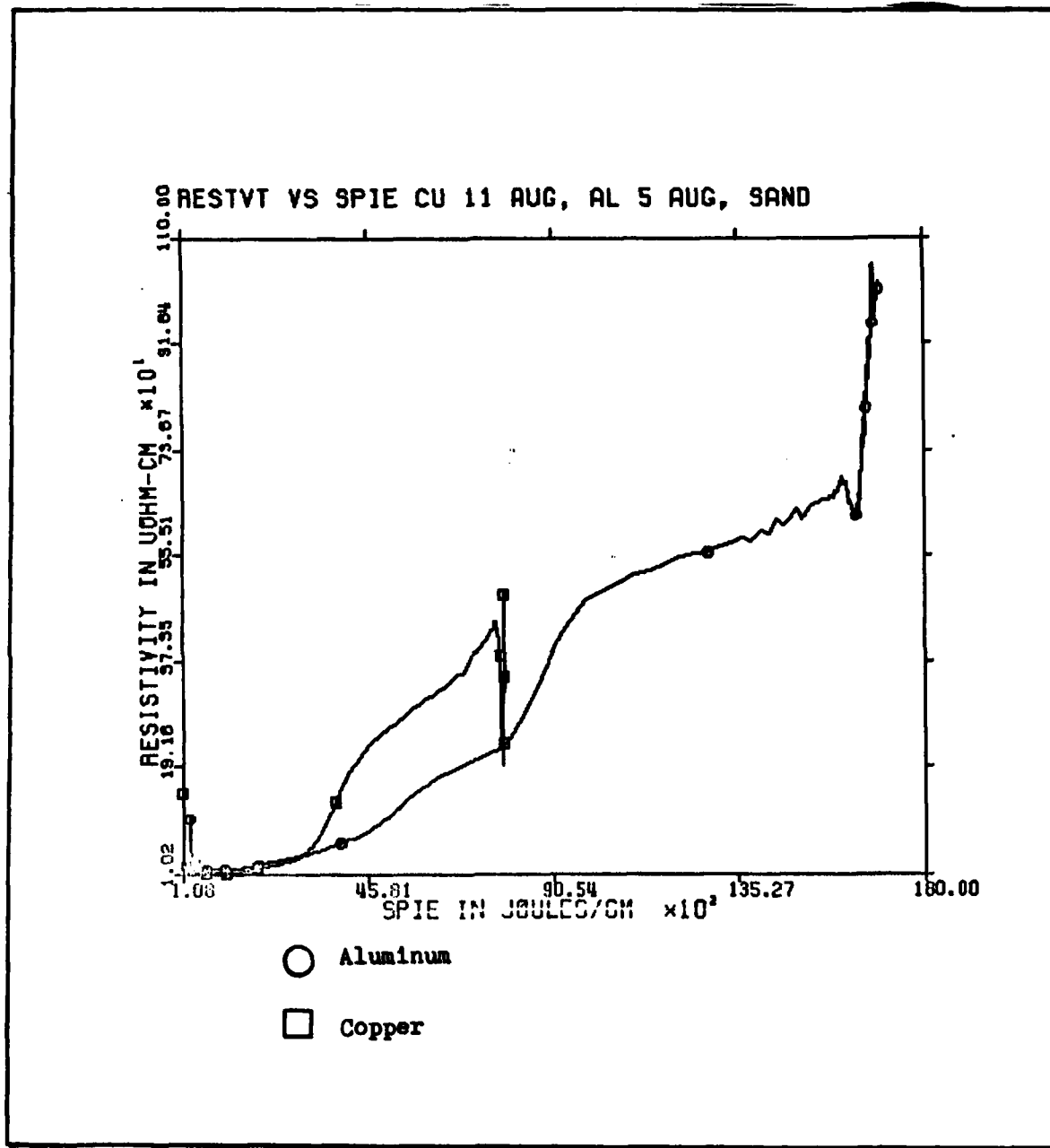


Fig 57. Preprocessed Resistivity Vs. Specific Energy

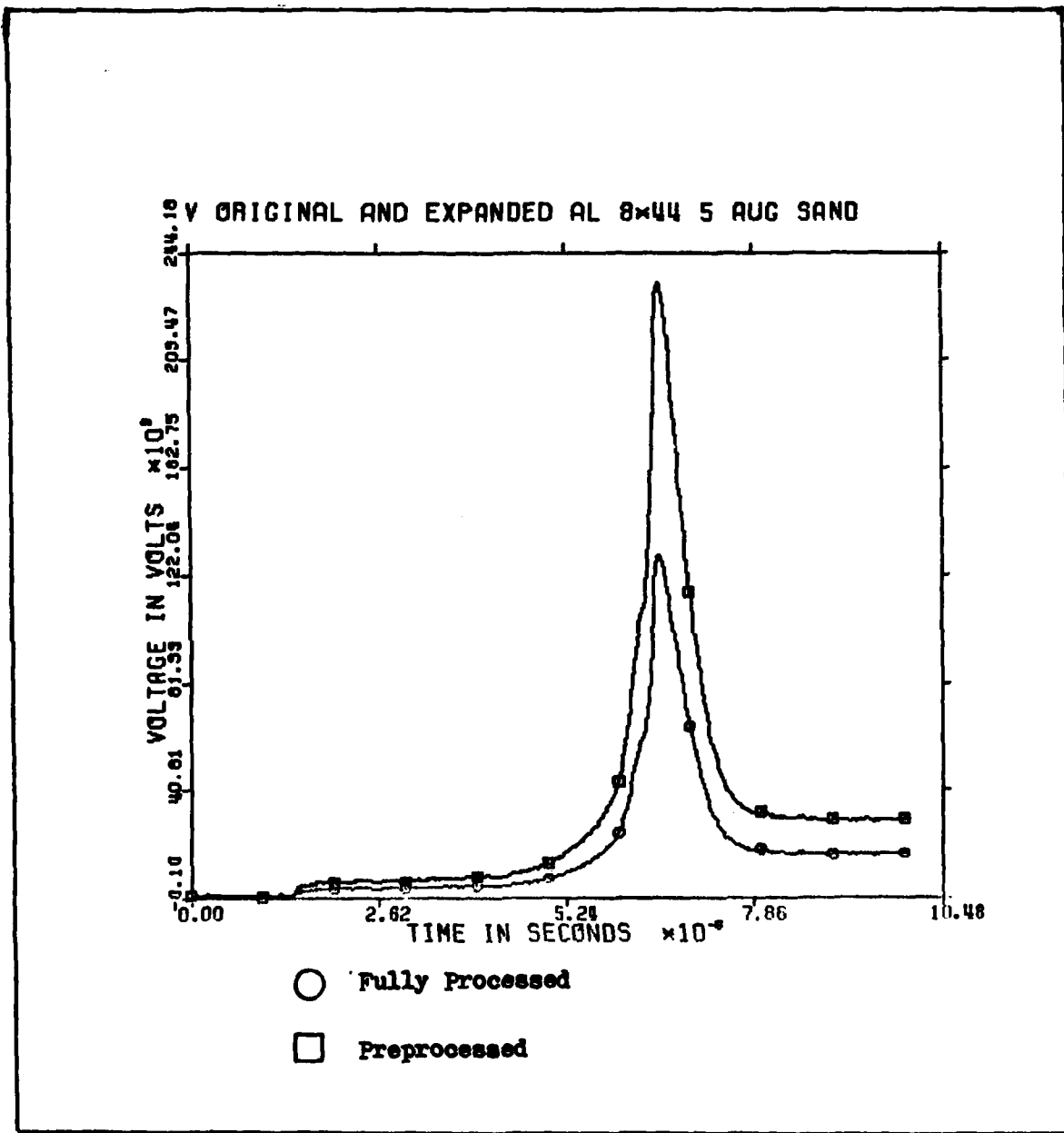


Fig 58. Original and Processed Fuse Voltage

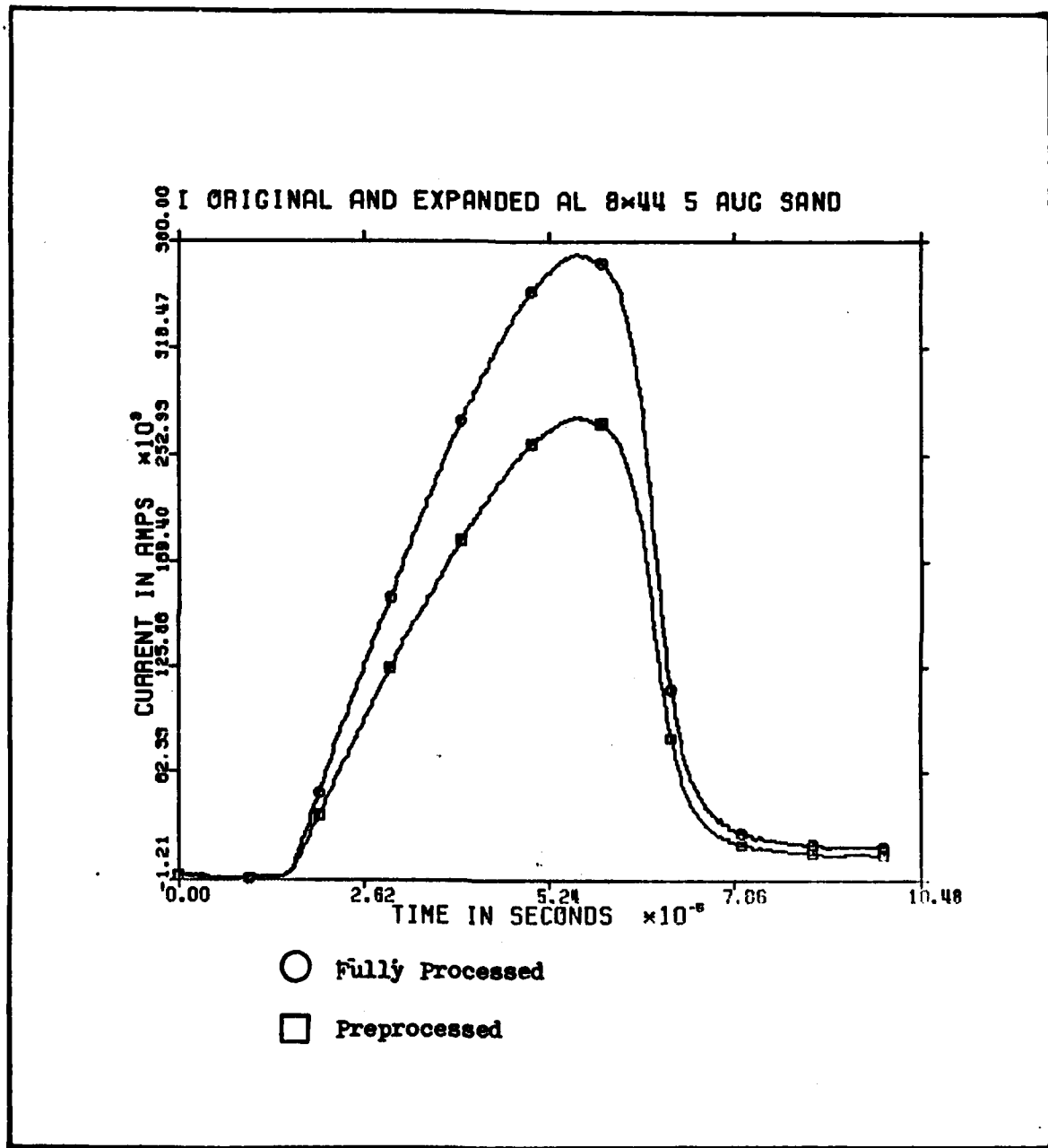


Fig 59. Original and Processed Fuse Current

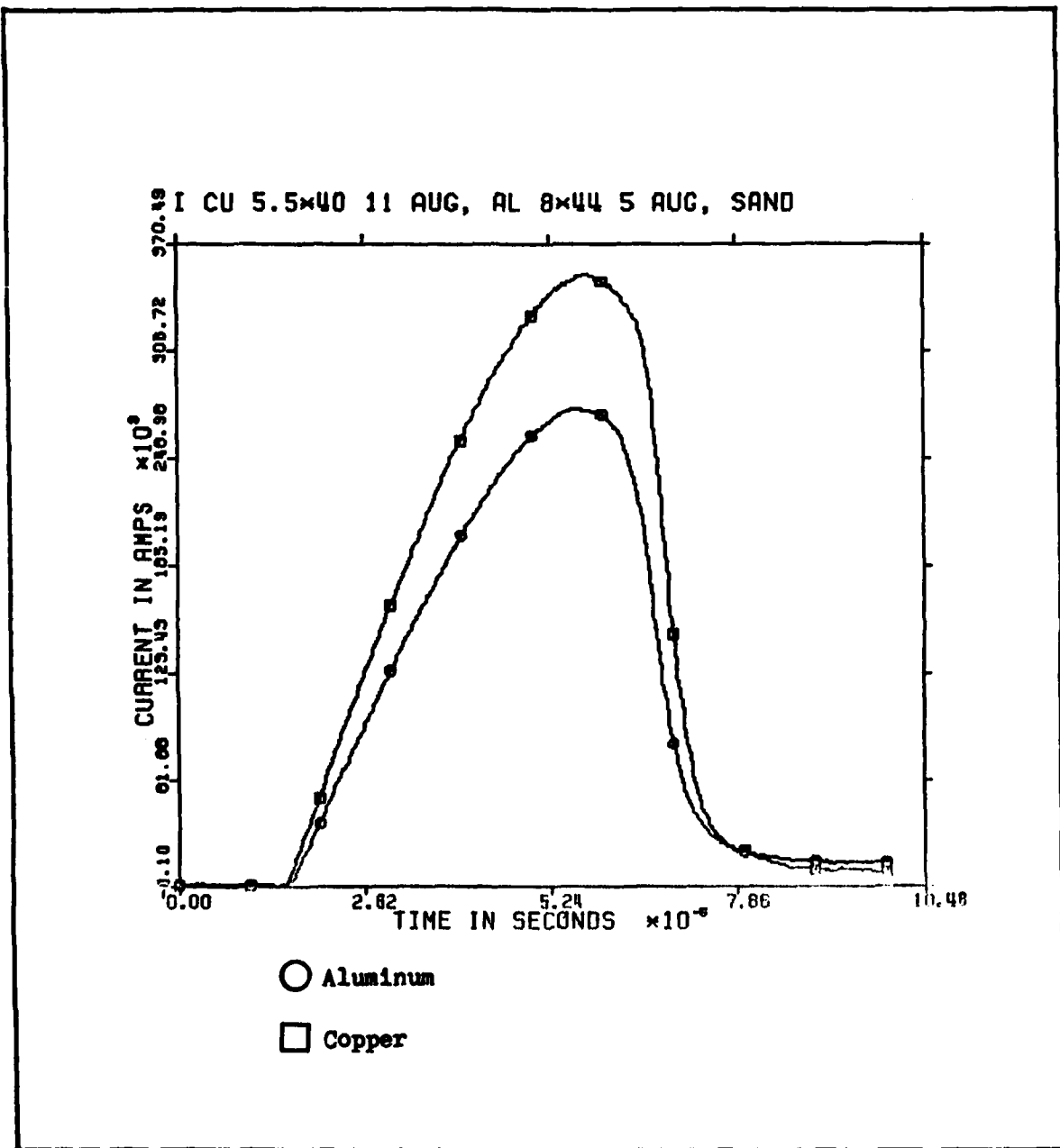


Fig 60. Original Fuse Currents

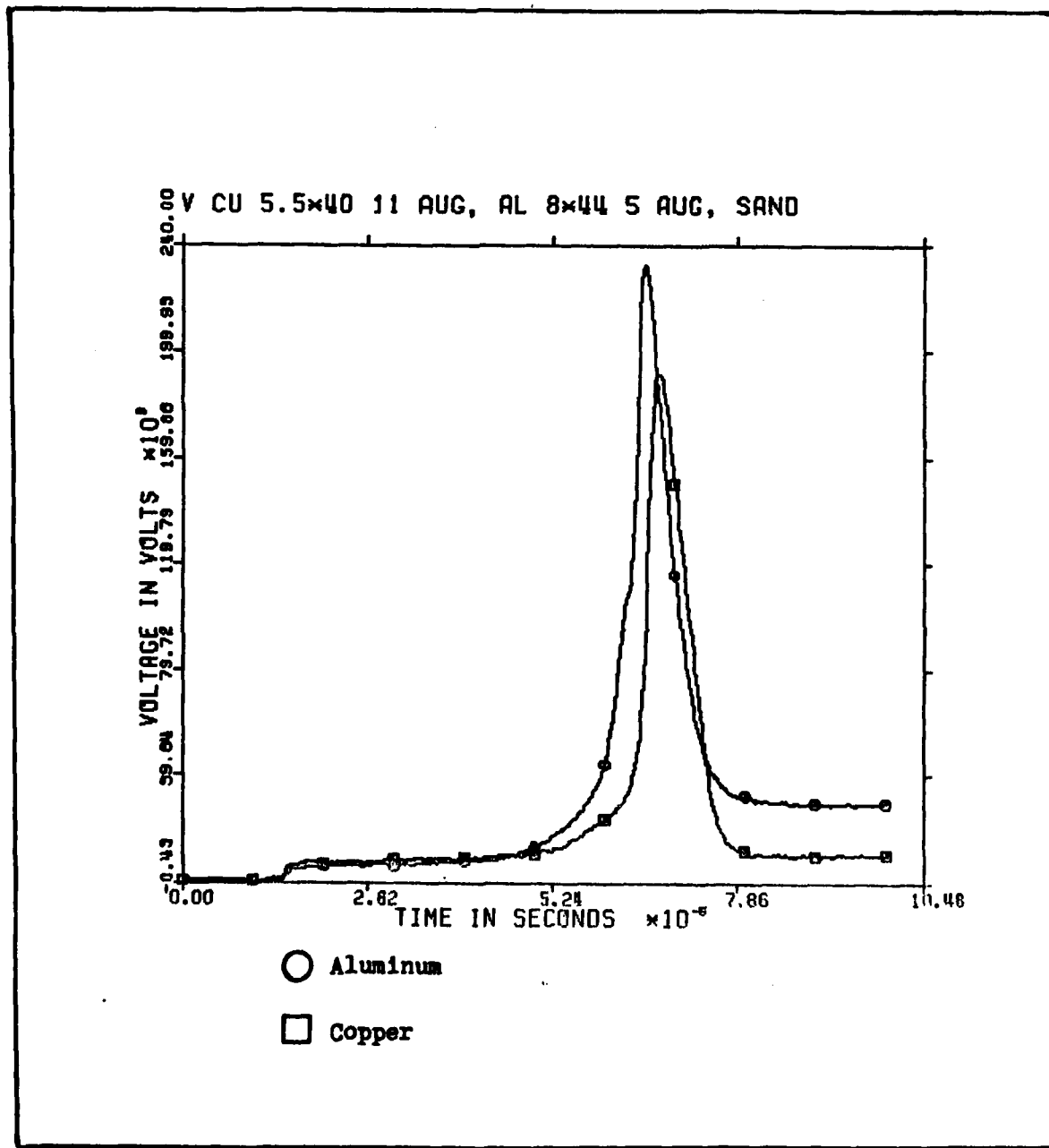


Fig 61. Original Fuse Voltages

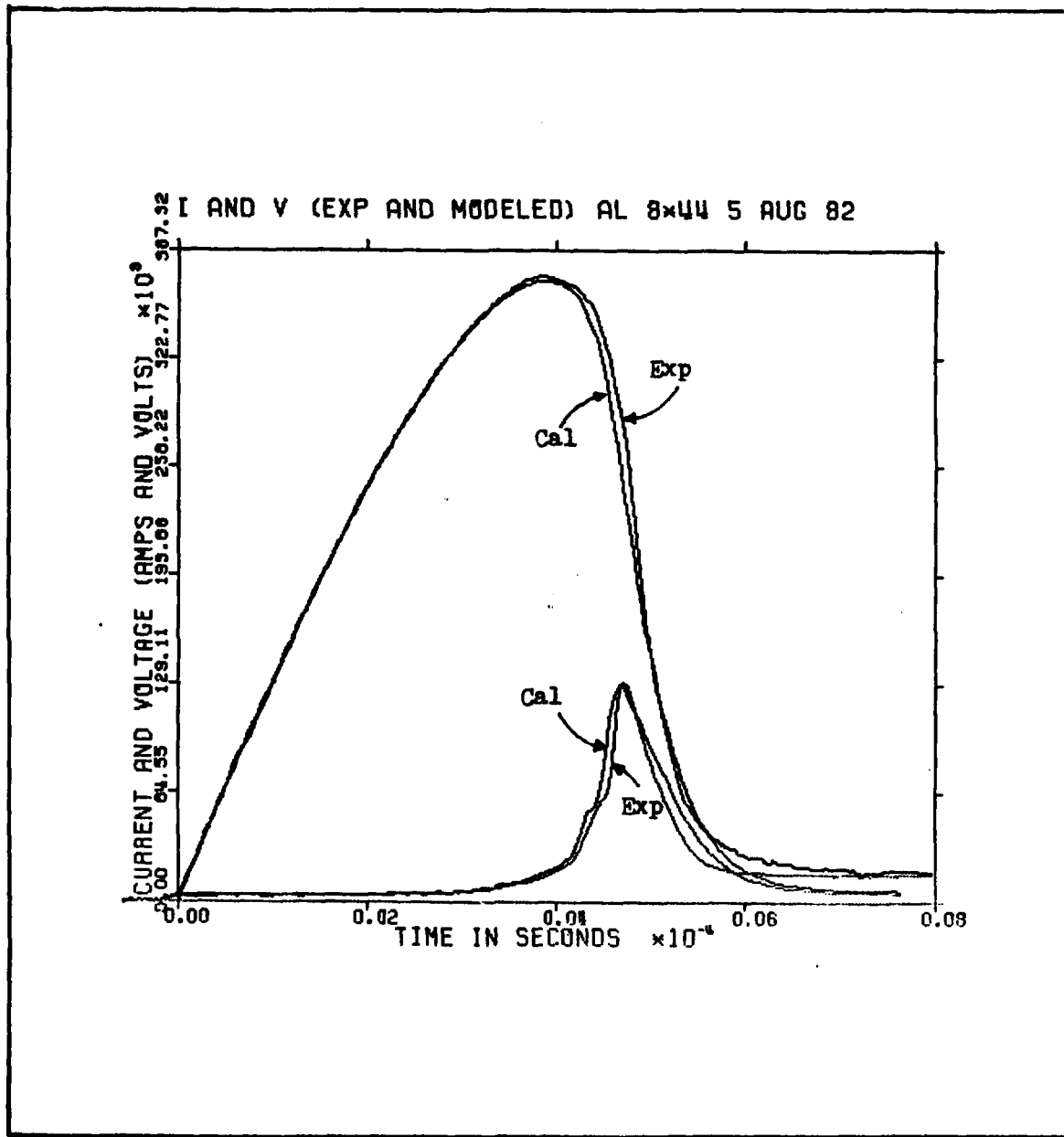
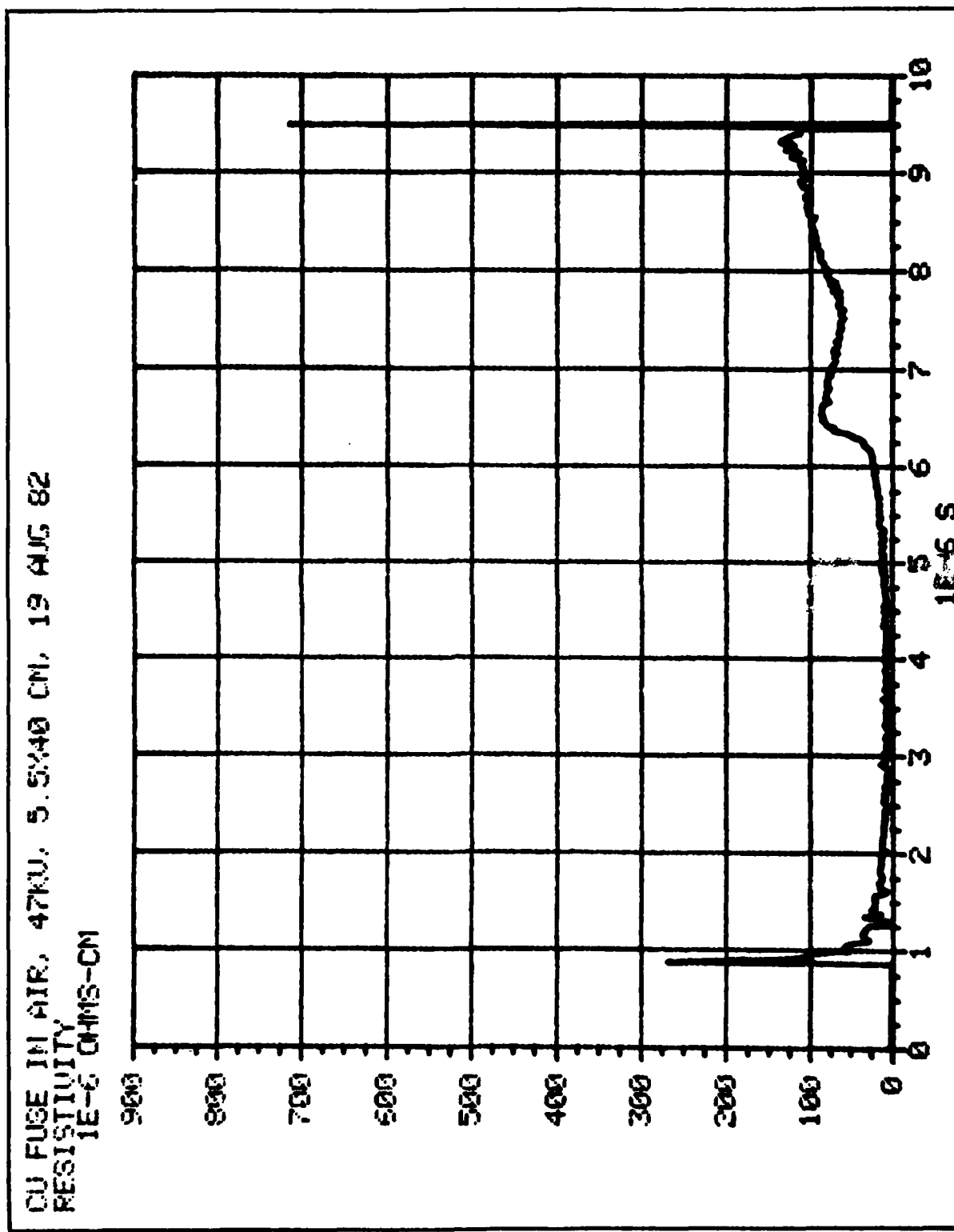


Fig 62. Processed and Calculated Fuse Voltage and Current



C-8

Fig. 63. Resistivity, Copper Fuse in Air

CU FUSE IN AIR. 4710. 5.5X40 CM. 12 AUG 82
MULTIPLY CURRENT - VOLTAGE IS DOTTED
1E-3 = 1

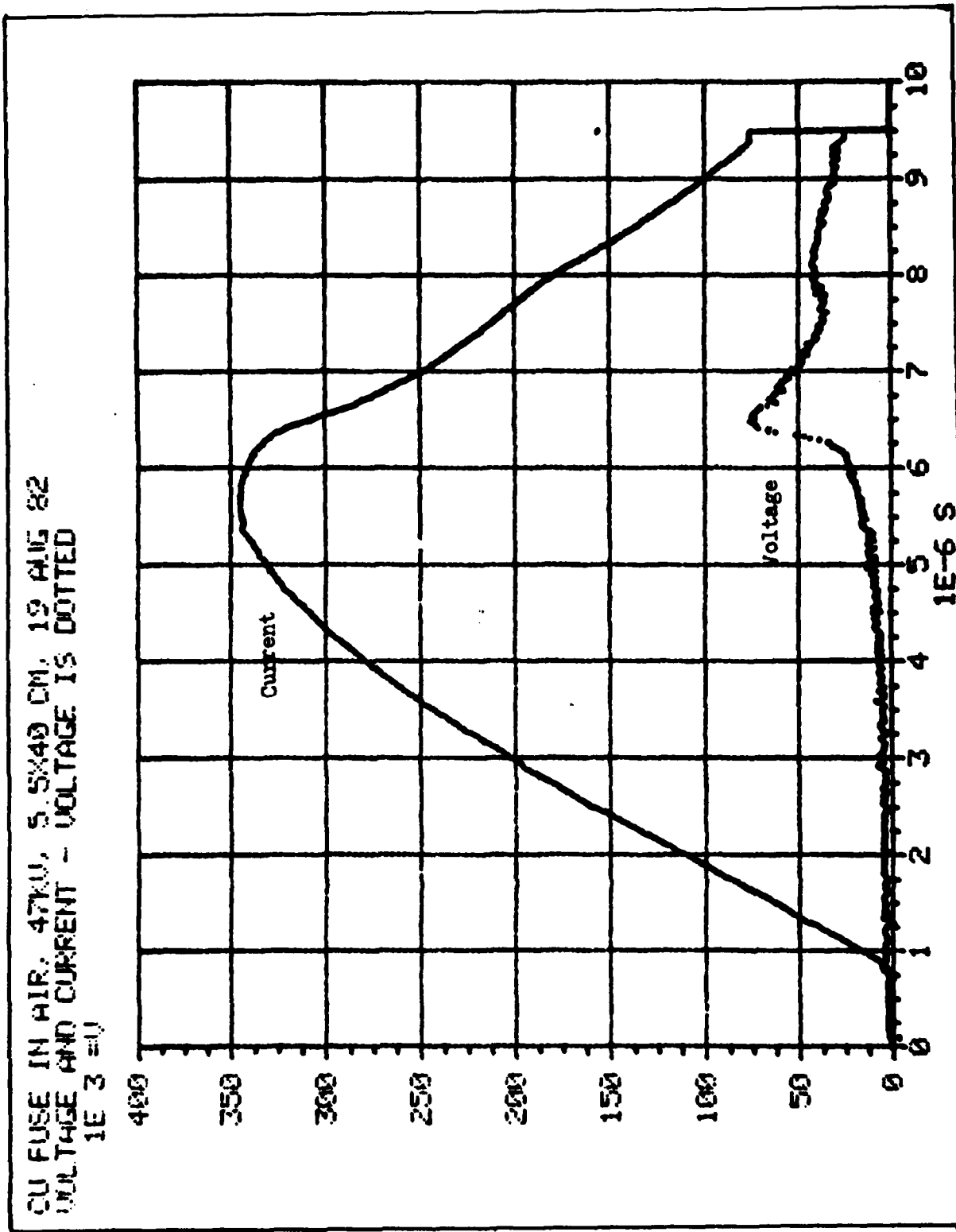


Fig 6. Voltage and Current, Copper Fuse in Air

AL FUSE IN SAND AT 47KU, 8%44 CM, 13 SEP 82
REFLECTIVE TIMING OF RESISTANCE, CURRENT AND VOLTAGE

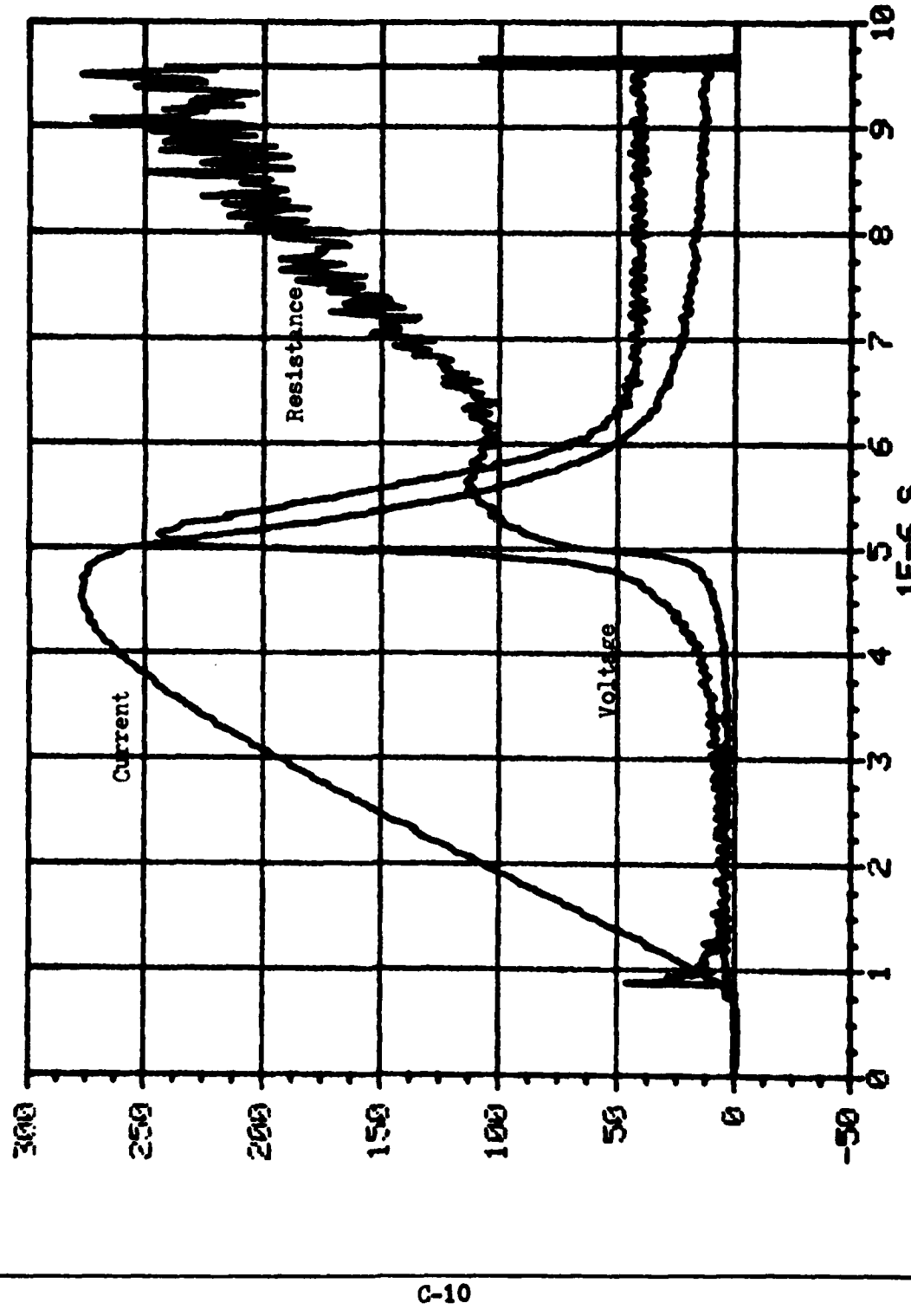


Fig 65. Reflective Timing, Voltage, Current, And Resistance

AL FUSE IN SAND AT 42KU, 8X44CM, 14 SEP 82
MAXIMUM AVAILABLE ENERGY, 1E-3 JULES
1E-3 JULES

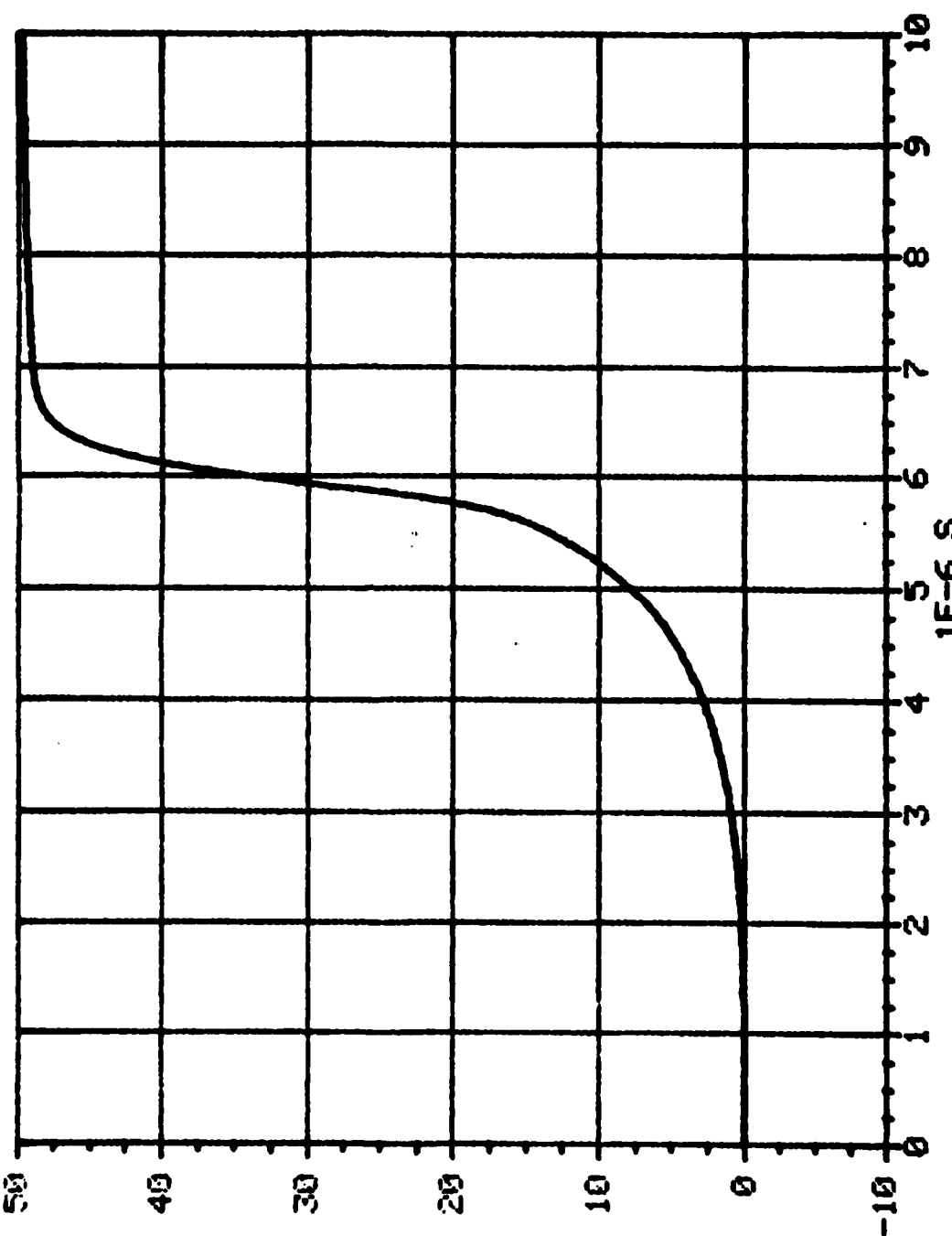
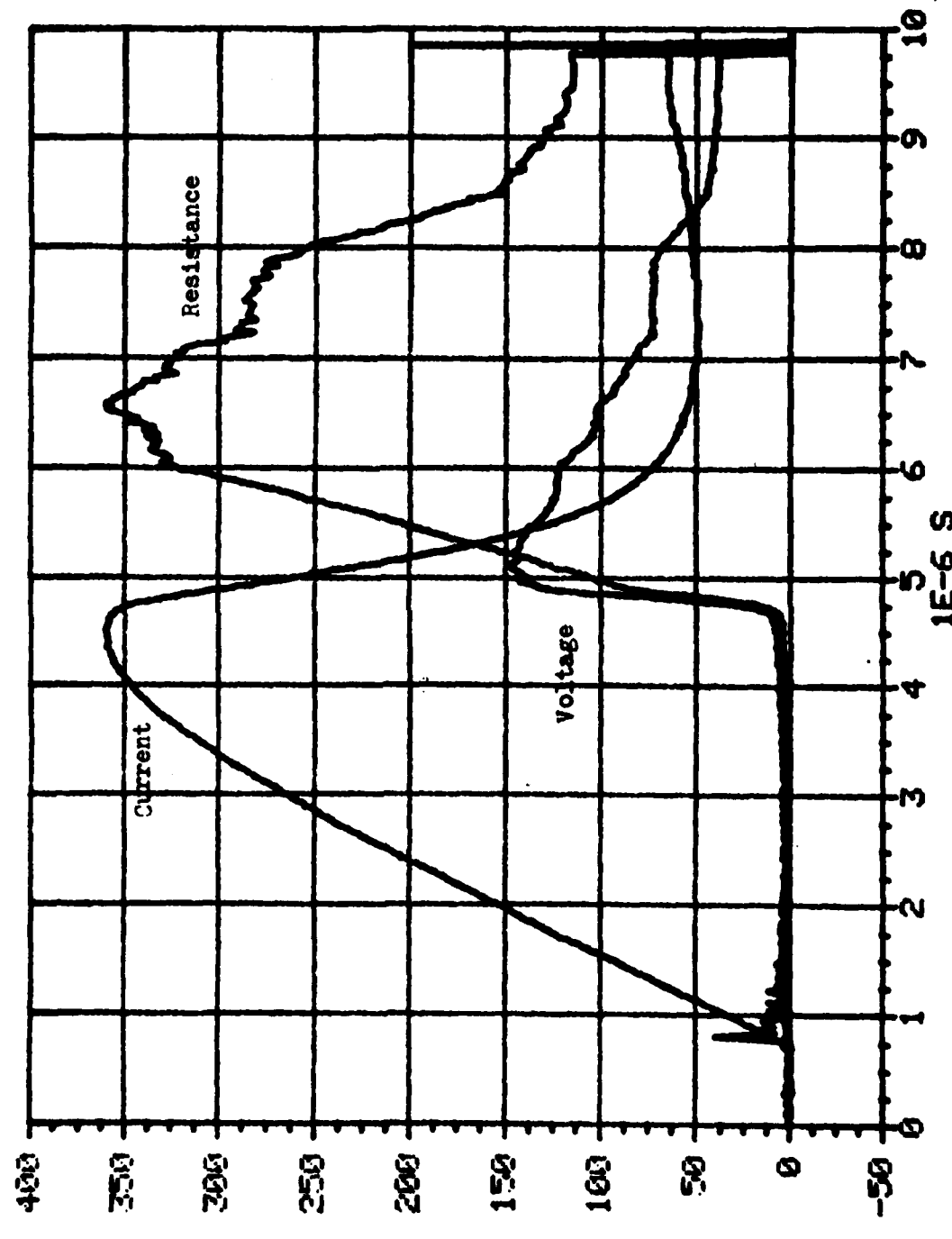


Fig 66. Fuse Energy (Energy Exceeds Max Available Energy Due To Cal. Errors)

AL FUSE IN COLD SAND, 47KU, 3X44CM, 27 JULY 82
RELATIVE TIMING, 1E 3 = 0



C-12

Fig 67. Relative Timing, Voltage, Current, and Resistance

VITA

Jerry Carroll Bueck was born on 16 October 1945 in Portsmouth, Virginia. He graduated from high school in 1964 and subsequently enlisted in the Air Force. After attending many colleges including Old Dominion University, Colorado State College, and the University of Colorado he received his degree in Electrical Engineering from New Mexico State University in 1973. Upon graduation he was commissioned a second lieutenant in the United State's Air Force after attending Officer's Training School. He then served as an Avionics Maintenance Officer at Myrtle Beach AFB, SC, and as an Aircraft Maintenance Officer at Yokota AB, Japan until he was reassigned to Edwards AFB, Flight Test Center, CA, as an Instrumentation Engineer. He entered the School of Engineering, Air Force Institute of Technology in June 1981.

Perminent address: 408 Beechwood Ave.

Norfolk, Virginia
23505

REPORT DOCUMENTATION PAGE		READ INSTRUCTIONS BEFORE COMPLETING FORM
1. REPORT NUMBER AFIT/GE/EE/82D-22	2. GOVT ACCESSION NO. AD-A124774	3. RECIPIENT'S CATALOG NUMBER
4. TITLE (and Subtitle) COMPARISON OF ALUMINUM AND COPPER FUSE OPENING SWITCHES UNDER ROOM AND CRYOGENIC TEMPERATURE CONDITIONS		5. TYPE OF REPORT & PERIOD COVERED MS Thesis
7. AUTHOR(s) Jerry C. Bueck	6. PERFORMING ORG. REPORT NUMBER	
9. PERFORMING ORGANIZATION NAME AND ADDRESS Air Force Institute of Technology (AFIT-EN) Wright Patterson AFB, OH 45433		10. PROGRAM ELEMENT, PROJECT, TASK AREA & WORK UNIT NUMBERS
11. CONTROLLING OFFICE NAME AND ADDRESS Air Force Weapons Laboratory Kirtland AFB, NM 78117		12. REPORT DATE December, 1982
14. MONITORING AGENCY NAME & ADDRESS (if different from Controlling Office)		13. NUMBER OF PAGES 116
16. DISTRIBUTION STATEMENT (of this Report)		15. SECURITY CLASS. (of this report) Unclassified
		15a. DECLASSIFICATION/DOWNGRADING SCHEDULE 4 JAN 1982
17. DISTRIBUTION STATEMENT (of the abstract entered in Block 20, if different from Report)		
18. SUPPLEMENTARY NOTES Approved for public release: IAW AFR 190-17. Lynn E. WCLAVER Dean for Research and Professional Development Air Force Institute of Technology (AFIT) Wright-Patterson AFB OH 45433		
19. KEY WORDS (Continue on reverse side if necessary and identify by block number) FUSES EXPLDING FOILS OPENING SWITCHES PULSE POWER EXPLDING FUSES		
20. ABSTRACT (Continue on reverse side if necessary and identify by block number) The characteristics of electrically exploded aluminum and copper foil fuses are investigated and compared under varying temperature conditions. A 34 to 39 KJ system is used to explode the fuses in room temperature glass beads (sand), sand cooled to approximately -77C, liquid nitrogen, and deionized water. The temperature of the quench medium is seen to have an effect on fuse behavior with aluminum fuses being more affected. Two data processing methods are used and are found to produce quite different results. Because of this difference only a qualitative comparison of the		

UNCLASSIFIED

SECURITY CLASSIFICATION OF THIS PAGE(When Data Entered)

20. cont.

behavior of the fuses is given. The first method involved using voltage and current data scalefactored and integrator droop corrected to compute resistivity. The second method used a self consistant solution to the circuit model to recalibrate the voltage and current signals and then compute resistivity.

UNCLASSIFIED

SECURITY CLASSIFICATION OF THIS PAGE(When Data Entered)

3-83

DTIC